Use of Kinematics to Minimize Construction Workers' Risk of Musculoskeletal Injury

by

Abdullatif Alwasel

A thesis
presented to the University of Waterloo
in fulfillment of the
thesis requirement for the degree of
Doctor of Philosophy
in
Systems Design Engineering

Waterloo, Ontario, Canada, 2017

Examining Committee Membership

The following served on the Examining Committee for this thesis. The decision of the Examining Committee is by majority vote.

External Examiner	Professor Mohamed Al-Hussein
Co-Supervisor	Professor Eihab Abdel-Rahman
Co-Supervisor	Professor Carl Haas
Internal Member	Professor John McPhee
Internal Member	Professor Bryan Tripp
Internal-external Member	Professor Emeritus Richard Wells

I hereby declare that I am the sole author of this thesis. This is a true copy of the thesis, including any required final revisions, as accepted by my examiners.

I understand that my thesis may be made electronically available to the public.

Abstract

Construction work requires more repetitive and highly physical effort than, for example, office work. Despite technological advancements in construction, the human factor is still an essential part of the industry. Hence, the need to maintain a healthy work environment is a shared interest between workers and industry. This thesis addresses the problem of cumulative injuries among construction workers, with emphasis on masons, and examines ways to improve safety and productivity simultaneously.

Vision-based motion capture and sensor-based joint angle measurement techniques were tested against a state-of-the-art Optotrak™ system. Results show that the overall error in joint angle measurements was $\pm 10\,\text{deg}$ for vision-based approaches compared to $\pm 3\,\text{deg}$ for optical encoders. Moreover, a noninvasive fatigue detection method was developed by applying time-delay embedding and phase-space warping (PSW) techniques to a single joint angle, exerted force, and electromyography (EMG) data. Results indicate that the method can detect a slowly changing variable, fatigue in a limb, from a single kinematic signal, limb exerted force, or its EMG signals.

Furthermore, twenty one masons distributed in four experience categories, ranging from novice to expert, took part in a study to evaluate safety and productivity in masonry work using inertial measurement units (IMUs). The study hypothesized that masons adopt safer

and more productive work techniques with experience and that these techniques can be identified and used to train novice workers. Results indicate that journeymen appear to develop more productive and safer work techniques compared to other groups. On the other hand, the three-years experience group was found to sustain the highest joint compression forces and moments. Results also show that a clear distinction exists between expert and inexpert mason motion patterns. Support Vector Machine (SVM) classifiers were able to identify these differences with an accuracy of %92.04 in 13 seconds using a linear kernel.

The thesis findings justify exploration of sensor fusion techniques to combine direct and indirect motion capture systems. The findings also suggest that PSW can be used in applications such as rehabilitation to access information about patient status hidden in the full-chain kinematics using a single kinematic signal. Finally, findings show the potential for training apprentices to excel in all three aspects: proficiency, productivity, and ergonomic safety by following the example of experts.

Acknowledgments

First of all, I would like to thank Allah, the Almighty, for guiding me and having made everything possible to do this thesis. I would like to thank my supervisors, Professor Eihab M. Abdel-Rahman and Professor Carl T. Haas for their help and guidance throughout my studies, this work could not be completed without your aid and support.

I would like to extend my gratitude to my examining committee; Professor John McPhee, Professor Bryan Tripp, Professor Richard Wells, and Professor Mohamed Al-Hussein for their help and feedback to enhance this thesis. I would also like to thank Professor Daniel Stashuk and Dr. Meena Abdel-Maseeh for their help in fatigue analysis. Also, Ms. Suzanne Moyer, Chair, Trades & Apprenticeship program, Conestoga College, for facilitating the data collection effort. I would like to extend my thanks to Mr. Rene Le Toile, Coordinator of the Brick and Stone programs, Conestoga College, for his help in recruiting participants and managing the data collection site. I would like to thank Dr. Mohammad Nahangi, Dr. JoonOh Seo, and Juhyeong Ryu for their help, support, and encouragement.

I would like to thank my colleagues and freinds Dr. Mahmoud Khater, Dr. Sangtak Park, Hamidreza Nafissi, Yasir Aljefri, Majed Alghamdi, Ayman Alnemi, Karim Elrayes, Hatem Sindi, Pim Vermeyden, Dr. Anne Vermeyden, and Dr. Ahmed Alhussain for their

support and encouragement.

Special thanks to my friends Talal Aldobaiki, Ahmed Aljarba, and Dr. Abdulrahman Alsuhaibani for their continuing support and encouragement.

Last but not the least I thank my family, my sisters and brothers: Sarah, Sulaiman, Haya, Saud, Monirah, Turki, Adel, and Khaled for their love and support. I could not have done it without all of you.

إهداء

أمي و أبي،

لا شئ مما حققته كان ممكناً بدون دعواتكم و حبكم و تشجيعكم لي منذ أن كنت طفلاً. أتمنى من كل قلبي أن أكون دائماً عند حسن ظنكم.

Dedication

My Mother and Father,

None of my achievements would have been possible without your prayers, love, and support since I was a kid. I sincerely hope that I always meet your expectations.

Table of Contents

List of Tables

List of Figures

Chapter 1

Introduction

1.1 Overview

Repetitive and highly physical [3], construction work requires more physical effort than, for example, office work. A person has to be capable of performing highly physical tasks to join the construction workforce. However, cumulative musculoskeletal injuries are reducing the construction labor force. The effects of these injuries extend to workers' social life and welfare. The impact also extends to a national level, considering that the number of construction workers is 1.3 and 11.1 million in Canada and the United States respectively [4, 5]. Not surprisingly, the construction industry is directly affected by musculoskeletal injuries as labor costs stand at 30–50 % of total project cost [6].

There are multiple causes of cumulative musculoskeletal injuries. Kumar [7] presented four theories for causes of musculoskeletal injuries, two of which are differential fatigue and cumulative load. These two paths to injuries are initiated by awkward postures and repetitive motions, both of which are common in construction trades. Further, in construction, like all trades, higher productivity is a major goal, which puts even more stress on workers. All of these factors contribute to the complexity of musculoskeletal injuries.

Best practices for health and safety for trades have emerged since the 1990's, spearheaded by organizations such as the Center to Protect Workers' Rights (CPWR), the Construction Industry Institute (CII), and the National Institute for Occupational Safety and Health (NIOSH). These practices include toolbox meetings, structured hazard analysis, drug testing, and cultural changes to encourage a safer environment. Occupational work and safety organizations have been addressing the musculoskeletal injury problem for a long time. Despite these efforts, the industry is still facing a high attrition rate, as approximately 56 % of craft trainees complete their training program [8].

Studies using advanced technology to address the attrition rate are on the rise. Researchers are using technologies such as motion tracking and machine learning algorithms to enhance safety in construction. These efforts face many hurdles: systemic (within the sector), peer pressure (within a project), and lack of awareness about the importance of musculoskeletal injuries. As a result, these interventions are not broadly implemented in

construction worksites or training facilities [9, 10]. This issue is partly caused by the perceived cost of adopting these changes in the workplace in terms of productivity loss, lower quality, and higher maintenance [10]. Thus, the industry is in need for an intervention that enhances productivity and safety in combination.

1.2 Motivation

Despite technological advancements in the construction sector, the human factor is still an essential part of the industry. Hence, the need to maintain a healthy work environment is a shared interest between workers and industry. Two important measures of workplace safety are the average number of days that a worker spends away from work due to an injury and the injury incidence rate. Another measure of safety is the average age of workers, which is an indicator of workers' longevity.

Construction and manufacturing sectors have one of the highest annual incidence rates of musculoskeletal injuries at 132.7 and 103.1 per 10,000 workers with an average of 10 days away from work compared to incidence rates of 26.6 and 25.4 with an average of 8 and 7 days away from work in management and technical services [11]. In addition, the 2011 Canadian census showed that the number of workers aged 55 or older is, for the first time, higher than workers aged 15 to 24 [12].

Construction trades are essential for national development and the human factor is an important asset of these trades. This thesis addresses the problem of cumulative injuries among construction workers and examines ways to improve safety and productivity jointly.

1.3 Objectives

This research aims to enhance construction workers' safety and productivity and to decrease their attrition rate. Various motion capture techniques were investigated and different analysis methods were tested to develop methods applicable in the field. Following is a list of specific objectives towards that goal:

- Testing the feasibility of direct motion measurement techniques in the field
- Finding noninvasive measures to evaluate muscle fatigue
- Testing the hypothesis that workers' safety and productivity are enhanced with experience
- Testing the hypothesis that workers' experience level can be identified from their motion patterns
- Creating a database for masons' motion patterns

The thesis was structured to examine tools for kinematic data collection in non-structured environments and to use this data to minimize the number of injuries among construction workers. Current work health and safety guidelines provide detailed instruction on how to conduct safe work, however, these guidelines are not often followed which in turn did not affect the overall workers health status. This thesis compares state-of-the-art data collection methods and conclude on their suitability for use in construction sites. Then kinematic signals are used to study on masonry workers with varying levels-of-experience to extract a motion pattern associated with the expert masons and test whether this pattern is associated safety and productivity combined.

1.4 Thesis Structure

This dissertation is comprised of seven chapters as shown in Figure 1.1. *The first chapter* is an introduction to the thesis topic. *The second chapter* is a review of relevant literature on theories of injury causation, musculoskeletal injuries in construction, kinematic data collection methods, fatigue detection, and current interventions to minimize injuries in construction and masonry work.

Chapter three, is a report from a collaborative study conducted to compare the performance of a state-of-the-art vision-based motion capture system and electrogoniometers

in non-structured environments. This chapter is based on papers submitted to the journal Robotica by Seo, Alwasel, Lee, Abdel-Rahman, and Haas [13] and published in the 30th International Symposium on Automation and Robotics in Construction and Mining by Alwasel, Elrayes, Abdel-Rahman, and Haas [14]. In this part, the thesis author was in charge of experimental design, data collection and analysis for the direct measurement system part.

Chapter four reports on a study conducted to examine the use of a nonlinear system identification technique to detect muscle fatigue from kinematic and electromyographic signals. This chapter is based on papers published in the Journal of Biomechanical Engineering and the 26th Conference on Mechanical Vibration and Noise by Alwasel, Yung, Abdel-Rahman, Wells, and Haas [15], Alwasel, Abdel-Rahman, and Haas [16]. In this part, the thesis author was in charge of data collection of kinematic signals as well as data analysis for all signals in addition to writing the papers.

Chapter five reports on a study conducted on twenty-one masons with various levels of expertise to examine the effect of their motion patterns on body joint forces and moments. This chapter is based on a paper published in the Journal of Construction Engineering and Management by Alwasel, Abdel-Rahman, Haas, and Lee [17]. In this part, the thesis author was in charge of data collection and analysis in addition to writing the paper.

Chapter six, deploys a Support Vector Machine-based machine learning algorithm to

classify workers' motion patterns into safe-productive and unsafe-unproductive based on their level of expertise. This chapter is based on a paper submitted to the Journal of Automation in Construction by Alwasel, Sabet, Nahangi, Haas, and Abdel-Rahman [18]. In this part, the thesis author was in charge of data collection and analysis in addition to writing the paper. *Chapter seven* summarizes the research conducted, presents conclusions, and suggests future research avenues.

1.5 Thesis Contributions

The data collection comparison study revealed that although indirect measurement methods have the benefit of being easy to use and cheap, implementing them in construction sites will result in inaccuracies compared to direct measurement system. Furthermore, for the first time, time-delay embedding and phase-space warping were used to detect muscles' fatigue using kinematic and physiological signals. Phase-space warping was, for the first time, shown to be able to differentiate between load sharing patterns using electromyography signals.

Moreover, for the first time, kinematic data from masons with different levels of experience were used to conduct comprehensive safety and productivity analysis. It was shown that expert masons adopt a method of work that minimizes the risk and increase

their productivity. For the first time, novice masons were shown to be safe workers but not productive and productivity increase with experience The 3-years experience group show high productivity but were associated with high levels of joint forces and moments. Furthermore, support vector machine was use, for the first time, to differentiate between masons with different experience levels. Thereby, the use of SVM on kinematic signals was shown, for the first time, to be able to detect motion patterns of safe and productive masons.

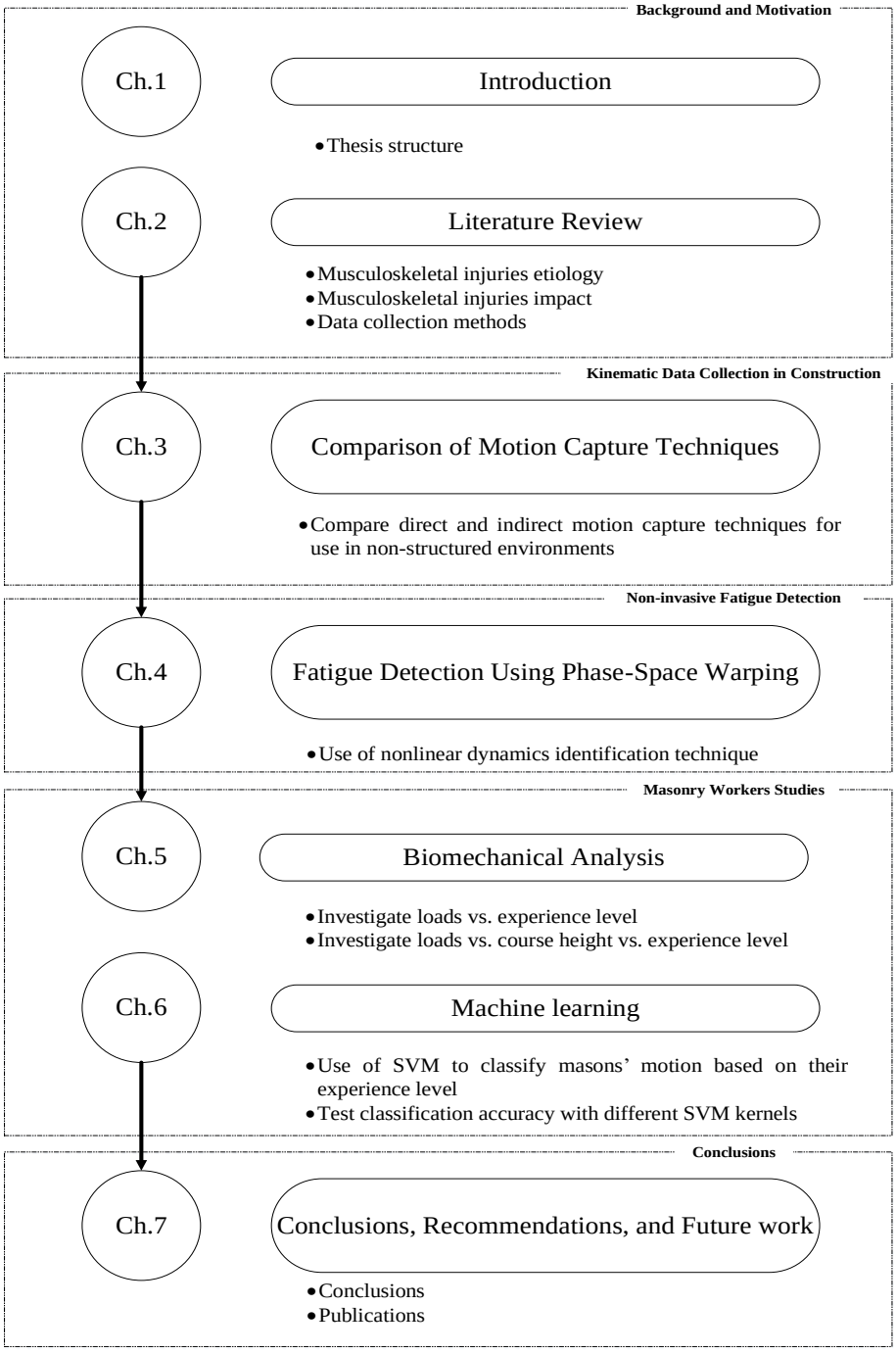

Figure 1.1: Illustration of the thesis topics

Chapter 2

Literature Review

This chapter is a review of literature relevant to this thesis.

2.1 Theories of Musculoskeletal Injury Causation

Musculoskeletal injuries (MSIs) are defined by the National Institute for Occupational Safety and Healthy (NIOSH) as those "that involve the nerves, tendons, muscles, and supporting structures of the body" [19]. The complexity of the MSIs stems from the multidisciplinary nature of its causes. Many theories have been developed to describe how MSIs occur. Kumar [7], through evidence published in the literature on workplace injuries, proposed four theories about how work-related injuries are developed: multivariate

interaction of musculoskeletal injury perception, differential fatigue, cumulative load, and overexertion. Each of these theories follows a series of actions leading to the perception of pain that indicate the existence of injury. The following subsections describe each theory in detail.

2.1.1 Multivariate Interaction Theory

This theory attributes the MSI precipitation to the interplay between morphological, biomechanical, psychosocial, and genetic elements. Morphological factors, such as muscle shape and size, are responsible for the ability of the body to withstand other factors leading to the injury. It explains the variability between individuals facing the same environment or performing the same task. For example, if all other factors leading to MSIs are controlled for two persons and the same type of force is applied on their bodies, different outcomes will be seen due to the difference in morphological characteristics.

Biomechanical factors change according to how much load is applied, at what angle, and to which part of the body. Human bodies react differently to applied forces. Even the same body sometimes reacts differently due to other factors such as fatigue. The inter- and intra-variability of the human body determines its variations in the ability to withstand applied forces.

Psychosocial elements can also decrease or increase the prevalence of injury. Bullying, racism, job demand, and job control are types of psychosocial factors that escalate or delay the process of wear and tear leading to MSIs. Hauke et al. [20] reviewed literature from 2000 to 2009 associating psychosocial factors (such as low social support, low job control, low decision authority, low job satisfaction) with MSIs. They found that a small but significant impact of psychosocial factors is causing MSIs. Furthermore, they found no evidence indicating that specific psychosocial factors are associated with a specific MSI or parts of the body.

The last element in the multivariate interaction theory is the genetic traits of the body; in fact, the genetic map of the body can provide information on whether it is susceptible to injury. Collins [21] reported on the association between some genetic sequences and some MSIs such as rotator cuff injuries. These genetic sequences are beyond the human control in the sense that under the same force, some people are more vulnerable to injury than others due to their genetic map.

The multivariate theory suggests that MSIs are multifactorial where there is no definite path specified for each injury. To address the problem of MSIs, many factors have to be monitored and managed, some tangible, such as biomechanical factors, while others are intangible. Thus, a system approach must be adopted to control the environment inside the human body, such as genetics, and outside the body, such as the psychosocial factors,

to eliminate the risk of injury.

2.1.2 Differential Fatigue Theory

The differential fatigue theory bases its assumption on the fact that effective industries rely on repetitive processes to achieve maximum production. A motion is constituted by multiple joints and muscles. These muscles are differentially loaded and their proportionality depends on many factors, such as posture and muscles' status. Differential loading leads to two effects. The short-term effect is that different muscles fatigue disproportionately due to the repeated loading and this fatigue results in distributing the load to other muscles and therefore lower productivity. In the long-term, when the muscles are continually fatigued due to repetitive forceful tasks, the body starts to change the optimum mechanism by which it originally was working to lower fatigue, and that response eventually results in pain.

2.1.3 Cumulative Load Theory

This theory highlights the idea that pain is not simply the result of a single incident of high load application but the result of accumulative load over a prolonged time, hence the cumulative fatigue. Muscles undergo damage at the micro level under the influence of

force. Further, muscles have the ability to self-repair their tissue with the removal of force for a period of time. Thus, the accumulation of low forces applied to the muscles for long periods is not the reason for injury. Rather, it is the absence of rest time for the muscles to repair themselves.

Rohmert [22] introduced a model to calculate the rest allowance required for a worker to avoid injury in industrial settings [22, 23]. The model calculates the required rest time based on the maximum exerted force. The effect of rest time pn m suggests that ergonomists and job designers must consider the resting allowance to produce an effective and safe work station. Rest time allows muscle tissue to self-repair itself before the application of the next set of forces. The rest allowance method works only if the force does not exceed the tissue tolerance limit. Whenever the force exceeds the tissue tolerance limit, the injury source becomes overexertion, which is the next theory.

2.1.4 Overexertion Theory

The last of Kumar's theories for MSI causation is the overexertion of force, position, motion, and duration, these four elements required to perform any effective task. Workers apply force to move an object from one position to another over a period of time. The MSI can happen due to overexertion of any of the four elements.

Overexertion of Force

Muscles are designed to produce force in contraction. To move an object, the muscles exert forces which are transmitted through the body parts through the joints. Muscles and joints have threshold limits under which they can tolerate forces, whenever the force level exceeds this threshold, injury happens.

In 2014, overexertion accounted for 33% of all non-fatal injuries reported by the U.S Department of Labor [11]. The problem with overexertion is that workers do not know that they are overexerting force until they have the symptom (pain), which is the later stage that researchers and health institutions are trying to prevent. Many intervention studies were conducted to lower the force required to perform tasks and the results were positive, indicating that redesigning the workstation or task lowers the incidence of MSIs [9, 24]. However, the end point is not promising because industries need to run at a certain pace that can be compromised through redesigned tasks, leading to delays in the production process.

Overexertion of Duration

Rohmert [25] demonstrated that for each force exertion level, a minimum muscle rest time is required to prevent MSIs, meaning the muscle threshold decreases with the prolonged

force exertion, making it easier for the worker to exceed the limit and thereby overexert force.

Therefore, the key issue is not only how much force is being exerted, but also how often this force is exerted and if the muscles are being rested. Many studies showed that repetitive motion is one of the causes of MSIs [19]. The repetitiveness itself is not the problem it is rather the lack of rest time for the muscles to regain their original shape and condition before the application of next set of force.

Overexertion of Posture

Joints are designed to work effectively within a defined range of motion. When a person exceeds this range of motion, muscles are required to produce more force to maintain the required posture. Kumar [7] demonstrated that the best position for any joint is the mid position, which requires the minimum amount of force. Any deviation of more than 20% from this position is going towards the dangerous zone.

For example, Alwasel et al. [26] investigated the risk factors for developing work-related shoulder MSIs among construction workers. They found that the risk factors are forceful work and range of motion and that, if workers maintained their upper arms below 90°of flexion, the number of shoulder MSIs could be decreased.

Interaction of Force, Duration, and Posture Overexertion

Finally, tissue is more vulnerable to injuries when subjected to the combination of forceful, prolonged, and awkward posture risk factors. In other words, certain forces may not harm the tissue in static mode but will injure it if repeated multiple times in a short duration. This interaction is performed in everyday life, and that is what makes MSIs appear in every sector. Thus, to decrease the MSIs prevalence, all of these factors have to be included when designing a task or a workstation, to guarantee that the person will perform the task at a low force level with repetitions spaced out enough to allow for the minimum rest time.

2.2 Impact of MSIs

Examining MSI risk factors, one can expect that the number of cases will be especially high among construction workers. MSIs can result from everyday activities in almost all work environments; furthermore, their impact on society is enormous, especially in countries such as Canada, where the health care system is socially funded. In this section, two aspects of MSIs impact are studied:

- Prevalence: using statistical analysis to examine the number of workers affected by MSIs in North America, the causes, and the cause-effect relationships.

- Severity: using statistical data to examine time lost due to injury.

2.2.1 Prevalence of MSIs

The many types of MSIs reported in statistical data published by Statistics Canada and the U.S Department of Labor's are categorized using two schemes according to the affected body part and/or the reported cause of injury.

In 2014, the number of MSI cases in the U.S. was 365,580 forming 32% of all injuries requiring days out of work. Construction cases accounted for 6.4%. Laborers, nursing assistants, heavy trucks and tractor-trailer drivers, janitors and cleaners, and stock clerks and registered nurses accounted for 85,830, constituting 7.4% of all injuries requiring days out of work [11].

In Canada, 51% of all injuries for working age Canadians 20 to 64 years old are sprains and/or strains out of which 18% are due to work. Thirty-three percent of all work injuries occur among workers in trade, transport, and equipment operations [27]. The similarity between Canadian and U.S data are due to the similar types of industry and population demographics. MSIs are widespread in North America especially, in work environments.

The prevalence of MSIs among workers is due to work conditions which involve all MSIs risk factors. This claim is supported by the number of cases in the occupations, making

up 7.4% of all injuries requiring days off work in the U.S and 33% of all work injuries in Canada. The cases resulting in these numbers are jobs in the same category, namely trading, transport, and labor.

The reason behind these figures is that workers in these jobs are often working under conditions that make them prone to the MSI risk factors discussed in 2.1. Generally, workers are not following the guidelines set by health regulators for their occupations to avoid injuries. Further, even if workers are working under those guidelines, their work conditions are not monitored in a way that would allow them to avoid stressful postures, such as working above head level, lifting heavy weights, or highly repetitive tasks with no rest time.

Those with jobs in trading, transport, and labor work under high stress, and in low income, low job security conditions, the worker is under psychosocial stress factors that may lead to the development of MSIs. Moreover, these jobs require more physical work compared to other jobs. Also, not enough health resources are available to workers in these categories. These circumstances meet the definition of an unhealthy environment as defined by the World Health Organization (WHO) [28].

Sprain, strain and, tears were responsible for 36.3% of all injuries requiring days away from work in 2014 [11]. These numbers indicate that one-third of injuries in the US were MSIs and two-thirds had other factors not directly related to MSIs. These numbers provide

a realistic picture of health conditions for workers, with the proviso that not all incidents are reported to the statistics bureau for reasons discussed by Kosny et al. [29]. They may also indicate the severity of injuries caused by non-obvious factors, such as psychosocial, overexertion of duration, and range of motion, which may contribute to the two-thirds figure [29].

In Canada, a similar pattern holds. Overexertion accounted for 28% of injuries among the working age adults 20 to 64 years old, whereas 35% of the injuries involve falling. Contact with sharp objects and being struck by an object contributed to 12%, and violence was responsible for 5% of injuries [27, 30].

The guidelines set by health regulators [31–33] provide tools for workers, employers, and policymakers to avoid MSIs in work sites by eliminating their risk factors. However, some risk factors are not obvious to workers; thus, avoiding these factors requires attention from the worker and/or employer. Such risk factors are responsible for the majority of MSIs in work sites according to statistics. These factors are hard to monitor without special types of equipment. Examples of these risk factors are force level, repeat frequency, and duration. Therefore, unlike overexertion in lifting and twisting, sprain/strain injuries are not controllable by the worker.

Back sprain/strain injuries in the U.S, made the top of the list with 17.3% of injuries followed by the knee at 9% and the shoulder at 7.7% [11]. In Canada, ankle and foot

injuries made the top of the list with 21% of all sprain/strain injuries followed by the wrist and hand at 16%. Back injuries accounted for 15.9% of all sprain/strain injuries and the knee constituted 15% [27].

The injury distribution by affected body part confirms the causality of some risk factors reported in the distribution by cause of injury. For example, the fact that back injuries are the most common result of overexertion in lifting and lowering supports research findings that confirm unsafe bending and carrying of overloads by overexerting force as risk factors in back MSI. However, the previous numbers provide an insight into the frequency of injury and the body part being affected but not into the severity of the problem.

2.2.2 Severity of MSIs

The severity of the MSIs can be measured by the period of time the injury requires for treatment. Further, the severity of the injury can be measured by examining the financial compensation provided to workers per injury and/or the total cost of MSIs to the national health care system.

Statistics Canada, in 2011, revealed that the average length of absence for workers in building and other support services was 8.6 days [34]. Figure 2.1 shows the average length of absence for the general work population, construction workers and helpers, and for those

in building and other support service from 2001 to 2011. The chart shows an ascending trend in the building and other support services from 6.6 days off work in 2001 to a peak of 9.1 in 2006. Henceforth, absence length stabilizes around 8.5 days, which is two days longer than the average absence in 2001. Several factors could underlie this trend: a large intake of inexperienced workers joining the workforce recently without the proper training to avoid injuries, a change in construction technology leading to more severe injuries, or an aging workforce requiring more time to recover. Regardless of the exact underlying causes, the data indicate that workers face a higher risk of developing severe injuries in the construction sector compared to 11 years ago.

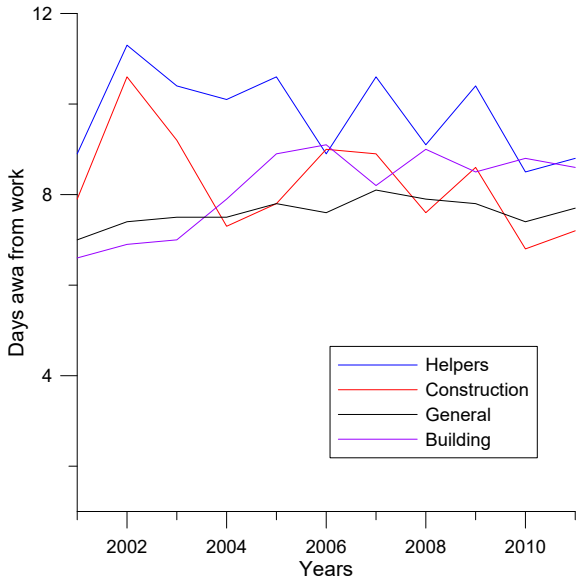

Figure 2.1: Number of days away from work due to injury

The trend is the same in the U.S.; the number of injured workers is on the rise. Tabulated data on absence rates grouped by the type of work and injured body part indicate heightened the risk of MSIs. According to the U.S. Bureau of Labor Statistics, the average number of days required for recovery from an MSI is 13 days [11].

MSIs are present across all occupations because of the existence of MSI risk factors in all environments, however, the degree to which they impact workers varies across occupations. Figure 2.2 shows how occupation affects the time required for treatment. Construction and manufacturing jobs required ten days of away time to recover compared to 5 and 6 for education and health care jobs. These numbers show the variation in the severity of MSIs by the type of occupation. Each occupation has its risk factors. The severity of MSIs depends on workers exposure to those risk factors.

There are two types of costs resulting from injury among workers. The first are the direct costs to treat workers and bring them back to the workforce; the second are the indirect costs of replacing the worker temporarily or permanently if necessary. The total cost of MSIs in Canada in 1994 was 3.4% of gross domestic product at 28$ billion CAD. The direct cost was 7.5$ billion and 18.1$ billion was indirect cost [35]. The direct and indirect costs of shoulder injuries were investigated by Alwasel [36], who found that when a worker is injured at the work site, this means that a worker's musculoskeletal system is severely worn due to work. Hence, the need to train a new worker to replace the injured

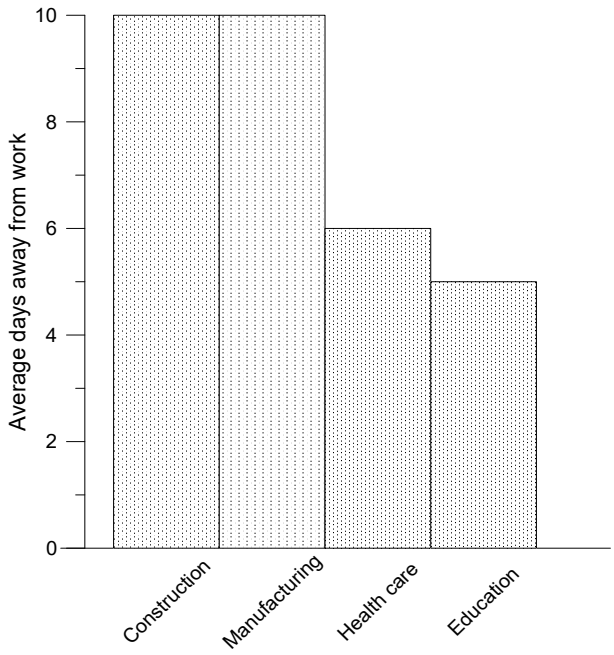

Figure 2.2: Number of days away from work due to injury, by occupation type

one this result in delays to the work schedule.

In the U.S, the burden of injuries in 2000 was $406 billion USD divided into $326 as indirect costs and $80 billion as direct costs [37]. Furthermore, the indirect costs of MSIs are not visible to the individual and can only be seen at the macro level. For small to medium businesses, the effect of injury is neither obvious nor important economically, however, at the society or large corporation level the economic burden is more clearly seen.

The burden of industrial MSIs and overall injuries could be minimized if policy makers developed more comprehensive plans to prevent injuries, plans which have been adopted by other countries and which have proven successful in eliminating the exposure to risk

factors [38]. Many researchers have tried to limit workers' exposure to MSI risk factors leading to injuries in their field. However, there are many challenges to these plans and their application in real situations.

Lahiri et al. [39] investigated the cost-effectiveness of four plans to decrease the burden of back pain resulting from work tasks: training, engineering control, training and control, and a comprehensive plan by the WHO. The authors found that the most cost-effective prevention method is training; however, the overall effectiveness of the training is low compared to other methods. Further, the study concluded that ergonomic control intervention and the full ergonomic plan are the most effective in the long term [39].

Morgan and Chow [40] investigated the economic impact of applying an ergonomic plan to decrease the burden for registered nurses (RN) injuries. They found that the cost to replace one RN leaving nursing due to back pain is between $25,000 to $38,000. The authors also found that applying an ergonomic plan that considers training, policy, and equipment use resulted in decreasing the number of back injuries among RNs and consequently reducing the economic burden resulting from back pain among RNs [40].

Thus, the financial burden from injuries in work environments is evident. Although businesses are mainly concerned with direct costs, the society as a whole is largely affected by an injury's indirect cost, which is always more significant than direct costs and yet not as obvious to individuals. These financial burdens do not cover the actual figure of the

injury for many reasons such as the multifactorial nature of the injury and the system that determines which injury to include as work-related.

2.3 Safety in Construction

Inspecting the number of injuries reported in the early 1900s compared to current statistics, one can conclude that construction work can be made safer. Historically, construction work was regarded as an environment with poor safety, health, and environmental conditions. For instance, the Golden Gate Bridge (San Francisco, USA), completed in 1937, was well regarded for its exceptional safety measures. At a cost of 35 million, there were only 11 worker deaths compared to the standard rate of one death for every million dollars spent [41].

Best practices in construction have emerged since the 1990's. Studies funded by organizations such as the Center to Protect Workers' Rights (CPWR), the Construction Industry Institute (CII), and the National Institute for Occupational Safety and Health (NIOSH), have developed best practices for all jobs in construction. These best practices include toolbox meetings, structured hazard analysis process, drug testing, and cultural changes to encourage a safer environment. These practices have improved work safety as evidenced by the industry's Lost Workday Case Incident Rate (LWCIR), which declined from 6.8

in 1989 to 2.2 in 2008, and the construction industry Total Recordable Incidence Rate (TRIR), which went from 14.3 in 1989 to 3.8 in 2013 [42].

However, the industry has begun to face a shortage in the workforce as the first baby boomer reached the age of retirement in 2011 [12]. On the other hand, the number of injuries in construction reported in the United States during 2014 for workers aged 45 and 54 was less than the younger categories [11]. This indicates that, although the worker population is aging, fewer injuries are reported among older workers than younger workers. The number of injuries reported vs. length of service with the same employer in construction provides a clearer picture of the problem. Workers with 3 months service or less reported 15% of the injuries, and workers with 3 months to 1 year reported 22.5% of the injuries. The percentage significantly increases for workers with 1 to 5 years to 34.2% of the injuries and then settles back to 26.5% of the injuries for workers with more than 5 years of service [11].

One of the many efforts to decrease the number of injuries among workers is the interventions by stakeholders to reduce the impact of MSIs on the industry. These interventions include regulatory procedures, such as the NIOSH lifting equation, which defines how much weight is considered safe for carrying [32, 43]. The impact of MSIs and other work-related injuries is widely seen through the number of studies conducted to investigate the injury source, assess its severity, and suggest solutions to decrease the injury prevalence. Types of

research include but are not limited to biomechanical studies to investigate the mechanics of the injury, epidemiological studies to investigate the nature of the injury, and ergonomic and management studies to suggest solutions to the injury problems.

There have been more recent attempts to implement ergonomics plans that decrease MSIs in the worksite and to continuously assess the impact of the solution in-situ. These studies are referred to as participatory ergonomics (PE). The advantage of intervention studies over other studies attempting to validate MSI solutions is that they do not need to mimic the environment in which the solutions will be applied. Thus, there is no effect of the environment on the study results. The effect of mimicking the environment of the industrial or crafting jobs was investigated by Moriguchi et al. [44]. The authors found that, due to lack of tools, researchers tend to neglect the subtasks performed in real settings when reproducing them in a lab environment. That oversight, in turn, led to the inaccurate representation of the task risk factors.

Cole et al. [45] investigated four PE studies to check their overall performance and evaluate the deficit of the theory and then suggest ways to improve the overall performance. The study evaluated the four studies and reported a mix of positive and negative results. In assessing the process, implementation, and effect of the changes on workers' health the study concluded that changes were limited due to management commitment, such that researchers had difficulty recruiting employees due to their management stress.

Authors reported theory deficits that contributed to limiting the outcomes of the four PE interventions; for example, ergonomic changes made to tools and workstations' layouts did not include capital equipment and production lines because of the financial burden on companies.

Denis et al. [9] divided the participatory ergonomics intervention studies in MSIs into three categories: complete, shortened, and turnkey. Dividing these studies is based on their evaluation of the preliminary results of MSIs, then a diagnosis of the problem, and a proposed solution. Authors found that, depending on the classification of the intervention, the results vary. Complete studies tend to cover most of the risk factors and work description whereas other classes tend to save time by skipping some of the risk factors and/or work descriptions.

Although researchers understand the importance of research in developing MSI solutions that are robust, comprehensive, and effective, they face problems when implementing them in reality, such as lack of funds or lack of management/worker cooperation. Thus, the impact of the research to develop solutions' to limit the expansion of MSI cases among workers is not noticeable.

Management commitment is a major player in the intervention game that determines whether interventions are successful. Middle management tends not to cooperate if the intervention does not directly reflect on their personal health or benefits. As a result,

workers might not be able to give up productivity over health because of the pressure from management. At the end of the day, supervisors are keeping track of productivity and not determining whether workers were using the safe technique [46].

The solution to the management commitment lies in developing a solution to MSIs that is independent and does not require management commitment at a high level. That is, securing the approval for applying a solution in a given field is not the problem; the problem lies in further observation of the application of the solutions in-situ. Thus, an independent solution would eliminate the burden set on management so they are not required to monitor the application of the solution in addition to their work as production managers.

Another form of interventions to reduce MSIs, job analysis, assesses work conditions for a given job and identifies potential dangers [47–54]. Results of these two types of interventions are often procedural guidelines for work with less exposure to risk factors leading to an increased number of work-related injuries.

Another type of intervention, implementing physical changes in the work environment by introducing new tools, aims at reducing the workload on workers' body and increasing productivity through the use of robotics [55], image-based tracking [56], or inertial measurements [57]. Though proven to have a positive impact on reducing exposure to risk factors, these interventions are not widely implemented in workplaces [9, 10].

Moreover, researchers are adopting emerging techniques from other fields and applying them to construction field, including the use of machine vision to classify human motion. Particularly, researchers are focusing on classification of workers' motion when performing tasks such as climbing a ladder, reaching far to the side of the ladder, standing, stooping, bending, walking, running, and crawling. They have achieved classification accuracies up to 99.5% compared to traditional marker-based motion tracking systems [58–62]. Range cameras, which translate depth information into grayscale images, are used to create a silhouette of the body, using software such as iPi Desktop Motion Capture and OpenNI, which encompass a predefined human model. The built-in algorithms can track the motion of the silhouette in space and time [63–67]. This method, using depth camera such as Kinect™, can function best in structured environments, such as a laboratory, because of its sensitivity to subject surroundings, self-occlusion, and short range (approximately 4m).

To overcome the shortcomings od the depth cameras [68], stereo-vision cameras have been used to collect 3D images outside laboratory environment [56, 69]. The system collects a point cloud of the body similar to those obtained by laser scanners. Utilizing the iPi software, the point cloud is tracked in a manner similar to the depth camera technique.

Inertial Measurement Units (IMUs) have been used to track human motion and work productivity in many environments [70–76] including construction settings [57, 77–84]. IMUs allow for unrestricted motion in non-structured environments. These sensors provide

translational and rotational accelerations of the body segment attached to them. A model-based software then uses these accelerations to estimate 3D coordinates of the body joint centers in space and time. Accuracies up to 80% were achieved in the classification of tasks compared to traditional motion tracking systems. Furthermore, productivity analyses were carried out with an accuracy of 85% compared to manual productivity analyses.

Body physical status monitoring (PSM) during tasks has been used to investigate the relationship between the physical status and productivity [85–87]. Although the use of PSM combined with location sensors such as UltraWideBand (UWB) trackers enables combined tracking of health and productivity, its accuracy is limited.

Despite these limitations, the field of automation in biomechanical analysis and safety training is rapidly advancing. The construction industry is in need of new innovations [88]. Researchers have used more sophisticated methods such as marker-based motion capture systems to create Cyber-Physical games that train workers in realistic construction settings [89]. Golabchi et al. [90] presented an automated method for job-site ergonomic safety analysis where they modeled a floor panel production line consisting of four stations. The proposed method has the advantage of simulating a job-site to investigate the outcomes of planned safety interventions. Seo et al. [56] proposed a method to perform on-site biomechanical analysis using Biovison Hierarchy (BVH) motion data extracted from vision-based approaches. The BVH file was converted into files readable to biomechanical

analysis tools such as 3DSSPP [91] and Opensim [92]. Using anthropometric parameters, they generated a multibody model and calculated the forces acting on body joints. This method is an improvement over traditional ergonomic analysis methods, which are based on observation and self-reporting and lack in-depth information.

Many complications hamper the application of these interventions in the field, particularly, at the sector, institution, and implementation levels: systemic sector-wide hurdles, peer pressure and lack of competition within the sector, and lack of awareness about musculoskeletal injuries across all three levels [93]. The cost of adopting those interventions, regarding productivity loss, job quality, or costly maintenance, is another major hurdle [10].

Thus, a potential solution to the MSI problem in the industry must be economical and not impede workers or their work quality. These features allow for overcoming the sector-wide hurdles. In addition, stakeholders have to be aware of the impact of MSIs and the benefit of lowering its prevalence.

2.3.1 Investigating Masonry Work

On-site analysis provides analytical and quantitative tools to guide a process of prevention-through-design. Significant efforts have been devoted to investigating the effects of masonry work on the human body [10, 47, 49, 94–101]. Faber et al. [97] studied aspects such as

work height, block mass, and single and dual-handed handling. A total of nine masons took part in the study. The authors measured the effects of varying block height and mass on the shoulder and L5/S1 joints and showed that masons are constantly subject to low back compression forces beyond NIOSH limit of 3.4 kN. Moreover, they found that working at heights below hip level significantly decreases the loads on the shoulder joint. They also reported that single-handed handling decreases the net extension moment of the lower back.

Moreover, the effect of experience level on posture during material handling has been studied in a laboratory setting [101, 102]. A total 30 material handlers took part in this study divided evenly between novices and experts. The participants lifted boxes weighing 15 and 32 kg from ground and 32 cm above ground. Researchers found that experts had significantly different postures from novices with the experts handling the material closer to their body. However, no significant difference was found between the two groups in the L5/S1 joint moment, and only minimal differences were found in peak moment, asymmetry, and cumulative loading at the L5/S1 joint.

Researchers have also investigated the use of different block materials to enhance masonry work environment. Hess et al. [47] found that using autoclaved aerated concrete resulted in shoulder and low back pain. However, they found that both concrete masonry units and autoclaved aerated concrete resulted in low back compression forces beyond the

NIOSH limit. The mean back compressive force using concrete masonry units was 4.3 kN while autoclaved aerated concrete has a significantly higher force at 4.9 kN.

U.S. Bureau of Labor Statistics [11] (BLS) data shows that the number of musculoskeletal injuries in those who worked five years or more with the same employer is almost equal to the number of novice worker injuries. This is also in agreement with the outcomes of Plamondon et al. [102] and Plamondon et al. [101] study. However, BLS statistics also show that the number of injuries for workers with 1 to 5 years employment with the same employer is significantly higher than for novice and expert groups. The reason for this discrepancy is not obvious and is critical to long-term retention of apprentices.

Manual lifting, an integral part of the masonry trade, poses a risk of cumulative stress injuries exacerbated by the length of exposure time. However, expert masons have been found to sustain far fewer injuries than less experienced masons. The reasons for this difference remain a quandary. Literature has analyzed the performance of experts and novices to draw conclusions about the relationship between experience and injury risks and productivity independent of each other. However, it has not covered the experience gap between them, namely the apprenticeship period, nor have the combined relationships among experience, productivity, and risk of musculoskeletal injury been quantified to date.

2.4 Data Collection in Construction

Body kinematics can be collected noninvasively by two techniques: vision-based and angular measurement. These two techniques can be categorized as indirect and direct measurement systems. The advantages and disadvantages of each technique determine the eligibility of a given techniques for use in the field.

2.4.1 Vision-based Techniques

Vision-based approaches aim to extract full-body motion data by processing 2D or 3D images [103]. Previous research efforts have developed several vision-based techniques, such as video camera combined with depth sensors (RGB-D) sensor-based[60, 63–65, 67], stereo-vision camera-based [104, 105], and multiple camera-based [106, 107] approaches. While RGB-D sensor-based and stereovision camera-based approaches take advantage of 3D imaging sensors that directly provide 3D information on scenes, a multiple cameras-based approach relies on the photogeometric acquisition of 3D body joint locations (i.e., 3D reconstruction) from tracked 2D joint locations of multi-view images.

RGB-D Sensor Technique

Several computer vision algorithms have been developed to estimate human poses by detecting the 3D positions of body joints directly from RGB-D images [63–65, 67]. Recently, motion capture solutions such as iPi Desktop Motion Capture (www.ipisoft.com) and OpenNI (www.openni.org) that use a Microsoft Kinect sensor have provided effective solutions for extracting skeleton-based motion data from 3D images obtained by RGB-D sensors.

The Kinect sensor that was initially developed for video gaming is capable of providing both depth and color information at a resolution of 640×480 and a rate of 30 frames per second [108]. This sensor is equipped with infrared (IR) projector, color camera, and IR camera. Using the projected structured IR lights, it measures the objects' depth, reconstructing 3D scenes with a point cloud [109]. Combined with the 3D sensing feature of the Kinect, the iPi Desktop Motion Capture software provides a marker-less solution for collecting full-body motion data. Figure 2.3 shows an example of an RGB-D image with a pre-defined body model, and the corresponding motion data. The algorithm is model-based, which means that motion data can be tracked by matching the surface of a pre-defined body model with a depth image, shown in Figure 2.3a. Then, the tracked motion data can be exported into any motion data format such as the Biovision Hierarchy

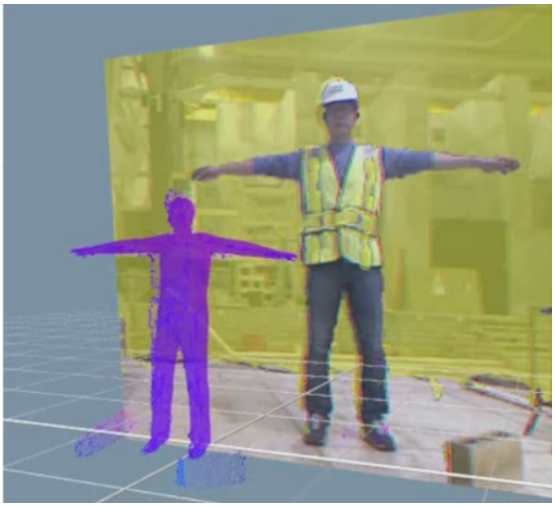

(a) RGB-D Image with a body model.

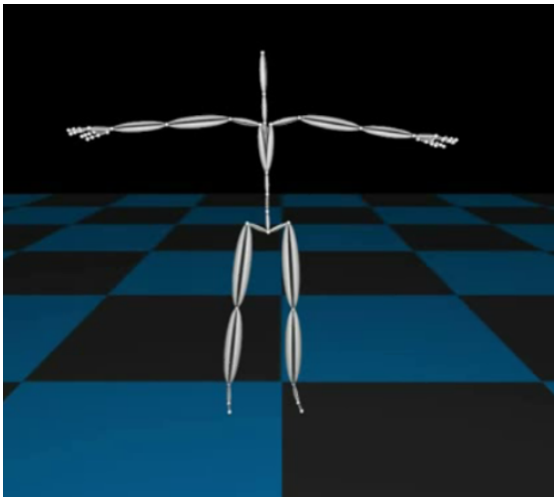

(b) Skeleton-based motion data (.BVH).

Figure 2.3: RGB-D Sensor-based motion capture.

(BVH) motion data, shown in Figure 2.3b. This software provides several post-processing algorithms to refine tracking and filtering algorithms for noise removal and smoothing.

The RGB-D sensor-based motion capture approach does not need markers or sensors attached to human body, which allows for motion capture without interfering with on-going work. Moreover, its low cost, approximately 150–250 USD, allows for easy access to industries, and they are an easy-to-use and easy-to-carry means of in-field motion data collection [60]. Furthermore, this approach is robust to self-occlusions because the iPi software provides an inverse kinematics algorithm that can adjust incorrectly tracked body parts due to occlusions. However, as the Kinect uses IR light, this approach is limited only to an indoor environment due to its sensitivity to sunlight. Also, the short operating range

of the Kinect sensor (within 4 m) is one of the disadvantages of this approach.

Stereovision Camera Technique

A stereovision system is designed to extract 3D information from a stereo image pair [110], works similar to 3D sensing in human vision. It begins with identifying image pixels that correspond to the same point in a physical scene observed by multiple cameras. The 3D position of a point can then be established by triangulation using a ray from each camera. The more corresponding pixels that can be identified, the more 3D points that can be determined with a single set of images. Correlation stereo methods attempt to obtain correspondences for every pixel in the stereo image, resulting in tens of thousands of 3D values generated with every stereo image. The Bumblebee XB3™, manufactured by Point Grey Technologies (www.ptgrey.com) is one of the widely used stereovision cameras. The stereo camera measures line-of-sight distance using two lenses with a narrow baseline in a self-contained unit. This allows for both optical and depth data to be collected with few environmental restrictions, such as outdoor environments and limited field-of-view.

Starbuck et al. [104] proposed a stereovision camera-based motion capture approach that addresses the short operating range of an RGB-D sensor. The 3D point cloud data collected from the stereovision camera was converted into a format used by an existing kinematic modeling software solution (iPi Motion Capture software) designed for use with

RGB-D sensors. Then, using the same algorithm used in the RGB-D sensor-based approach, skeleton-based motion data was extracted from the 3D point cloud data. Through a laboratory test, the proposed method was shown to be comparable to the traditional RGB-D sensor-based approach [104].

A stereovision camera-based approach provides additional advantages, beyond the benefits from the RGB-D sensor-based approach. For example, this approach does not depend on environmental conditions, allowing both indoor and outdoor applications. Also, the operating range of the stereovision camera is flexible according to lens field-of-view, lens separation, and image size [68]. However, as computing depth information from two images is a computationally intensive task, the frame rate relies on the hardware performance [68].

Multiple Camera-based Technique

A multiple camera-based motion capture technique aims to estimate the 3D locations of body joints by processing 2D images from two different views using multiple video cameras or a 3D camcorder that has two lenses in one camera. Han and Lee [106] proposed a motion capture process that consists of 2D pose estimation from one view of images, correspondence matching of body joints on the other view of images, and 3D reconstruction of body joints using the corresponding joint locations identified. However, this approach requires extensive training images to detect joint locations on testing images, and significant

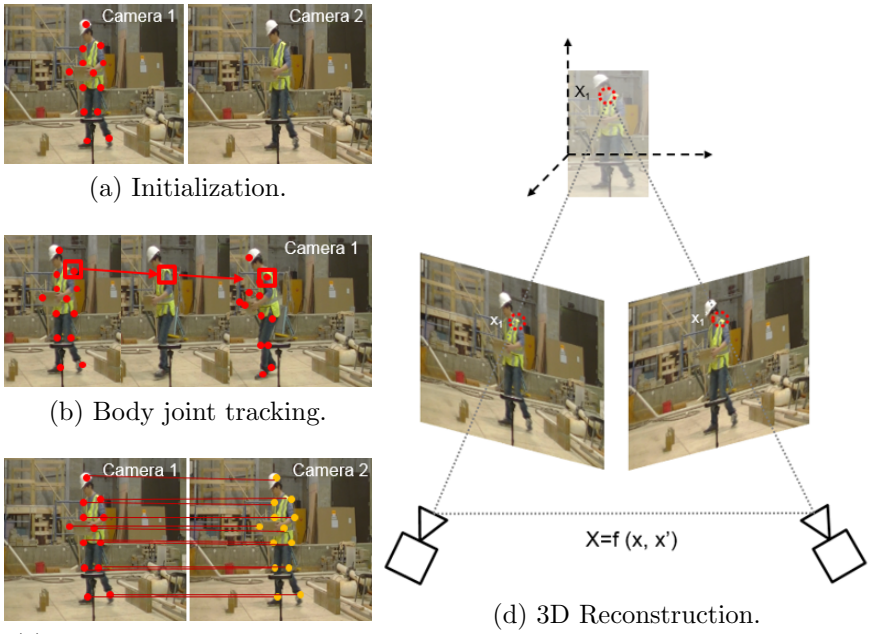

(a) Initialization.

(b) Body joint tracking.

(c) Correspondance matching.

(d) 3D Reconstruction.

Figure 2.4: An Overview of a Multiple Camera-based Motion Capture Technique

computation time for 2D pose estimation. To address this issue, Liu et al. [107] modified this approach by proposing body joints tracking that accelerates the 2D pose estimation process without the prior knowledge (training images for joint detection). Figure 2.4 shows an overview of the modified approach.

The idea of 2D joint tracking is that continuous tracking of body joints on consecutive image frames enables fast estimation of 2D skeletons [107]. Once the target joints are initialized in the first frame, shown in Figure 2.4a, the algorithm tracks the joints in consecutive images by detecting the image patch with the most similar color histogram with that of the initialized target. To reduce computation time, a modified particle filter tracker

was applied to specify the number of reliable candidates for the targets in the subsequent frames [111]. The tracking of different body joints is performed independently, resulting in a 2D skeleton model, shown in Figure 2.4b. The next process is to identify the corresponding body joints on the image from the other viewpoint by comparing the features of a pixel with the feature descriptors, such as Scale-Invariant Feature Transform (SIFT) [112] and Speeded Up Robust Features (SURF) [113, 114], shown in Figure 2.4c. To obtain more reliable corresponding locations of body joints, the search space is constrained by epipolar geometry [115] and homography [106]. Once pairs of corresponding body joints are detected from two different viewpoints of images, a 3D reconstruction algorithm detects the 3D positions of each joint through triangulation, resulting in 3D full-body skeleton-based motion data as shown in Figure 2.4d. Camera intrinsic and extrinsic parameters required for 3D reconstruction are obtained by using Zhang [116] camera calibration technique.

The strength of a multiple camera-based motion capture technique is that we can use ordinary video cameras to obtain motion data. Thus, this approach is less hardware dependent than RGB-D sensor-based and stereovision camera-based techniques. Moreover, it is not only cost effective but also it benefits from zoom lenses that collect video images from a distance. Even though environmental conditions such as illuminations may affect the performance of 3D skeleton extraction, post image processing enables us to obtain clear images even in a noisy environment. From previous studies that investigated the

accuracy of this approach, about ±10 cm of errors in body length and up to 20 deg of errors in joint rotation angles have been reported [106, 107]. These errors result from either incorrectly detected joint locations or inaccurate camera calibration process. Especially, the performance of this approach is significantly affected by frequent self-occlusions of the forearm, such as elbows and hands, which led to larger errors.

2.4.2 Angular Measurement Techniques

Angular measurement sensor-based approaches directly measure joint angles using sensors attached to specific body joints without the need for any mathematical transformation in space or time. Examples of sensors include goniometers and strain gauges.

Goniometers

Goniometers have been used to measure joints' range of motion. Traditional goniometers were made of a mechanical compass that measures the static relative angle between two body segments [117]. Modern goniometers are made of an electrical compass (potentiometer-based) which can measure static and dynamic relative angles [16, 117]. The potentiometer changes its resistance with the rotation of the two body segments connected to it. The principle of operation is that the voltage drop (V) across the potentiometer due to a constant electric current (I) passing through it will depend on the resistance (R) following

Ohm's law:

$$V = I \times R$$

Calibration of the potentiometer (goniometer) from 0 deg to a full range of motion is conducted once to produce a calibration chart that describes the relationship between the change in joint angle and the measured voltage. The use of potentiometer allows for detection of rotary motion as well as for placement of the sensor at the center of joint rotation.

Strain gauges

Strain gauges work on the same principles as goniometers except that the sensing element in a strain gauge responds to translation (change in length (ΔL)) represented as change in resistance (ΔR)

$$\frac{\Delta R}{R} = \frac{\Delta L}{L}$$

Measuring the joint angle depends on the placement of the strain gauge with respect to the axis of joint rotation [118]. Misalignment can produce significant errors due to the complexity of placing a translational sensor to detect rotatory motion [119].

2.5 Fatigue Detection

Muscles serve as the actuators of the neuromusculoskeletal system. In the rehabilitation process, it is important to monitor the level of fatigue of the musculoskeletal system, which provides objective feedback to the health professional. In ergonomics, fatigue may be linked to productivity and quality deficits, as well as musculoskeletal disorders, in the longer term [120].

The action potential generated by motor units (MU) initiates contraction forces that form, in aggregate, the muscle force. Indwelling electromyography detects the action potential of one or a few motor units. Surface EMG aggregates the action potentials contained in the muscle volume between two electrodes.

Although surface EMG is less invasive than indwelling EMG, the signal obtained using surface EMG cannot be used directly. Also, the surface EMG signal undergoes filtration and is subject to artifacts due to the presence of skin tissue and body fat between the muscle and surface electrodes. It has to go through multiple stages of signal processing before it can be used to study the muscle condition. Hence, signal processing is essential to the use of EMG signals [121]. Nevertheless, EMG has been used for the last six decades to study the relationship between muscle force and action potential. It enables researchers to investigate the characteristics of the neuromusculoskeletal system including muscle fatigue.

Indwelling EMG has been used to obtain detailed information about MUs and their characteristics. It enables researchers to draw conclusions about abnormalities of MUs at a central level [122]. De Luca [121, 123] used surface EMG to detect fatigue in the lower back. Gerdle et al. [124] used surface EMG to detect fatigue in thigh muscles; they used EMG mean frequency (MNF) and amplitude RMS as fatigue indices. Tsai et al. [125] used joint torque measurement as an indicator of fatigue for the shoulder joint. Ebaugh et al. [126] used the mean power frequency of raw EMG signal as an indicator of fatigue in the shoulder muscle. While it is a simpler alternative to indwelling EMG, it measures more fibers with the resulting signal reflects the average muscle state, since surface EMG measures the aggregate of action potentials from multiple MUs, the number of muscles fibers under testing depends on the size, location, and spacing between two electrodes.

A less intrusive alternative to EMG measures the exerted force or torque across a joint since it does not require the use of electrodes. This method takes into account the sum of forces exerted by individual muscles recruited to perform a task. It monitors the state of the dynamic link between two body segments. For example, Bini et al. [127] used this approach to investigate fatigue effects in the lower limb during cycling. While EMG signals are not collected explicitly, in this case, it is assumed that the forces they produce serve as indicator of their states.

At a higher level, the kinematics of body segment motions resulting from those forces

and torques represent easier and less cumbersome signals to collect and monitor. In this case, kinematics serve as the output of a dynamic system controlling body segment motions while muscle forces serve as the input. Therefore, the output kinematics can be used as an indicator of the state of the input forces and the underlying force producing muscles.

Chapter 3

Comparison of Direct and Indirect Motion Measurement Techniques

This chapter describes the result of an experiment to compare the accuracy of three indirect measurement techniques (vision-based motion capture techniques) and one direct measurement technique (angular measurement sensor-based). The techniques are RGB-D sensor-based, stereovision camera-based, multiple camera-based, and an optical encoder (a potentiometer-based electrogoniometer).

3.1 Methodology

Vision-based motion capture and an angular measurement sensor-based techniques were tested in two independent testing sessions as shown in figure 3.1. An exoskeleton is used to align the optical encoder with the knee flexion axis of rotation. The straps used to attach the exoskeleton to the lower limb were indistinguishable from the subject's clothes and skin. As a result, they could affect the performance of image processing for the vision-based approaches, especially the multiple cameras-based approach that tracks body joints using color information. To avoid this, the angular measurement sensor-based approach was tested in a separate session from the vision-based approaches.

Figure 3.1 shows experimental conditions for each testing session. In the session for vision-based approaches, shown in figure 3.1, three image sensors were located in front of a subject to collect 2D or 3D images from a front view. The Kinect™ that has 640×480 resolution with 30 fps, Bumblebee XB3™ stereovision camera that has 320×240 resolution with 10 fps, and 3D camcorder that has 1920×1080 resolution with 29 fps were positioned 4, 6 and 8 meters away from the subject, respectively. The positions of the Kinect™ and Bumblebee XB3™ were determined based on the optimal operating distance proposed by their manufacturers. They were placed at the border of their manufacturer's suggested distance to allow for a limit test. As the 3D camcorder has zoom lenses, its position was

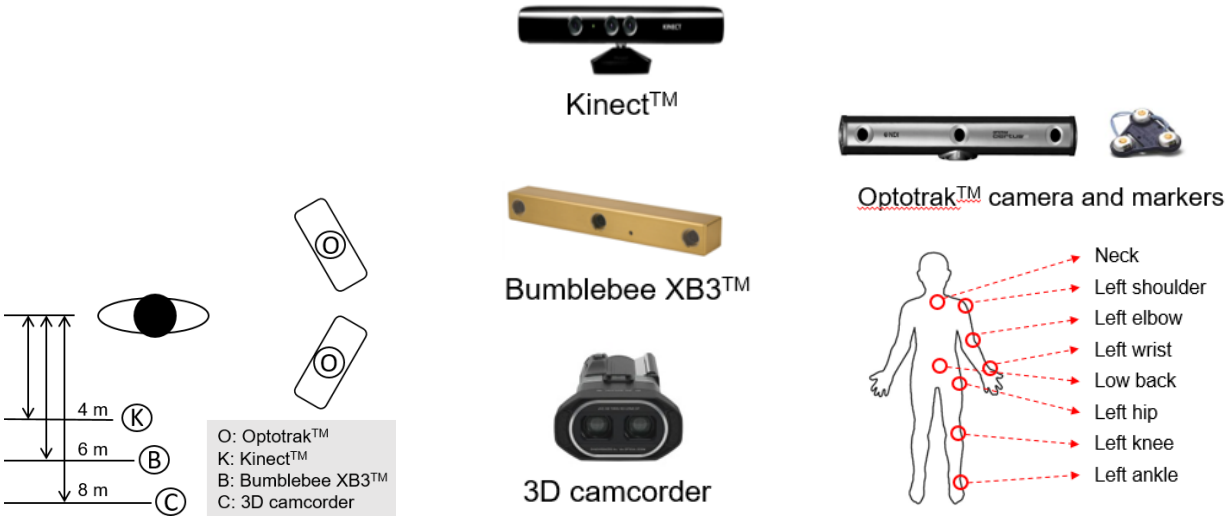

(a) Test setup. (b) Types of camera. (c) Reference measure.

Figure 3.1: Test condition for indirect measurement techniques.

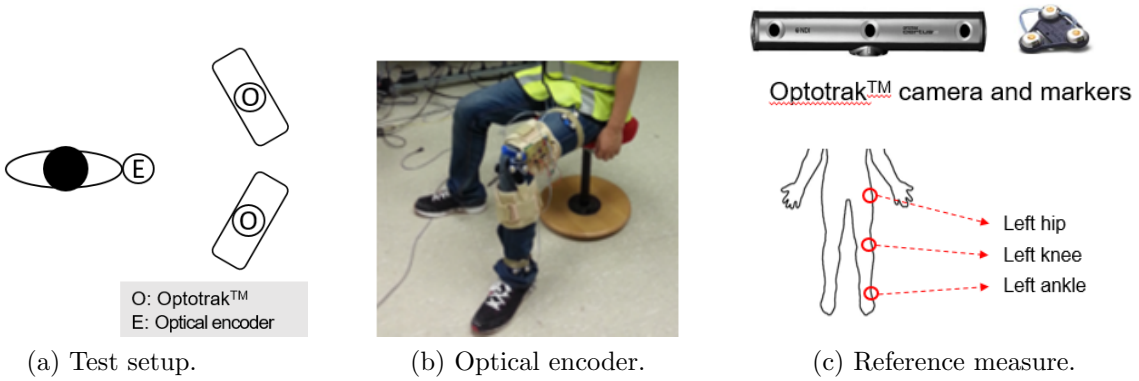

(a) Test setup. (b) Optical encoder. (c) Reference measure.

Figure 3.2: Test condition for direct measurement techniques.

Figure 3.3: Experimental setup

selected to obtain a clear view of the subject's whole body. Motion data obtained from Optotrak™ system served as a ground truth. The Optotrak™ uses active markers attached on the center of body joints to track body motions. If the markers are captured by at least one of the cameras, the system can provide accurate 3D positions of the markers with an accuracy of up to 0.1 mm. The markers were attached to the subject's trunk and left side body joints, including neck, low back, shoulder, elbow, wrist, hip, knee and ankle joints. In addition, the markers' attachment served in securing the participant's clothing in place to minimize signal noise. Two Optotrak™ cameras were positioned to the left side of the subject to prevent possible data loss due to markers' occlusions.

In the angular measurement sensor-based session test, shown in figure 3.2, the optical encoder that has 550 samples per second was positioned across the left knee to measure knee-included angles, the optical encoder was placed using a specially designed exoskeleton to reduce the effect of soft tissue movements. The system uses an optical encoder placed noninvasively along the axis of the joint rotation, the knee in joint in this case. The optical encoder [128] is mounted to an exoskeleton, an off-the-shelf knee brace (Flexlite hinged knee support). The brace as shown in figure 3.4 has two axes, one aligned with the thigh and the other is aligned with the shank. The optical encoder is inserted at the intersection of these two axes. This configuration allows the brace to reduce knee motions to a simple hinge joint rotation that follows knee flexion. The optical encoder contains a rotating and

a fixed part. The fixed part is rigidly attached to one of the brace arms, while the moving part is fixed to the other arm. Figure 3.4 shows the brace configuration.

The sensor system is controlled by a PIC18F46J50 microcontroller from Microchip Company. The controller receives the two signals from the encoder and saves them temporarily in the buffer before sending them into an SD card attached to the circuit. The data is stored in the SD card for later processing to obtain the results. The system runs on 550 sample/s sampling rate. The system runs on a 9V battery with a voltage regulator to supply the components with 5 and 3 volts.

Data transmission from the sensor to the storage unit is performed in two steps, one from the sensor to microcontroller the second is from the microcontroller to SD card (storage unit). The system includes a mini USB interface that provides the ability interface the PC to the sensor system.

With the rotation of the knee, the brace arms follow the motion of the shank and thigh. Similarly, the encoder rotates mimicking knee flexion and yielding a direct measurement of the knee flexion angle. To obtain ground truth angles, active markers were attached to the left hip, left knee and left ankle joints. Two Optotrak™ cameras were also positioned to the left side of the subject. In each session, subjects' motion was simultaneously recorded with these devices. For the synchronization of motion data, the subject was asked to hold a T-pose at the beginning of the recording. Data synchronization was manually performed

Figure 3.4: Configuration of the sensor system attached to the knee joint

by identifying the T-pose frame across all measurement techniques.

Testing Tasks

To compare the accuracy of motion data for diverse tasks, one male subject simulated three types of tasks, as shown in figures 3.5, 3.6, and 3.7, they are basic tasks with movements upper and lower body parts, lifting and placing, and walking. The basic tasks were designed to test the measurement accuracy for simple motions that involve movements of specific

(a) Arm extension.

(b) Arms abduction.

(c) Elbow flexion.

(d) Back bending.

(e) Twisting.

(f) Knee flexion.

Figure 3.5: Basic motion test.

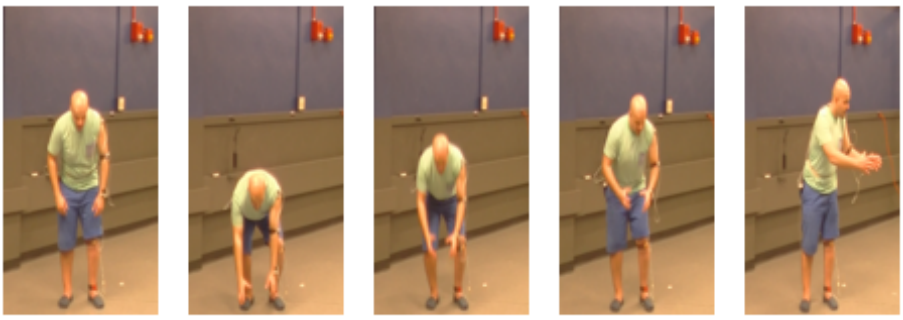

Figure 3.6: Lifting and placing task

Figure 3.7: Walking task

body parts.

Those include arm extension and abduction, elbow flexion, back bending, twisting, and knee flexion, which are also common motions in manual work such as construction. A lifting and placing task was selected for motions involving coordinated body movements. Specifically, the subject was asked to simulate the lifting task by lifting an imaginary object from the ground and placing it to the side. Lastly, a walking task was intended to test the measurement accuracy for rapid repetitive movements. To perform identical tasks for two independent sessions, the subject was asked to practice the task in question for several times before recording two the test sessions.

Accuracy Metrics

As measures of motion data accuracy for vision-based motion capture techniques, previous studies have used 3D positions of body joints' centers, body link lengths, or joint rotation angles [60, 104, 106, 107]. However, due to the difference in body models used in each vision-based approach, the use of these measures may lead to bias in accuracy comparison. For example, joint locations and corresponding body link lengths in a multiple cameras-based technique can be calculated based on the subject's measured joint center locations. On the other hand, the RGB-D sensor-based and stereovision camera-based techniques capture motions by matching 3D point clouds with a pre-defined body model, and thus the body link length from the captured motion data is affected by the anthropometric mismatch

between the model and subject. Also, while both RGB-D sensor-based and stereovision camera-based approaches provide motion data in a BVH file format that defines body postures using joint rotational angles, these angles are not available in the motion data from the multiple cameras-based technique used in this test [106, 107].

To address this issue, new body angles were defined, which can be measured by all vision-based techniques as shown in figure 3.8. Specifically, the body angles of each body part were defined as the angles between the vector along the body segment and the vertical vector. For example, the upper arm vector is obtained using 3D shoulder and elbow locations, thus, the angle between the upper arm vector of and the vertical vector (y-axis) is calculated as an upper arm (shoulder) angle. The other body angles such as forearm (elbow), trunk flexion, upper leg (hip) and lower leg (knee) angles are calculated using the same method. However, the trunk axial rotation angle that indicates the twisting angle was computed by using shoulder and hip vectors that were projected onto the $x-y$ plane. As the motion data from the three vision-based techniques and OptotrakTM provides 3D locations of body joints, all these angles can be calculated using vectors defined by two selected 3D joint locations, enabling accuracy comparison.

To measure the accuracy of body angles from an angular measurement sensor-based techniques, knee-included angles directly obtained from the optical encoder were compared with the angles determined by 3D locations of markers attached to the hip, knee and ankle

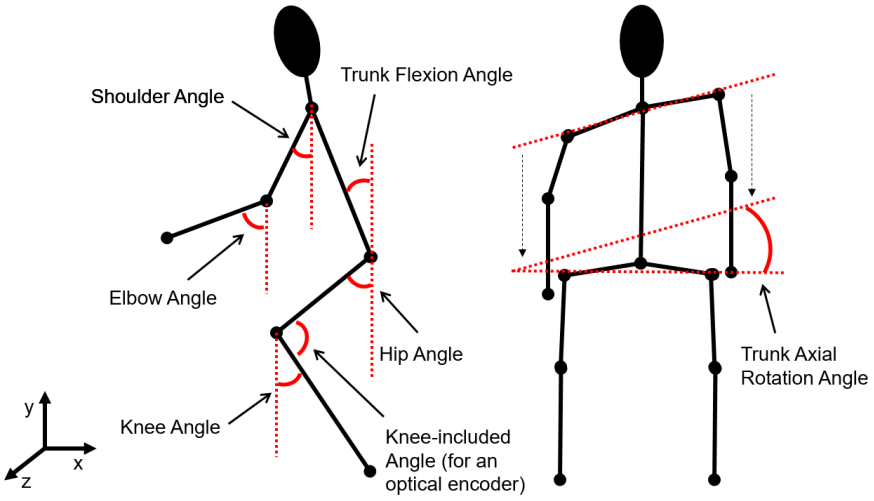

Figure 3.8: Body Angles to be Compared.

joints. Ground truth body angles were calculated based on 3D marker positions from Optotrak™. The markers were attached to the skin near the joints, not the centers of body joints. As a result, body angles from Optotrak™may slightly differ from the angles from vision-based and angular measurement sensor-based techniques. To adjust possible discrepancies, the body angles were calibrated using the angles from a T-pose. Also, the body angles from each approach were smoothed using a Savitzky-Golay filter [129] that has been widely used for post processing of motion data [130].

3.2 Results

3.2.1 Vision-based techniques

Figure 3.2.1 shows plots of body angles obtained from vision-based motion capture techniques during one cycle of various basic tasks. Through the visual investigation, it was found that overall body angles from each approach were closely matched with body angles from an Optotrak™, while back (flexion and twisting) and hip angles, figures 3.9d,3.9e, and 3.9f, from a multiple camera-based techniques showed discrepancies during the middle of the tasks.

For the quantitative assessment during these tasks, mean and standard deviation of absolute errors (MAEs and S.D. of AEs), and maximum and minimum errors (MAX and MIN) in body angles between three different techniques and an Optotrak™were calculated as shown in table 3.1 The RGB-D sensor-based captured the most accurate (4.2 deg of average MAEs) and reliable (2.8 deg of average S.D.) results for all body angles. The stereovision camera-based technique also provided relatively accurate motion data, resulting in 6.2 deg of MAE, but showed higher variations (4.2 deg of average S.D.) than an RGB-D sensor-based approach. The least accurate results (11.6 deg of average MAEs) were obtained from a multiple camera-based approach, especially due to relatively larger errors in lower arm (16.2 deg of MAEs), truck flexion (12.5 deg of MAEs) and trunk rotation

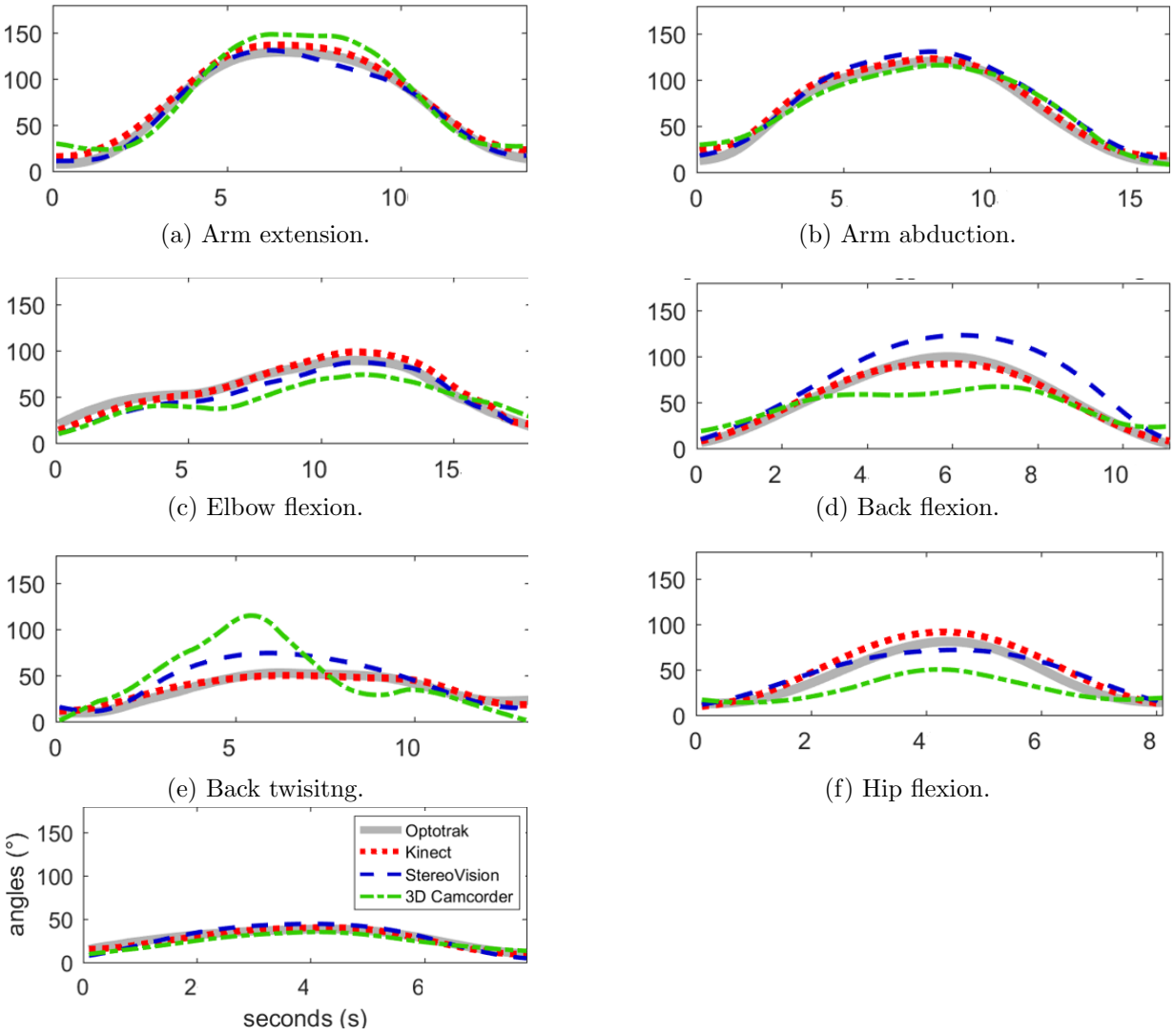

(a) Arm extension.

(b) Arm abduction.

(c) Elbow flexion.

(d) Back flexion.

(e) Back twisitng.

(f) Hip flexion.

(g) Knee flexion.

Figure 3.9: Comparison of body angles from different vision-based motion capture techniques during basic tasks.

Table 3.1: Accuracy of body angles from vision-based techniques during basic tasks

Body Angles	**Metrics**	**RGB-D Sensor (Kinect™)**	**Stereovision Camera (Bumblebee XB3™)**	**Multiple Camera (3D Camcorder)**
Arm				
Extension	MAE	5.9	3	11.3
	S.D. of AE	2.5	2.6	6.8
	MIN/MAX	-9.9 – -0.6	-3.2 – 9.9	-22.0 – 12.0
Abduction	MAE	4.7	8.2	7.6
	S.D. of AE	2.3	3.8	4.2
	MIN/MAX	-11.1 – -1.9	-14.3 – -0.3	-16.8 – 7.6
Elbow				
Flexion	MAE	4.9	8.1	16.2
	S.D. of AE	3.4	4	4.2
	MIN/MAX	-9.8 – 8.6	-2.7 – 14.0	10.1 – 24.5
Back				
Flexion	MAE	2.5	15.5	12.5
	S.D. of AE	2.1	11.2	12.5
	MIN/MAX	7.6	0	39
	MIN	-3.9	-34.3	-19.7
Twisting	MAE	3.1	11	21.9
	S.D. of AE	1.9	8.6	18.5
	MIN/MAX	-6.5 – 4.6	-23.8 – 8.6	-64.6 – 22.5
Leg				
Hip flexion	MAE	5.4	4.3	9.8
	S.D. of AE	5.5	4.6	12
	MIN/MAX	-13.7 – 3.3	-14.0 – 9.3	-4.9 – 32.4
Knee flexion	MAE	1	2.4	2.7
	S.D. of AE	1.1	2.6	2.8
	MIN/MAX	-1.7 – 4.1	-6.5 – 7.6	-3.3 – 8.1
Average MAE		**4.2**	**6.2**	**11.6**
Average S.D.		**2.8**	**4.4**	**8.1**

(21.9 deg of MAEs) angles than other body angles.

Figure 3.2.1 shows body angles from vision-based techniques during one cycle of a lifting and placing task. Even for a complex task that involves simultaneous total body motion, all the approaches provided robust body angle measurements for all body parts. Unlike basic tasks, no major discrepancies in body angles from a multiple cameras-based technique were observed.

Average MAEs during a lifting and placing task were 6.5 (RGB-D sensor-based), 6.6

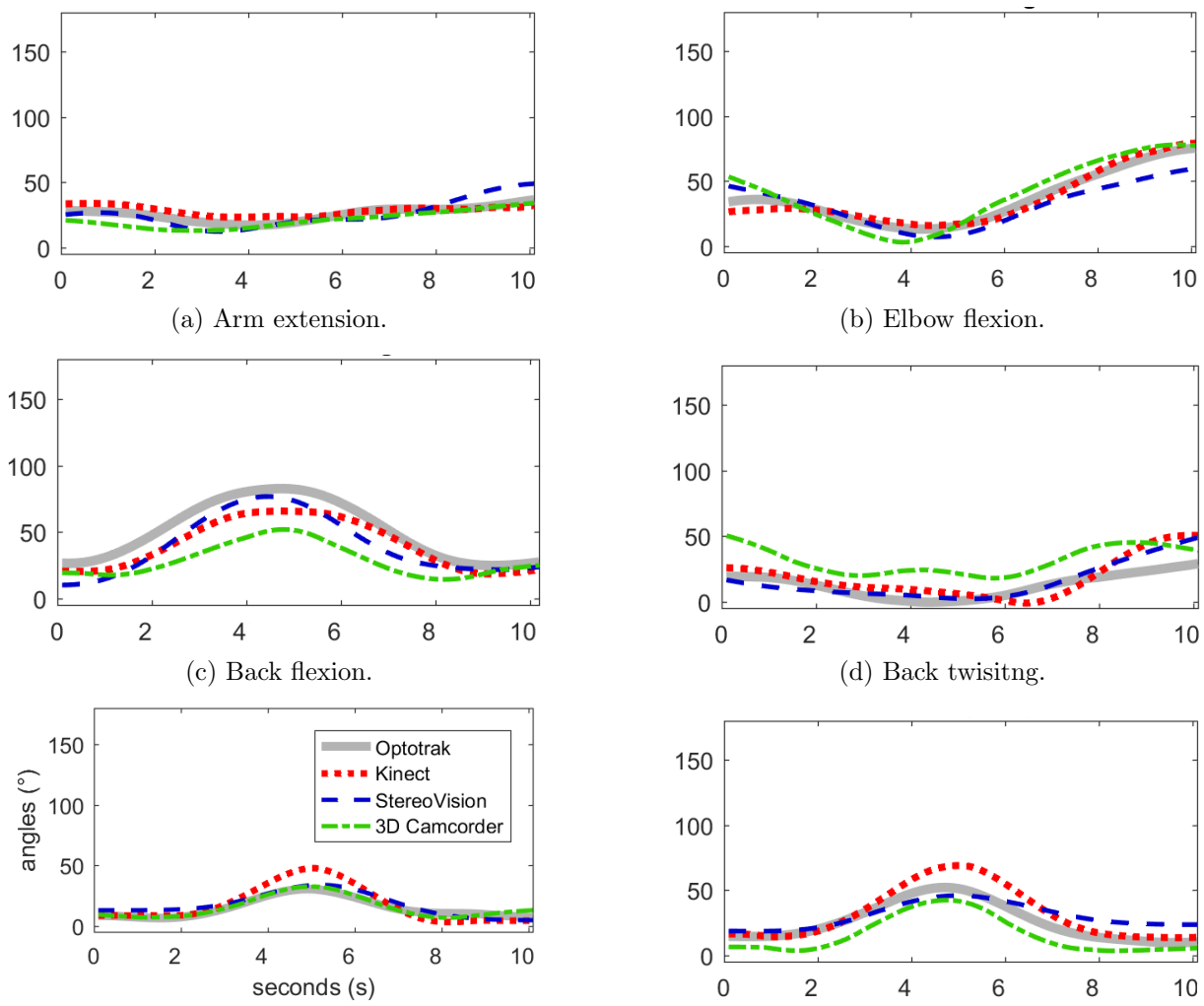

(a) Arm extension.

(b) Elbow flexion.

(c) Back flexion.

(d) Back twisitng.

(e) Knee flexion.

(f) Hip flexion.

Figure 3.10: Comparison of body angles from vision-based techniques during lifting and placing task.

Table 3.2: Accuracy of body angles from vision-based techniques during lifting and placing task

Body Angles	**Metrics**	**RGB-D Sensor (Kinect™)**	**Stereovision Camera (Bumblebee XB3™)**	**Multiple Camera (3D Camcorder)**
Arm extension	MAE	3.5	4.6	4.4
	S.D. of AE	2.4	3.8	3.3
	MIN/MAX	-6.3 to 4.4	-13.1 to 6.5	0.3 to 10.4
Elbow flexion	MAE	3.6	7.6	7.5
	S.D. of AE	1.9	4.7	3.6
	MIN/MAX	-4.9 to 8.3	-12.1 to 16.2	-19.3 to 11.1
Back Flexion	MAE	10.3	11	22.7
	S.D. of AE	5.1	5.2	11.2
	MIN/MAX	2.9 to 16.9	3.1 to 18.4	2.2 to 35.5
Back twisting	MAE	8.4	5.5	18.8
	S.D. of AE	6.2	5.2	4.8
	MIN/MAX	-23.4 to 11.3	-20.0 to 7.2	-31.1 to -10.5
Hip flexion	MAE	6.9	7.1	10.3
	S.D. of AE	6.2	4.7	2.7
	MIN/MAX	-19.4 to 1.5	-13.9 to 7.0	4.6 to 14.9
Knee flexion	MAE	6	4	1.5
	S.D. of AE	5	1.8	1.4
	MIN/MAX	-17.5 to 7.2	-6.7 to 4.0	-6.1 to 3.7
Average MAE		**6.5**	**6.6**	**10.9**
Average S.D.		**4.5**	**4.2**	**4.5**

(stereovision camera-based), and 10.9 (multiple camera-based) deg, showing similar errors in body angles during basic tasks, table 3.2. Both RGB-D sensor- and stereovision camera-based showed robust results in this task, even though errors in body angles in the RGB-D sensor-based were slightly high. Again, in motion data from a multiple camera-based, larger errors in back (torso flexion and rotation) angles were observed while upper arm angles were relatively accurate.

Finally, the walking task showed higher discrepancies in body angles from all vision-based as shown in figure 3.2.1. Motion data from the RGB-D sensor- and multiple camera-based induced similar errors (7.1 and 11.0 deg of average MAEs, respectively) with other

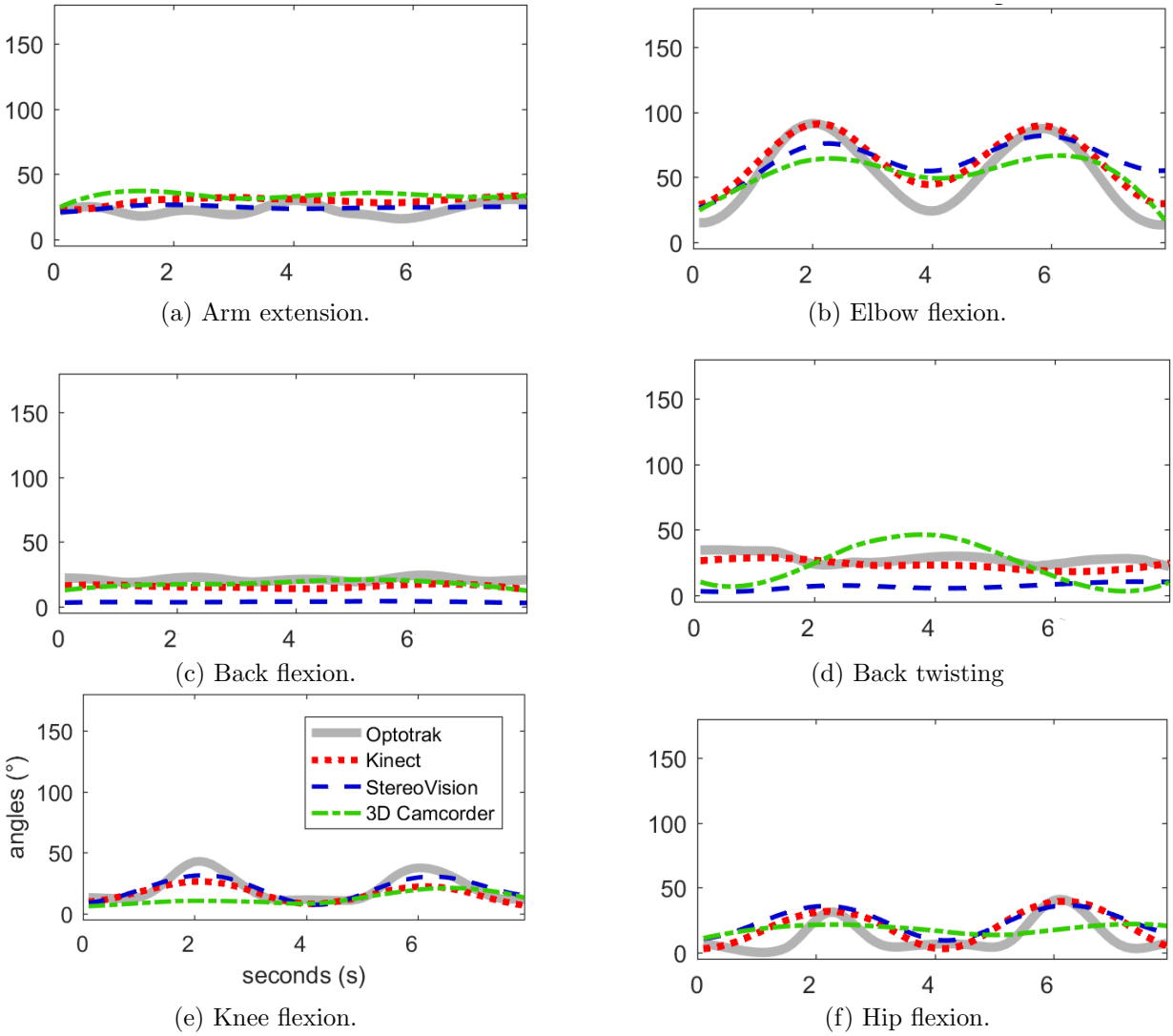

(a) Arm extension.

(b) Elbow flexion.

(c) Back flexion.

(d) Back twisting

(e) Knee flexion.

(f) Hip flexion.

Figure 3.11: Comparison of body angles from vision-based techniques during walking task.

tasks while a stereovision camera-based approach showed the largest errors (12.6 degrees of average MAEs) among three tasks, table 3.3.

Table 3.3: Accuracy of vision-based motion capture techniques during walking task

Body Angles	**Metrics**	**RGB-D Sensor (Kinect™)**	**Stereovision Camera (Bumblebee XB3™)**	**Multiple Camera (3D Camcorder)**
Upper Arm	MAE	7.1	4.5	10.9
	S.D. of AE	4	2.3	5.5
	MIN/MAX	-13.3 to 1.8	-8.7 to 6.5	-19.3 to -2.0
Lower Arm	MAE	10.7	15.9	15
	S.D. of AE	6.3	11.6	7.7
	MIN/MAX	-20.6 to 1.1	-41.8 to 17.1	-25.4 to 28.0
Back Flexion	MAE	5.4	17.3	3.5
	S.D. of AE	1.5	1.4	2.2
	MIN/MAX	2.3 to 7.9	15.0 to 20.4	-1.7 to 9.4
Back Axial Rotation	MAE	4.8	21.3	15.3
	S.D. of AE	4.8	5.3	8.1
	MIN/MAX	-24.4 to 8.8	14.6 to 32.0	-18.6 to 27.9
Upper Leg	MAE	8.8	12.1	11.6
	S.D. of AE	6.6	7.2	5.5
	MIN/MAX	-21.2 to 3.8	-27.3 to 4.9	-18.9 to 23.1
Lower Leg	MAE	5.6	4.2	9.7
	S.D. of AE	5.1	2.7	8.9
	MIN/MAX	-4.3 to 16.6	-6.9 to 11.6	-5.0 to 32.5
Average MAE		**7.1**	**12.6**	**11**
Average S.D.		**4.7**	**5.9**	**6.3**

3.2.2 Angular measurement sensor-based technique

Figure 3.12 shows plots of knee-included angles measured using an optical encoder and an Optotak™during three tasks. Note that among basic tasks; only the knee-bending task was tested because the sensor was configured to measure knee flexion angle which is constant in the other basic tasks. Two plots almost matched each other, indicating an accurate angular measurement of an optical encoder for all three tasks. However, small discrepancies were observed at the beginning and end of the cycle of knee-bending, and lifting and placing tasks.

A MAE for knee flexion angles obtained from the optical encoder was 2.9, 3.8 and 3.0

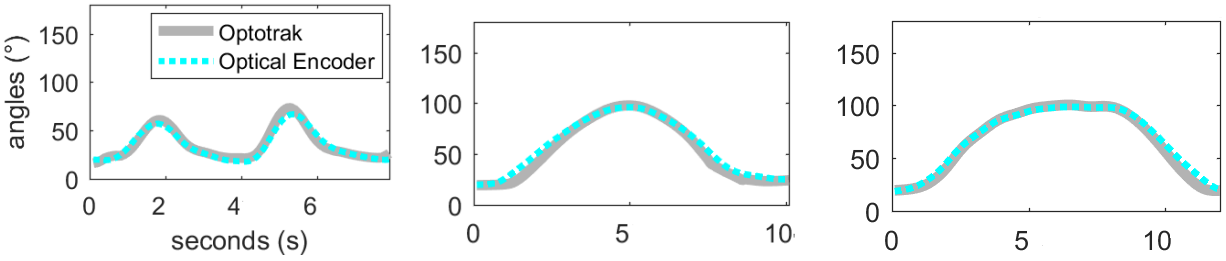

(a) Walking. (b) Lifting. (c) Knee bending.

Figure 3.12: Comparison of Knee flexion Angles obtained by angular measurement sensor-based during three tasks.

Table 3.4: Accuracy of an angular measurement sensor-based techniques during three tasks

Body Angles	Metrics	Basic Task	Lifting and Placing Task	Walking Task
Knee flexion	MAE	2.9	3.8	3
	S.D. of AE	2.7	3.1	2.1
	MIN/MAX	-10.1 to 2.0	-10.7 to 1.8	-5.6 to 8.8

deg for the three tasks, respectively, table 3.4. Compared with the RGB-D sensor-based that showed the most accurate measurements for hip and knee angles (1.0–8.8 degrees of MAEs) among vision-based techniques, this approach provided the most accurate and reliable angular measurements across all tasks.

3.3 Discussion

Specifications and accuracies of three vision-based motion capture techniques and the optical encoder are summarized in table 3.5. The experimental tests in the previous section

presented 5.9, 8.5, 11.2 and 3.2 deg of average MAEs for the RGD-D sensor-based, the stereovision camera-based, the multiple camera-based, and the optical encoder, respectively. The motion capture performance of each approach relies on the specifications of devices, such as types of raw data, resolution, and fps. For better decisions on appropriate uses of these approaches in construction, it is important not only to compare the accuracy but also to understand comparative advantages and limitations.

Among vision-based techniques, the RGB-D sensor-based showed the most accurate and reliable results for all three tasks as it uses data-rich 3D images and has a high resolution and frame rate. It is also expected that rapid technological development of this technique will enable us to collect more accurate and reliable 3D point cloud data, contributing to the improvement of motion tracking performance. Despite the robust performance of this approach, its short operating range (less than 4m) and sensitivity to sunlight limit its application to confined and indoor areas.

Alternatively, the stereovision camera-based can be a practical solution due to its ability to collect 3D images at both indoor and outdoor conditions and its longer operating range. The accuracy of body angles from this technique was not significantly different from the RGB-D sensor-based, excluding the walking task. Considering that walking involves more rapid movements than other tasks in this test, it was likely that the low frame rate (8-10 fps) of the stereovision resulted in tracking errors of certain body parts (such as upper

Table 3.5: Comparison of specifications and accuracies of vision-based motion capture techniques

Performance		**RGB-D Sensor (Kinect™)**	**Stereovision Camera (Bumblebee XB3™)**	**Multiple Camera (3D Camcorder)**	**Optical Encoder**
Specifications	Raw Data	3D images	3D images	2D images	Body angles
	Operating Range	Less than 4m	Less than 10 m (unlimited with zoom lenses)	Unlimited with zoom lenses	Unlimited
	Resolution	640 × 480	320 × 240	1920 × 1080	–
	fps	30	8–10	29	550
Accuracy (MAEs)	Basic Tasks	4.2	6.2	11.6	2.9
	Lifting and Placing	6.5	6.6	10.9	3.8
	Walking	7.1	12.6	11.0	3.0
	Average	**5.9**	**8.5**	**11.2**	**3.2**

limbs) that moved quickly. As the frame rate of a stereovision camera is determined by the computational time for 3D reconstruction and the performance of hardware, the use of an advanced 3D reconstruction algorithm and a high-performance computer can achieve a higher frame rate that helps to reduce errors in motion data, particularly during tasks involving rapid body movements. The operating range of the stereovision camera-based is recommended to set by Bumblebee XB3™within 10 m as the quality of 3D point clouds is significantly affected by its distance from the subject. However, a binocular stereovision system theoretically works with any two 2D cameras that are separated by a short distance, and are mounted parallel to one another. As a result, this technique is flexible in terms of operating ranges if zoom lenses are used. Recently, a stereovision system with adjustable zoom lens control has been introduced [131], enabling more practical application of this

approach.

The multiple camera-based approach showed larger errors in body angles than the other two vision-based techniques. Both the RGB-D sensor-based and stereovision camera-based approaches benefit from 3D imaging hardware that provides richer information, such as, RGB pixel values and depth information on scenes. However, the multiple camera-based approach need to extract motion data by processing only 2D images that contain less information, such as, RGB pixel values. Inaccurate camera calibration process could also lead to errors in the 3D triangulation of body joints from two images. Considering these limitations, the multiple camera-based approach with about 10 degrees of error in body angles is promising. Despite relatively larger errors, a multiple camera-based approach has several competitive advantages from a practical point of view, compared to the other two techniques.

For example, as any type of ordinary cameras can be used to collect 2D images, additional investments in devices are not required. Due to the use of zoom lenses, its operating range is theoretically unlimited. Less sensitivity to rapid movements is another strength of this approach. In addition, there is room for further improvement if occlusion issues are handled. One of the reasons for the least accurate results from a multiple camera-based is that it showed relatively larger errors in the elbow, back flexion and back twisting angles than other body angles. As shown in figures 3.9c, 3.9d, and 3.9e, an elbow or a hip

was occluded by a lower arm or a torso (i.e., self-occlusions), which may lead to incorrect detections of these joints in a multiple camera-based. In these tests, a 3D camcorder was used to obtain two images from different views. As the distance between two lenses is very short (3.5 cm), both images are affected by self-occlusions. If two independent cameras are positioned away from each other, it could be possible to obtain at least one clear view of images, reducing errors due to self-occlusions.

The optical encoder provided accurate measurements for knee flexion angles across all types of tasks. Further, as these sensors are attached to body joints to directly measure joint angles, they can provide robust angular measurements for body joints with one degree of freedom under any condition. Although angular measurement sensors, such as, the optical encoder can be used for all body joints, the use of these sensors could be limited due to the need for straps or exoskeletons that may lead to interfering with on-going work. Instead, using angular measurement sensor-based for selected body joints can offset the limitation of vision-based approaches that are sensitive to self-occlusions.

However, soft tissue movements may result in errors in body angles from these sensors. For example, during the testing of this approach, small differences in knee-included angles were observed at the beginning and end of cycles, which can be attributed to soft tissue movements, especially when straps are not firmly secured to the leg. Securing straps firmly to the body to hold the sensor in position is an important factor to obtain accurate body

angles from the sensor [132].

3.3.1 Study limitations

The results of this study does not account for the differences in the body mases which can alter the results of indirect techniques and can increase soft tissue motion in direct techniques. This study was conducted in a controlled environment, aspect such as lighting and line-of-sight was controlled. This level of control is not found in construction sites, hence, these results might be different in a construction site.

3.4 Potential Applications in Construction

Vision and angular measurement sensor-based motion capture techniques investigated in this study are considered practical means of in-field motion capture, even though about 5–10 degrees of error in body angles from the vision-based and approximately 3 degrees of error from the angular measurement sensor-based still exist. In construction, tasks are performed in unstructured and varying environments, and thus work methods and postures are changing over time. Collecting motion data using these non-invasive and cost-effective approaches enable us to understand how workers interact with the environment at construction sites and to identify potential safety and health risks under given environments,

specifically when accuracies would not significantly matter such as rough postural assessment, time and motion study, and trajectory analysis.

These techniques can be used to specify the severity of working postures. Existing postural ergonomic risk assessment methods determine the level of ergonomic risks based on pre-classified postures through human observation [133]. Some methods such as Rapid Upper Limb Assessment (RULA) [51] and Rapid Entire Body Assessment (REBA) [134] require detailed segmentations of body postures according to body angles. For example, in RULA, trunk postures are categorized into four groups according to trunk flexion angles (0, 0–20, 20–60 and over 60deg). Body angles obtained from these techniques can be used for rough posture classification that is needed for postural risk assessments. Also, as continuously measured workers' motions during performing tasks is enabled, several in-depth motion analysis for understanding physical demands can be facilitated. Traditionally, pre-determined-motion-time-systems have been widely used to identify workloads during occupational tasks [135]. As these systems rely on human observations to describe workers' manual activities, significant human efforts are generally required. However, by using a time series motion data from the presented techniques, it is possible to accurately and automatically quantify motion-time values for these systems. In addition, trajectory analysis through in-field motion measurements helps to evaluate work efficiency, as well as the risk of ergonomic injuries. For example, shorter trajectories of body movements may

indicate more efficient movements of a human body, indicating smaller physical demands. Previous studies on movement patterns during occupational tasks found that a more 'dynamic' pattern of movements is believed to be associated with a lower incidence of WMSD development [136, 137]. Analysis of motion patterns and trajectories using vision-based motion data can broaden our understanding on the job from an ergonomic perspective.

In-field kinematic measurement using vision- and angular measurement sensor-based motion capture techniques also has great potential to be used for more in-depth analysis of physical demands such as biomechanical analysis, even though further improvement of motion data accuracy is required [56]. The biomechanical analysis aims to estimate musculoskeletal stresses as a function of motion and external force data [138, 139]. Previous biomechanical studies have relied on laboratory experiments to collect motion data using marker-based motion capture approaches, which can be replaced by in-field motion capture approaches that enable on-site biomechanical analysis. As an accurate measurement of all joint angles is necessary for reliable biomechanical analysis, further accuracy improvement of vision-based motion capture approaches is required.

However, the sensitivity of biomechanical analysis results to motion errors vary depending on body joints [140]. For example, Chaffin and Erig [140] found that an error of ± 10 deg in the limiting joint angles such as, knees and ankles could cause the biomechanical analysis results to vary up to $\pm 12\%$ during lifting, pushing and pulling tasks, whereas

errors in other joints could have little or no effect. This result indicates that some angular errors in body joints that do not involve forceful exertions are acceptable for biomechanical analysis while it is important to obtain accurate body angles for stressful body joints. So, complemented by relatively accurate angular measurement sensors such as optical encoders that are applied to the limiting joints, vision-based motion capture techniques enable researchers to perform biomechanical analysis without significantly sacrificing the reliability of biomechanical analysis.

3.5 Conclusion

This chapter describes the potential of vision-based and angular measurement sensor-based techniques as a means of measuring workers' motions. These techniques were compared through laboratory tests while performing three different types of tasks. The accuracy of these approaches was computed by comparing body angles from each approach and a marker-based motion capture. The comparison results indicated that the overall errors in body angles from vision-based approaches are ± 10 deg, while the optical encoder, that is one example of angular measurement sensors, can provide quite an accurate body angle measurements ± 3 deg for specific body joints with one degree of freedom. Moreover, self-occlusions and rapid movements are major factors that lead to errors in vision-based

techniques.

From a practical point of view, vision-based and angular measurement sensor-based have great potential as non-invasive motion data collection methods at construction sites. Even though several obstacles, such as a limited operating range (RGB-D sensor-based), low frame rates (stereovision camera) and occlusions (multiple camera-based) remain to obtain more accurate data from these approaches. Further algorithm refinements and hardware developments are expected to address these issues. The angular measurement sensor-based technique can provide robust measurements of specific joint movements, despite a small possibility of discomfort by attached sensors. Furthermore, combined with vision-based motion capture, the angular measurement sensor-based can enhance the accuracy of in-field motion measurements. Motion data from these techniques can be used for diverse in-depth analysis without sacrificing its reliability to better understand workers' physical demands during occupational tasks including construction. Also, understanding how workers behave under given working environments through kinematics measurements and analysis helps to ergonomically design automated machines and assistive robots, aiming at both reducing physical demands and enhancing workers' capabilities.

Chapter 4

Fatigue Detection Using Phase-Space Warping

4.1 Introduction

Time delay embedding was introduced in the 80s as a method to reconstruct inaccessible states of a dynamic system [141–143]. The method uses the time-history of a single accessible state in a coupled dynamic system to reconstruct the full system states. The time-history of the available state is delayed by 'an optimal' time step to reconstruct the other states. For example, when using time delay embedding one can measure the thigh displacement to estimate the other state variable of the lower limb dynamic system, such

as leg displacement.

Time delay embedding methods analyze the state variable time-history to determine the minimum system dimension that can describe its dynamics and the time delays corresponding to each of them. One method particularly searches for the dimension and time-delay that maximally fills the phase-space [142].

The reconstructed phase-space can then be used to track damage evolution. An approach to achieve this is phase-space warping (PSW) [144–146]. PSW uses the healthy system response to construct local maps in phase-space that describe the characteristics of the healthy system response. It then compares the actual system response in phase-space over time to the healthy local maps to extract a tracking metric for a slowly drifting inaccessible variable in the system.

PSW has been previously used to track changes in walking kinematics [147] and to investigate local muscle fatigue during sawing tasks using smooth orthogonal decomposition in upper extremity muscles [148]. A similar approach looked at the local state-space temporal fluctuation and used these fluctuations as a fatigue index during repetitive tasks [149].

In this chapter, a novel application of PSW to detect fatigue in the musculoskeletal system using time delay embedding is presented. Since muscle tissue undergoes mechanical degradation, cumulative fatigue, termed by Kumar [7], PSW is used to construct a

metric to track it. First, time delay embedding is used to reconstruct the dynamics of the musculoskeletal system. Second, the PSW method is used to extract a fatigue metric in the time domain. Implementing these methods allow for extracting a fatigue metric out of three types of signals: an invasive signal (i.e., EMG) and two non-invasive signals (i.e., kinematics and force).

4.2 Methodology

4.2.1 Kinematic experiment

Participants

Five male participants (average age 28.8 years$\pm$1.3(SD), height 172.82 cm $\pm$9.67(SD), weight 95.8 kg $\pm$6.9(SD)), with no injury history were recruited from the University of Waterloo student population to perform the kinematic experiments of this study.

Procedure

Kinematic signals were collected using a customized instrumented knee brace described in Chapter 3 and shown in figure 4.1. Participants were asked to walk on a treadmill (Horizon CT5.4, Horizon Fitness, WI, USA). A treadmill was chosen to provide an external pace

for the participant walking exercise. This eliminates the tendency of self-pace and self-regulation from the collected kinematic data.

Figure 4.1: Instrumented knee brace used to measure the knee flexion angle in sagittal plane

Participants were instructed to come to the laboratory 30 minutes prior to data collection, allowing for preparation of the knee brace. Each participant's left knee was fitted with the instrumented knee brace, figure 4.1, to measure the knee flexion angle in the sagittal plane. An initial experiment was conducted to measure each participant maximum walking speed (MWS), defined as the speed beyond which they would start running. It was

determined by asking the participant to walk on a treadmill while the operator increases speed gradually until the participant started running and recorded as

$$MWS = RS - 0.1km/h \tag{4.1}$$

where RS is the participant running speed. The average maximum walking speed of the participants was 4.54 km/h $\pm$0.61(SD).

During the experiment, the treadmill speed was increased from 0 to MWS instantaneously. Once the treadmill speed reached maximum walking speed, data collection commenced. The participants were asked to walk on the treadmill until they could no longer keep up with it, at which point the experiment was terminated.

Instrumentation

The knee angle was recorded using an untethered 'knee angle direct measurement system' shown in figure 4.1. The system measures the flexion angles using an encoder (Penny & Giles Company) placed at the intersection of the thigh and shank in the sagittal plane. The flexion angle is sampled and recorded through a custom made DAQ with an on-board SD memory card. The sampling rate is set to 500 Hz ($T_s = 2ms$).

4.2.2 Physiological experiment

Participants

Five male participants (average age 25 years ±5.59(SD), upper arm circumference 34.38 cm ±2.64(SD), height 176.72 cm ±4.22(SD), weight 74.8 kg ±11.22(SD)), with no injury history to their elbows, upper arm, and forearm, were recruited from the University of Waterloo student population to perform the physiological experiments of this study. Twenty-four hours prior to each test session, each participant was instructed not to consume alcohol and caffeine and to avoid exercise. Each participant provided informed consent to all experimental procedures, as approved by the University of Waterloo Office of Research Ethics.

Procedure

The exercises, shown schematically in figure 4.2, were chosen to cover a wide range of muscle fatigue processes. For example, a sinusoidal-shaped force profile has a slower rate of change in force compared to the other stepwise functions [150]. The session's force magnitude [151–153], cycle time [150, 154–156], and duty cycle [150, 156] were set in accordance with previous studies. These settings were selected since they have been demonstrated to induce fatigue over a 60 minute period [157, 158].

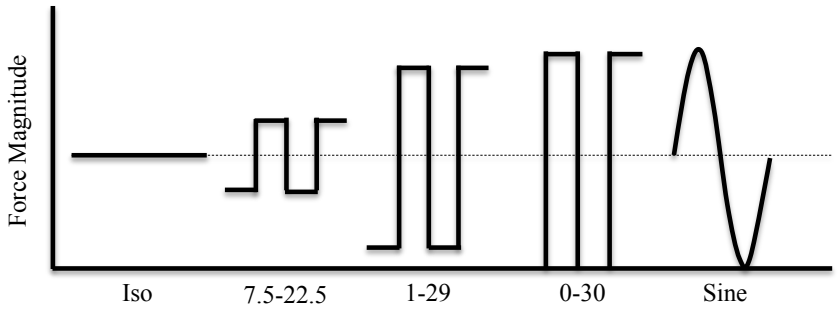

Figure 4.2: Schematic diagram for the Iso, 7.5–22.5, 1–29, 0–30, and Sine exercises, respectively, performed in the physiological experiment.

Five experimental exercises were performed by each participant. Across all exercises, participants exerted a mean force of 15 % maximum voluntary contraction (MVC) with a duty cycle set at 50% of a 6 s cycle time. The five exercises are:

- Iso: uninterrupted isometric elbow extension at 15 % MVC.
- 0–30: a stepwise elbow extension cycling between 0 and 30 % MVC.
- 1–29: a stepwise elbow extension cycling between 1 and 29% MVC.
- 7.5–22.5: a stepwise elbow extension cycling between 7.5 and 22.5 % MVC.
- Sine: a sinusoidal wave form with a peak of 30 % MVC.

The participant was asked to come to the laboratory a day before the data collection to get familiar with the experimental exercise and to collect an MVC. The MVC was

calculated as the average force during the middle 3 s of a 5 s exertion. These MVC forces were used to determine the absolute force required to achieve 15% MVC and 30% MVC for the five exercise conditions.

Each exercise condition consisted of a 10 minutes baseline activity followed by the exercise protocol, and then a 60 minute recovery period. The participants were instructed to exert forces during the exercise protocol for 60 minutes or until the participants could no longer match the force magnitude (exhaustion).

Continuous electromyography measurement was collected for the medial and lateral triceps muscles as well as the biceps muscle. At least seven days of rest, between sessions, was provided to minimize carryover effects between exercise conditions. Laboratory room temperature was kept between $22 - 24°C$. Figure 4.3 shows a participant equipped arm on the apparatus.

Data were sampled at a frequency of 2048 Hz using NAID Collection software (version 1.0.0.10, University of Waterloo 2001). Offline post-processing was conducted using Chart 4.0 (ADInstruments, Colorado Springs, CO, USA) and Mathematica 9.0 (Wolfram, Champaign, IL, USA).

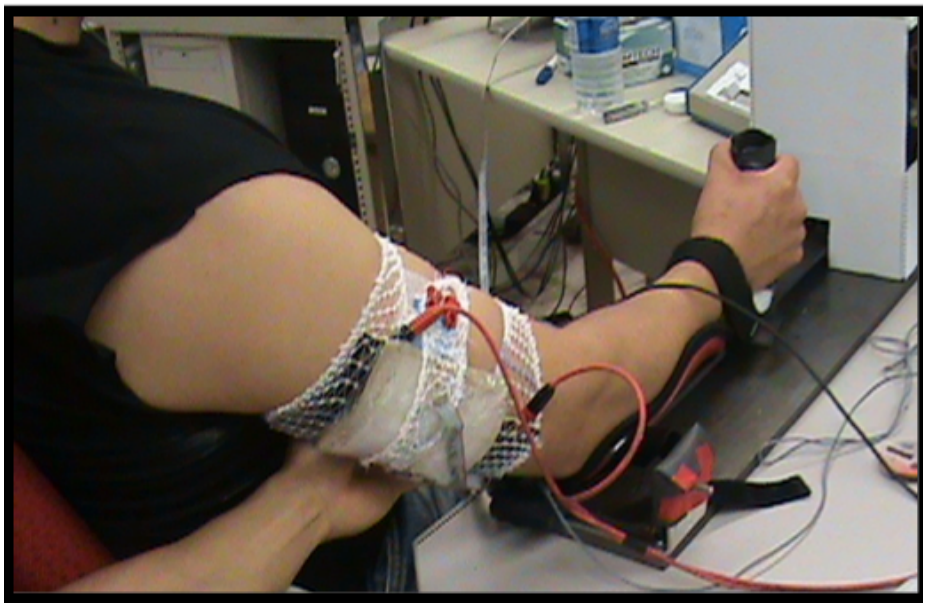

Figure 4.3: Elbow extension and EMG data collection from Triceps and Biceps muscles

Instrumentation

A custom fabricated apparatus, figure 4.3, was designed to support the arm. The apparatus allowed for modulating the exercise profile for isometric elbow extension. It also allowed for measurement of MVC and testing of contraction torque without removing the arm.

The system involves a brushless 200 VAC servomotor, custom-designed armrest, servo amplifier, and encoder. It is controlled by a programmable motion controller (DMC-1417, Galil Motion Control Inc., California). The servomotor was controlled using position and torque through Galil software. In addition to proprioceptive feedback, visual feedback was provided for the participant to maintain a fixed position. Counter-weights were added to

the apparatus to balance the weight at the beginning of each exercise.

Bipolar surface electrodes were used to collect EMG signals (Ag-AgCl electrodes, Ambu Blue Sensor N, Denmark). Electrodes were placed at the belly of the lateral triceps, medial triceps, and biceps brachii. Inter-electrodes distance was 20 mm. Hair was removed by razor and skin was abraded by ethanol and prepared with NuPrep Gel (Weaver and Company, CO, USA). EMG signals were collected using an eight channel data system (Bortec Octopus, Calgary AL; common mode rejection ratio > 115 dB; band-pass filter 10–1000 Hz) amplified with a gain of $1000, \pm 5$ V.

Although biceps brachii, unlike the triceps muscles, is not a major contributor to elbow extension [159], EMG signals were collected for all three muscles. Therefore, EMG signals for the biceps muscle served as a control case to examine whether the fatigue detection method proposed here can distinguish between the presence and absence of muscle loading and fatigue patterns in the EMG signals. DC offset was removed and the instantaneous root mean square (RMS) amplitude was calculated, normalized to the MVC exerted during baseline activity of that trial, averaged for a 30s window.

4.3 Analysis

4.3.1 Time Delay Embedding

Time delay embedding is used to reconstruct the phase-space of a coupled dynamic system using the sampled time-history of a system state variable $y(t)$, such as the knee flexion angle. It yields information about the minimum system dimension $d_\circ$ required to represent the coupled dynamic system; the lower limb kinematic chain in this case. The method calls for the determination of the optimal time delay $\tau_\circ$ of y required to reconstruct the state vector as:

$$\mathbf{y}(t) = \begin{Bmatrix} y(t) \\ y(t+\tau) \\ \vdots \\ y\big(t+\tau(d-1)\big) \end{Bmatrix} \tag{4.2}$$

The fill factor algorithm [142] was used to calculate $d_\circ$ and $\tau_\circ$. The algorithm uses the function

$$F(\tau) = \frac{\sum_{i=1}^{N_s} |Det[M_d]|}{N_s (y_{max} - y_{min})^d} \tag{4.3}$$

where $Det[M_d]$ is a measure of the hyper-area occupied by the orbit in phase-space, ob-

tained by calculating the determinant of d randomly selected vectors with the same base point, N_s is the number of random evaluations of the hyper-area, and y_{max} and y_{min} are the largest and smallest values of the state variable, respectively, recorded in the time series. It calculates $F(\tau)$ as a measure of the area occupied by orbits in the reconstructed phase-space of dimension d as a function of the delay time τ. The process is repeated as the number of dimensions d is increased.

The minimum number of dimension d_o is determined using the $F(\tau)$ curves and defined as the dimension beyond which the $F(\tau)$ curves do not add any new significant features as the dimension increases. In other words, no new maxima or minima in the curve, which is the $F(\tau)$ curves become essentially parallel to each other.

4.3.2 Phase-space Warping

PSW calls for distinction among three time-scales:

1. a sampling (fast) time-scale $\sim T_s$.

2. an averaging (intermediate) time-scale $\sim T_m$.

3. a tracking (slow) time-scale where muscle fatigue can be observed.

The initial M cycles of the signal $y(t)$ time-history are used as a reference set utilized to represent the system's healthy status. Local linear maps are constructed for populated areas of the phase-space. Each of the 'rested' return maps

$$\mathbf{y}_{n+1} = P(\mathbf{y}_n) \tag{4.4}$$

represents the healthy system return map at that point in phase-space [144]. The reference set size is chosen to be large enough to average out cycle-to-cycle differences, due to the stochastic nature of the neuromuscular system and non-stationarity. Moreover, it is chosen to be not too large to avoid contaminating the reference set with the fatigue onset. The rest of the time-history is divided into S snapshots each made of M cycles.

It is important to note that in equation (4.4), the map is not accounting for intrinsic physiological noise. That is because, in this analysis, it is assumed that there is an underlying deterministic process existing over the intermediate time-scale and a deterministic fatigue process existing over the slow time-scale. Also, there are stochastic noise processes existing in the fast time-scale. Moreover, there may be other un-modeled neuromuscular processes due to the central nervous system (CNS) that exist across all three time-scales. However, this analysis assumes that their effects are not dominant compared to those of the deterministic process.

The local linear map is composed of a parameter matrix $\mathbf{A}_n$ and a parameter vector $\mathbf{a}_n$ that describe the k$^{\text{th}}$ return of the state variable vector $\mathbf{y}_n$ according to:

$$\mathbf{y}_{(n+k)} = \mathbf{A}_n \mathbf{y}_n + \mathbf{a}_n \tag{4.5}$$

The map parameters $\mathbf{A}_n$ and $\mathbf{a}_n$, are calculated following the algorithm described in Chelidze et al. [144] from the matrices

$$\begin{aligned} \mathbf{Y}_n &= [\mathbf{y}_n^1 \quad \mathbf{y}_n^2 \quad \dots \quad \mathbf{y}_n^B] \\ \mathbf{Y}_{n+k} &= [\mathbf{y}_{n+k}^1 \quad \mathbf{y}_{n+k}^2 \quad \dots \quad \mathbf{y}_{n+k}^B] \end{aligned} \tag{4.6}$$

constructed out of the B nearest neighbors of the state variable vectors $\mathbf{y}_n$ and $\mathbf{y}_{n+k}$ in the reference set.

As muscles fatigue, the measured state variable vector represents a return map:

$$\mathbf{y}_{n+1} = \hat{P}(\mathbf{y}_n, \phi) \tag{4.7}$$

containing information about ϕ, a parameter representing muscle fatigue. Therefore, fatigue can be estimated as the difference between the rested return map prediction of the

k^{th} return and the fatigued return map:

$$e_{n+k} = ||\hat{P}(\mathbf{y}_{n+k-1}, \phi) - P^k(\mathbf{y}_n)|| \tag{4.8}$$

Alternatively, a fatigue tracking metric e_n can be calculated by comparing the k^{th} return predicted by the rested return map to the reconstructed state variable vector at that point in time:

$$e_{n+k} = ||\mathbf{y}_{n+k} - P^k(\mathbf{y}_n)|| \tag{4.9}$$

The fatigue metric is averaged out over each snapshot to reduce fast and intermediate time-scales noise. Therefore, the fatigue metric for snapshot j is evaluated as:

$$E_j = \frac{1}{NM} \sum_{i=0}^{NM} e_i \tag{4.10}$$

where $N = \lfloor \frac{T_m}{T_s} \rceil$.

4.4 Results

4.4.1 Kinematic experiment

Data collection sessions lasted an average of 7.41 minutes ±4.7(SD) at which point participants could no longer keep up with the treadmill 'subjective fatigue exhaustion.' The average gait cycle was estimated from the reference set as $T_m = 1.18s \pm .044(\text{SD})$.

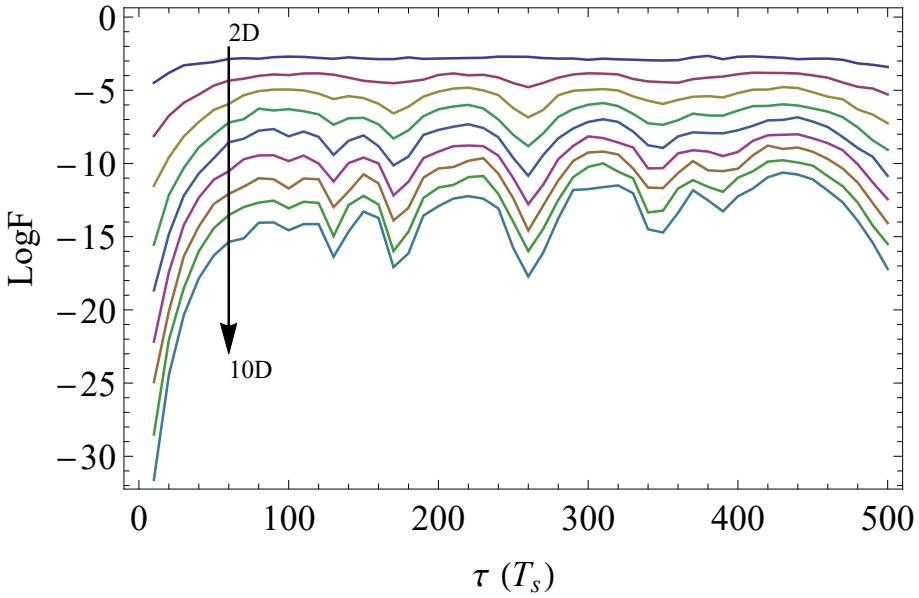

Figure 4.4: Log scale plot of the fill factor $F(\tau)$ as a function of the time delay for state variable vector dimensions in the range of d=2–10.

The time delay $\tau_\circ$ and minimum system dimension $d_\circ$ were determined using the fill factor algorithm discussed above. The fill factor curves Log$F$ vs. τ for the first participant are shown in figure 4.4, for state variable vector dimensions from $d = 2$ to 10 and time

delays in the range of $\tau = 1$–$500T_s$. Inspecting the fill factor curves for all participants, we observe that no new minima or maxima are added beyond $d = 5$, which indicates that the minimum dimension required to represent the coupled dynamic system, $d_\circ$, of the lower limb is five. The fill factor curve F vs. τ, shown in figure 4.5, is used to determine the optimal time delay $\tau_\circ$. By inspecting the curve, it was found that the first maxima occurs at $\tau_\circ = 100T_s$.

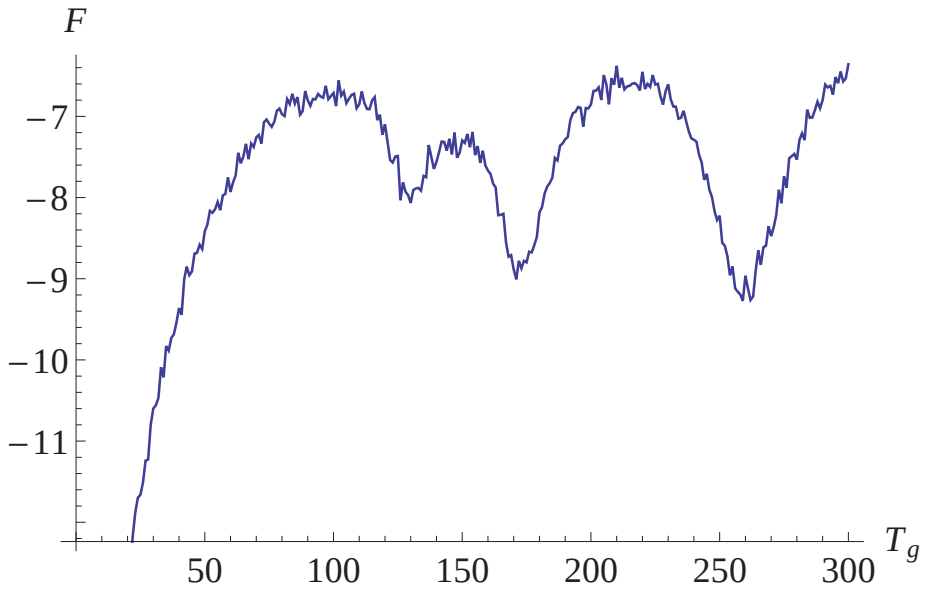

Figure 4.5: The fill factor F as a function of time delay τ for a state variable vector of dimension $d_\circ = 5$

.

The reference set was made of 24000 data points representing the first 48 seconds of the exercise and equivalent to 40 gait cycles. Each snapshot was made of $M = 10$ gait cycles. The number of nearest neighbors used to construct the local linear maps was set to $B = 15$.

The tracking function e_j was calculated for each snapshot including the reference set. The numerical values of e_j represent the average change of the gait orbit in the reconstructed phase-space.

The tracking metric e_j for all five participants is shown in figure 4.6 as a function of the normalized session time. It represents the lower limb health (fatigue) for each participant. Indications of fatigue appear progressively over the session time and a large change in the fatigue metric is observed towards the end of the session. Participants 2, 3, and 4 appear to temporarily recover in the second half of the session until they can no longer keep up with the treadmill speed. This may indicate deployment of different muscles to cope with fatigue. The average change in fatigue metric was 0.34 ± 0.17(SD).

4.4.2 Physiological experiment

All physiological data analysis was carried out on raw data, a sample is shown in figure 4.7, to avoid distorting the signal spectral content. Some participants were not able to complete the entire 60 minute exercise.

The reference set for physiological signals was made of the first 50000 data points representing the first 24 seconds of each exercise and equivalent to 40 exercise cycles. Each snapshot was made of $M = 10$ cycles. The number of nearest neighbors used to construct

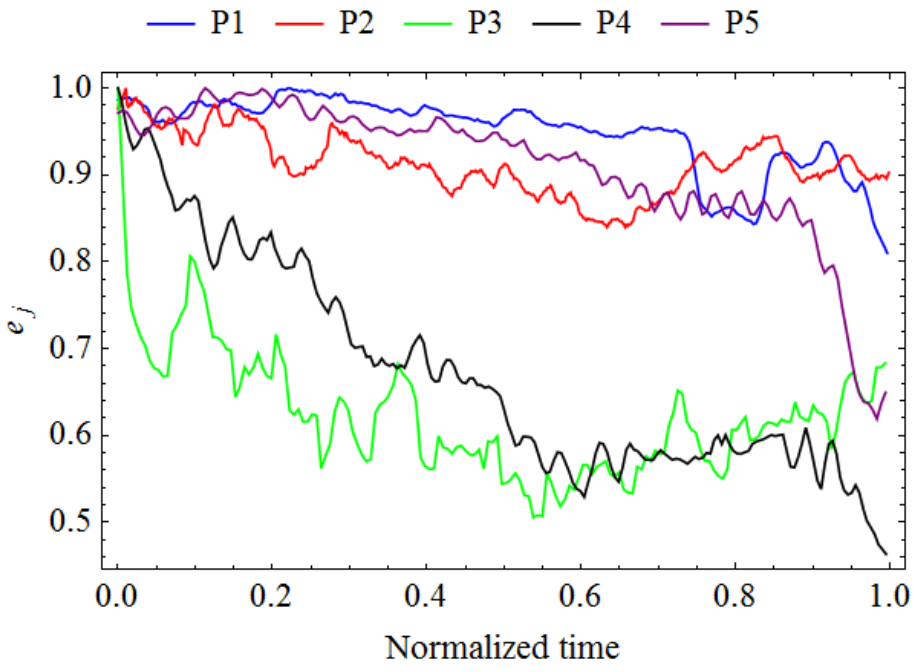

Figure 4.6: Fatigue indices of the lower limb E_j as function of normalized session time.

the local linear maps was set to $B = 300$. The use of a significantly lower number of nearest neighbors resulted in a singularity in the neighborhood matrices, equation (4.6), as a result of a loss in diversity of the neighborhood points.

The intermediate time-scale was set equal to exercise cycle period $T_m = 6s$. For the case of Iso exercise where no exercise cycle was applied, the intermediate time-scale was set equal to the average period of individual MU action potential $T_m = \frac{1}{25}$s [160, 161].

The FFT of the EMG signal in the initial 24 s, the reference set, for the five elbow exercises shows, a dominant peak in the frequency range 60–70 Hz, Table 4.1. This peak

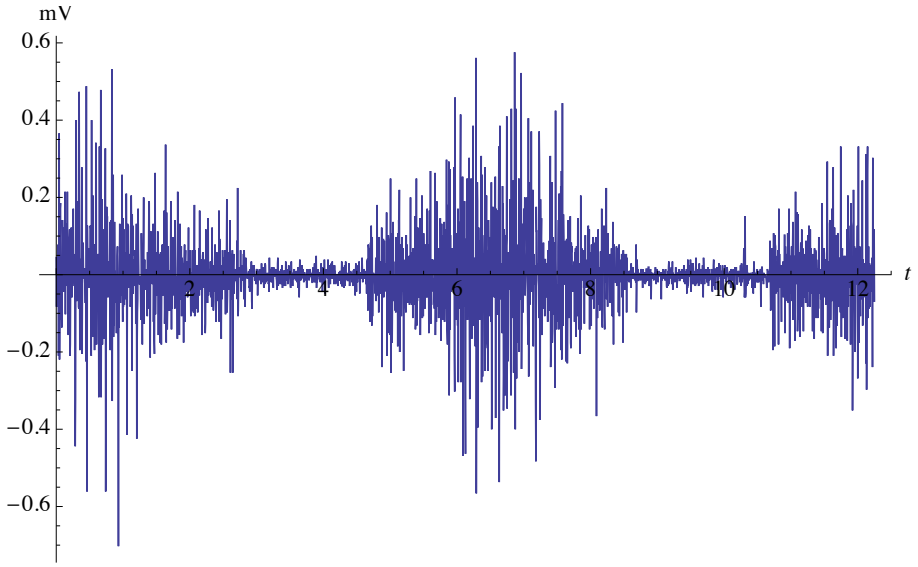

Figure 4.7: Raw EMG signal obtained during the 0–30 % Sine exercise.

appears to correspond with the Piper rhythm observed in previous studies [162, 163]. Figure 4.8 shows the frequency spectrum of the Iso exercise. The peaks appearing at 60 Hz and its harmonics are due to the power line electromagnetic radiation.

Table 4.1: Dominant frequency.

Experiment	Dominant frequency
Iso	68 Hz
0–30	75 Hz
7.5–22.5	71 Hz
1–29	67 Hz
Sine	68 Hz

Despite the lack of a cyclic process in the Iso exercise, the frequency-domain analysis

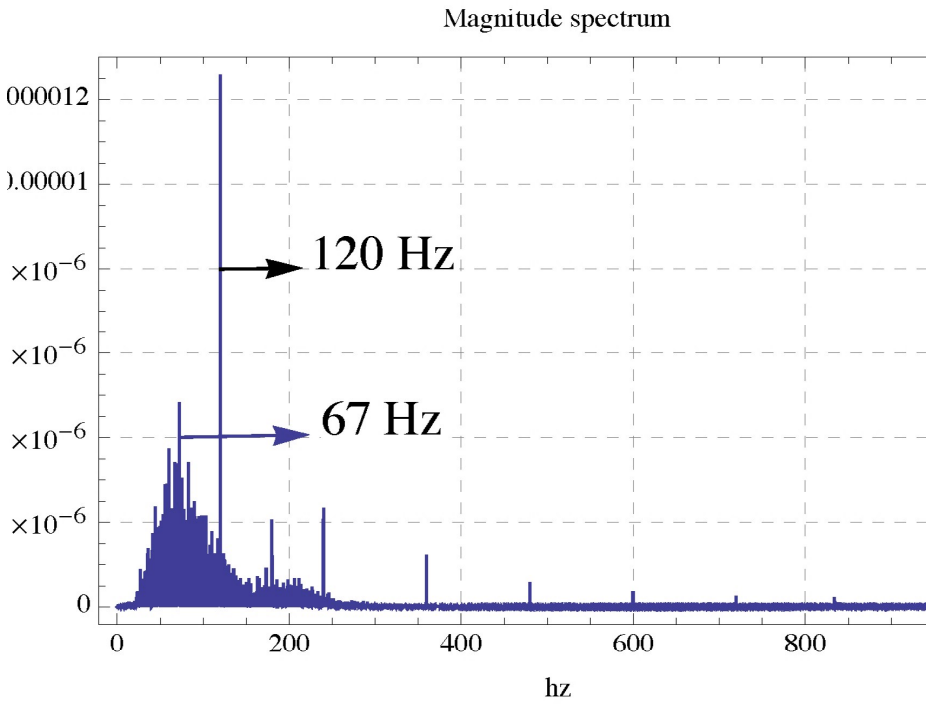

Figure 4.8: The FFT of the EMG signal obtained in the Iso exercise.

revealed the existence of a periodic process with a dominant frequency at 67 Hz. This periodic process is due to the central nervous system effort to keep the force at a constant value. In other words, it represents the average firing rate of the muscle as a whole.

The fill factor curves Log$F$ vs. τ were constructed for observable experimental state vector dimension from 2 to 10 as the time-delay varied in the range $\tau = 1 - 50\ T_s$. The minimum dimensions required to represent the full dynamic system fully was found, through inspection of the fill factor curves, to be d_o=5. The optimal time-delay for each exercise was found by inspecting the corresponding Log$F$ vs. τ curve at d_o=5 for the first

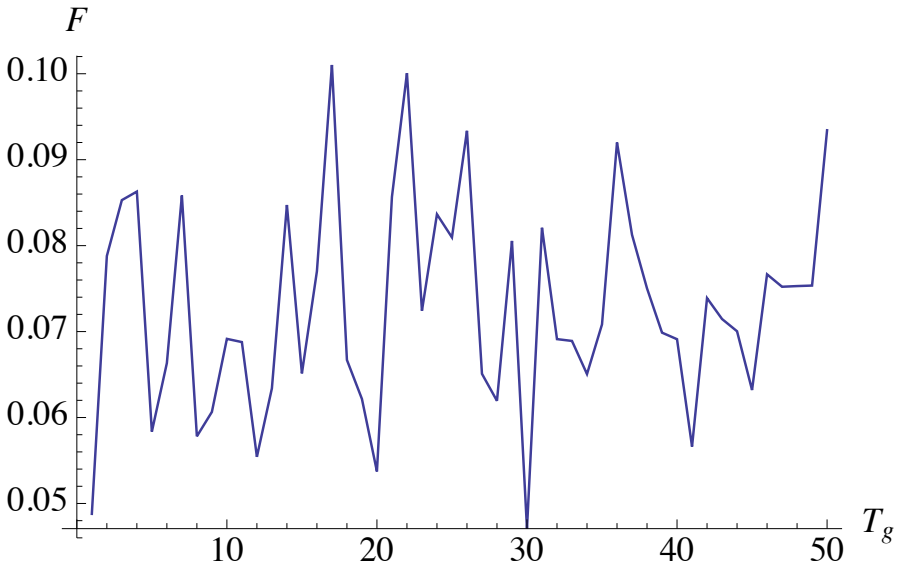

Figure 4.9: Fill factor curve for dimension five.

maximum. Figure 4.9 shows that the first maximum for the isometric exercise is happening at 4 T_m. The time delay for all exercises are listed in Table 4.2.

Table 4.2: Optimal time-delays.

Experiment	Delayed time steps
Iso	5 T_s
0–30	4 T_s
1–29	4 T_s
7.5–22.5	3 T_s
Sine	4 T_s

The fatigue detection procedure described above was applied to the force and EMG signals in each of the physiological experiments except for the Iso exercise where it was

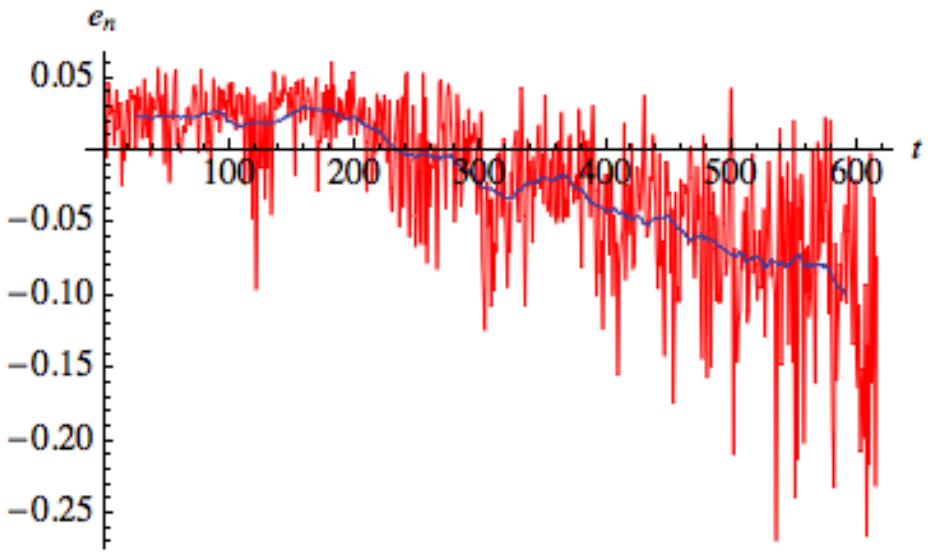

Figure 4.10: The fatigue tracking metric (red line) and its moving average (blue line) for the lateral triceps during Iso

applied to EMG signals only due to lack of force variation. The red line in the Fig.4.10 shows the magnitude of the fatigue tracking metric for each snapshot of the EMG signal in the lateral triceps during the Iso exercise. To overcome the high-frequency cycle-on-cycle variation observed in the results, a 50-cycle moving average is used to obtain the trend of the fatigue index over slow-time and shown as the blue line in Fig. 4.10.

The fatigue indices obtained from measurement of the force exerted by elbow extensors for participant 1 are shown in figure 4.11 In all four exercises where time-varying force measurements are available, the fatigue index increases indicating progressive fatigue in the elbow extensor muscle group, the medial triceps, the lateral triceps, and biceps. Fatigue indices in the 7.5–22.5 and 0–30 exercises were much larger than those for the Sine and 1–29

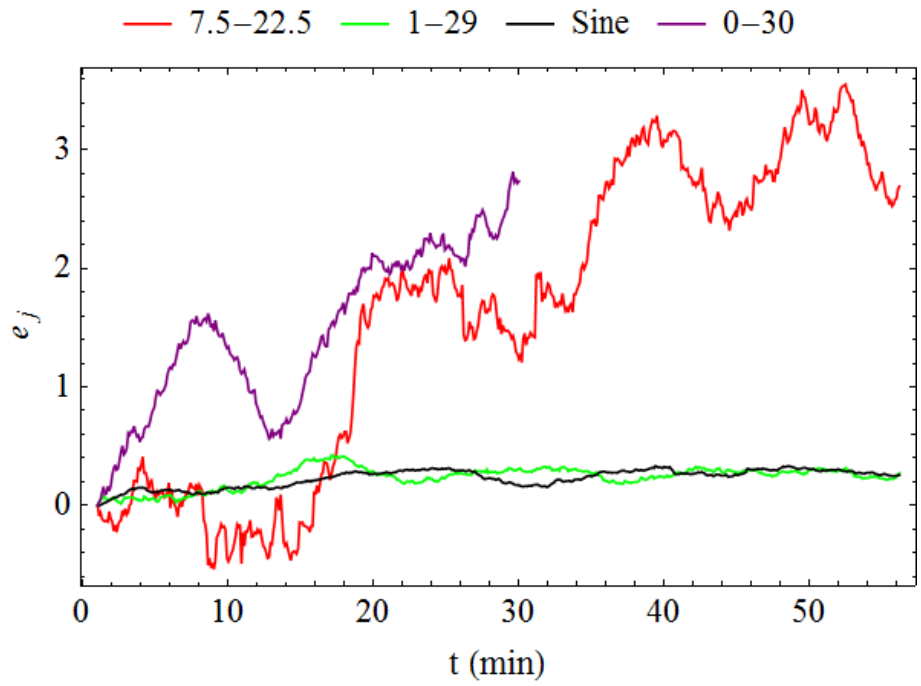

Figure 4.11: Fatigue indices obtained from measured force during the four cyclic elbow exercises

exercises. The fatigue indices for the 1–29 and Sine exercises are nearly indistinguishable.

The fatigue indices for the lateral triceps, medial triceps, and biceps for participant 1 are shown in figures 4.12, 4.13, and 4.14, respectively, as functions of time. These results were obtained by analyzing the EMG signals collected simultaneously for all three muscles during the five exercises described above.

The fatigue indices in figures 4.12, 4.13, and 4.14 show that participant 1 lateral and medial triceps experienced significant fatigue while the biceps muscle demonstrated minimal or no fatigue across all experiments. This is in agreement with An et al. [159], who

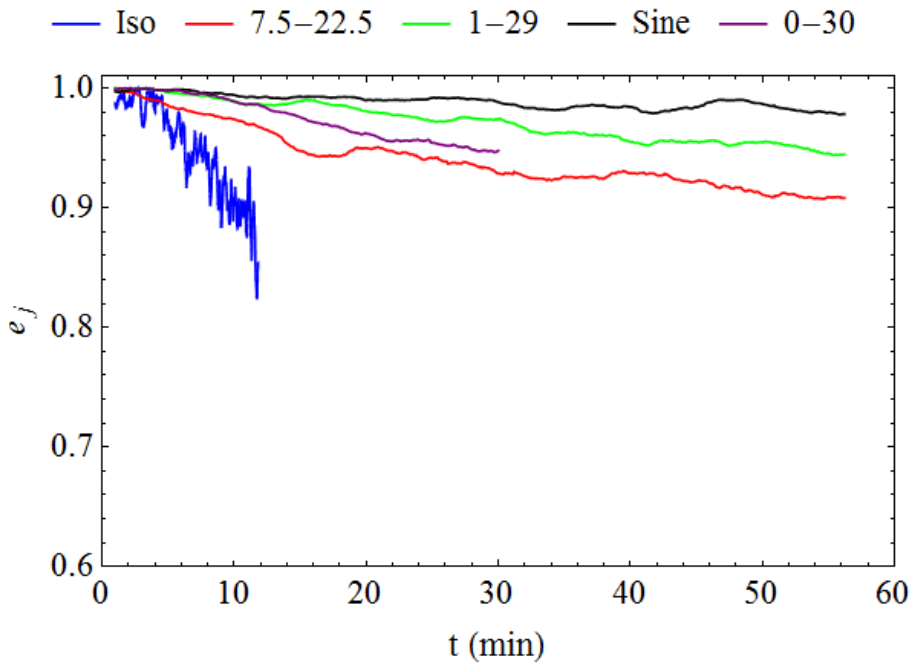

Figure 4.12: Fatigue indices obtained from the EMG signal of the lateral triceps during five elbow exercises.

found that the lateral and medial triceps are major contributors to elbow extension, while the biceps did not play a major role. Moreover, the results show that the lateral and medial triceps have different fatigue patterns (slopes) corresponding to differences in their load sharing patterns during elbow extension.

The muscle fatigue indices were similarly evaluated for each of the four other participants. Table 4.3 lists the average and standard error (SE) of the change in muscle fatigue index Δe_j over the course of the exercise period for the five participants. The standard error is one order-of-magnitude less than the fatigue indices for the medial and lateral

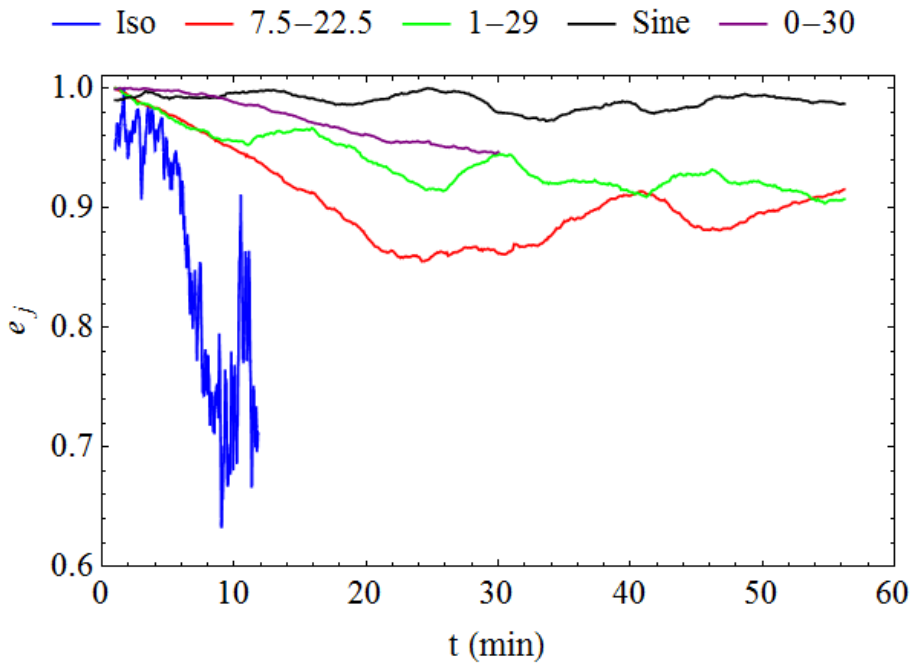

Figure 4.13: Fatigue indices obtained from the EMG signal of the medial triceps during five elbow exercises.

triceps confirming the meaningful change in the muscle state over the exercise period.

4.5 Discussion

4.5.1 Method Validation

A standard method of fatigue detection is the observation of a downward shift in the mean or median frequency of the EMG spectrum during an isometric exercise [121]. The FFT was obtained for the first and last 50000 points, respectively, of the EMG signal in the

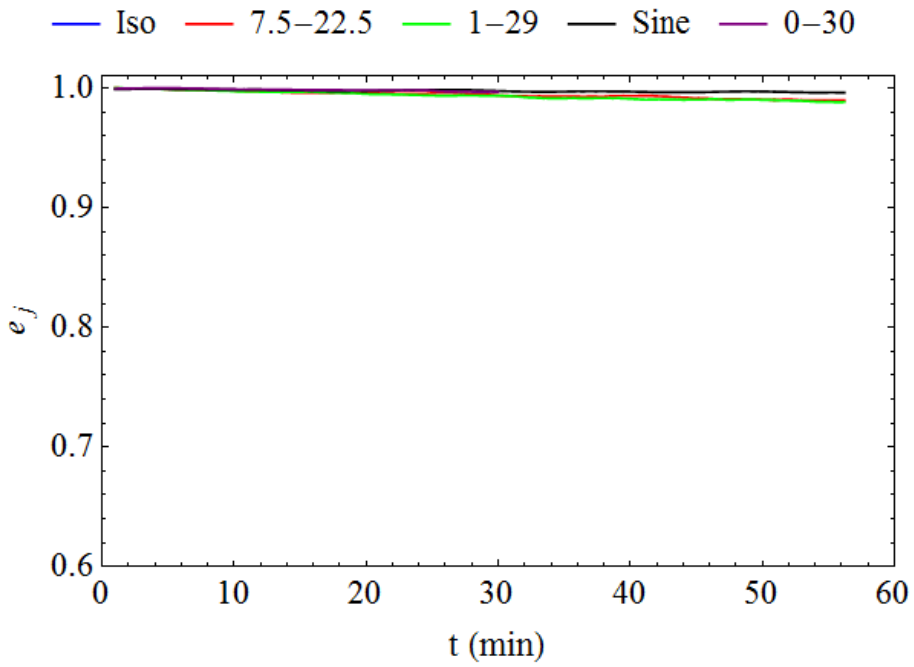

Figure 4.14: Fatigue indices obtained from the EMG signal of the biceps brachii during five elbow exercises.

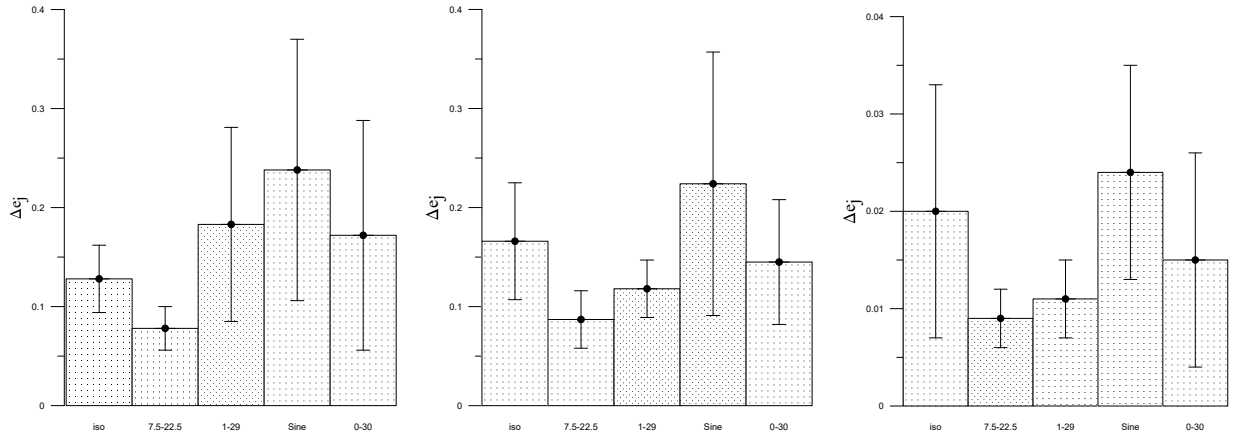

(a) Lateral. (b) Medial. (c) Biceps.

Figure 4.15: Average change in fatigue metric for muscles and force in all exercises.

Table 4.3: Average change in fatigue index for the five exercises.

Experiment	iso		7.5–22.5		1–29		Sine		0–30	
Muscle	Δe_j	±SE	Δe_j	±SE	Δe_j	±SE	Δe_j	±SE	Δe_j	±SE
Lateral	0.128	0.034	0.077	0.022	0.183	0.098	0.237	0.132	0.172	0.116
Medial	0.166	0.059	0.087	0.029	0.118	0.029	0.224	0.133	0.145	0.063
Biceps	0.02	0.013	0.009	0.004	0.011	0.004	0.024	0.011	0.015	0.011
Force			0.638	0.184	0.482	0.227	0.84	0.605	0.707	0.148

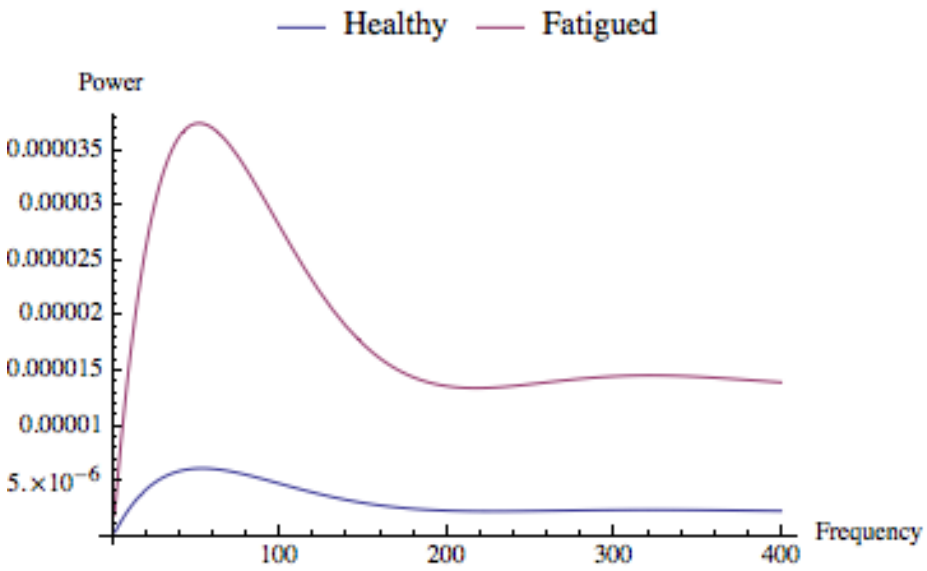

Figure 4.16: Iso signal vs. mean frequency power

lateral triceps muscle during the Iso exercise representing the first and last 24 s of the exercise. Figure 4.16 shows tenth-order polynomial fits for the frequency spectra of the two FFTs. Comparing the initial to the final 24 s, an increase in the power level across the spectrum can be observed. Further, the dominant frequency shifted from 67 to 59 Hz as the muscle fatigued over the 15 minutes time span of the exercise. These results validate

our finding of fatigue in the EMG signals of the medial and lateral triceps using PSW, figures 4.12 and 4.13.

Tracking the frequency shift is shown in Fig. 4.17, the curve represents the change in fundamental frequency with time in samples. In addition, the controlled physiological lab

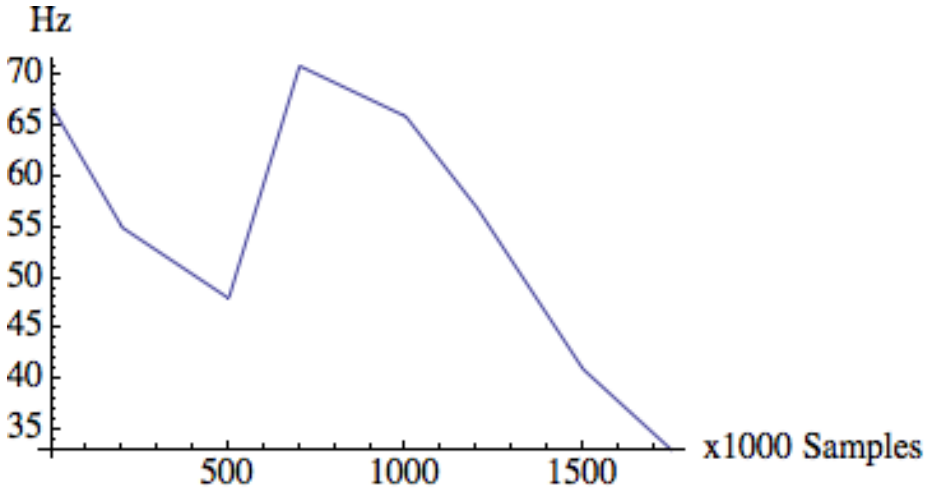

Figure 4.17: Iso exercise frequency shift

experiment proved that PSW can discriminate the presence of fatigue in EMG signals. Specifically, the fatigue detection method proposed here was able to distinguish significant fatigue in the agonist muscles(i.e., lateral and medial triceps) from the antagonist muscle (i.e., biceps) during the Iso, 7.5–22.5, 1–29, and 0–30 exercises.

Since participants in the physiological and kinematic experiments were instructed to complete the tasks until they are no longer able to keep up, our results show qualitative agreement among fatigue detection indices obtained from EMG signals, force signals, and

kinematic signals. This indicates that fatigue can be successfully detected using invasive and non-invasive signals. However, the more invasive EMG signals allow for investigation of muscle participation in various motion patterns and load sharing relationships among various muscles during those motion patterns.

4.5.2 Results Interpretation

The fatigue indices obtained from the PSW can be used for qualitative and quantitative comparison among the states of a muscle (or a muscle group) over time during the same exercise or different exercises as well as for comparison among the states of different muscles. However, a quantitative comparison can only be carried out for exercises with similar dynamics, for example, exercises that share a similar time period. In addition, the measured signal has to be treated with the same signal processing procedure and the same normalization parameters.

For example, the large changes in the fatigue indices of the lateral and medial triceps during the Iso exercise, when compared to the cyclic exercises, do not necessarily mean that those muscles are experiencing greater *severity* of fatigue. The nature of the exercise and the lack of an exercise period precludes the quantitative comparison between the isometric condition and the time-varying exercises. Nonetheless, the fatigue indices of the medial and lateral triceps during the Iso exercise, figures 4.12 and 4.13, show that the muscles are

rapidly fatiguing compared to the cyclic exercises.

It is important to note that conclusions about fatigue onset and comparison of fatigue patterns to study load sharing among muscles are subject to the uncertainty level in the fatigue index. An estimate of the level of uncertainty can be obtained from the standard error of the fatigue index as demonstrated in table 4.3 and figure 4.15.

4.5.3 Kinematic Experiment

The kinematic system under investigation in this analysis is an open kinematic chain that extends from the trunk through the lower extremities to end at the foot. The knee flexion angles θ data collected provide information about part of the chain. The angle also carries information about the other state variables of the coupled dynamic system of the lower limb. Using time delay embedding, the minimum dimension required to represent the coupled system was found to be $d_\circ = 5$, which is consistent with previous gait studies using phase-space reconstruction [164, 165].

This result is also consistent with the standard model of the lower limb dynamics in the sagittal plane which consists of two rigid bodies, the shank and thigh, connected by a hinge joint, the knee. This model is represented by four independent state variables, knee and thigh flexion angles θ and α and their angular speeds $\dot{\theta}$ and $\dot{\alpha}$. The fifth state variable in

our reconstructed phase-space corresponds to the forcing phase angle $\beta(t)$ imposed on the system by the treadmill. Thus, the state variables vector of the dynamic system underlying the reconstructed phase-space can be written as $\mathbf{y}(t) = [\theta,\ \dot{\theta},\ \ \alpha,\ \dot{\alpha},\ \beta]^T$.

The pseudo phase-space, therefore, represents the discrete time evolution of the state variables vector $\mathbf{y}_n$. Orbits of the gait cycle in the pseudo phase-space, projected onto a plane described by the first two elements of the reconstructed state variables vector figure 4.18, show qualitative agreement with those measured by Winter 2009 [1] and projected onto the θ-$\dot{\theta}$ plane of phase-space figure 4.19. The latter figure was obtained by plotting the measured knee flexion angle θ versus the numerically differentiated angular speed $\dot{\theta}$.

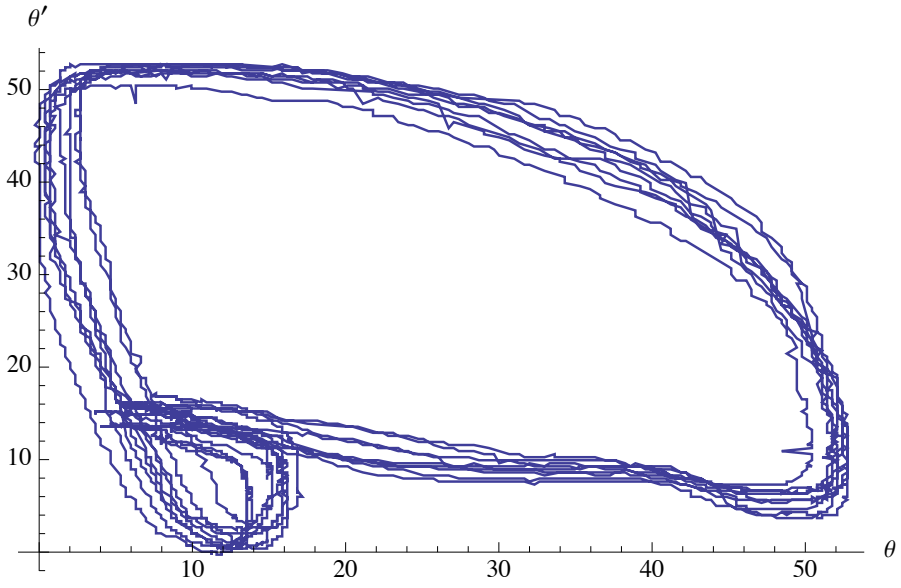

Figure 4.18: The pseudo phase-portrait of the gait cycle obtained from reconstructed phase-space.

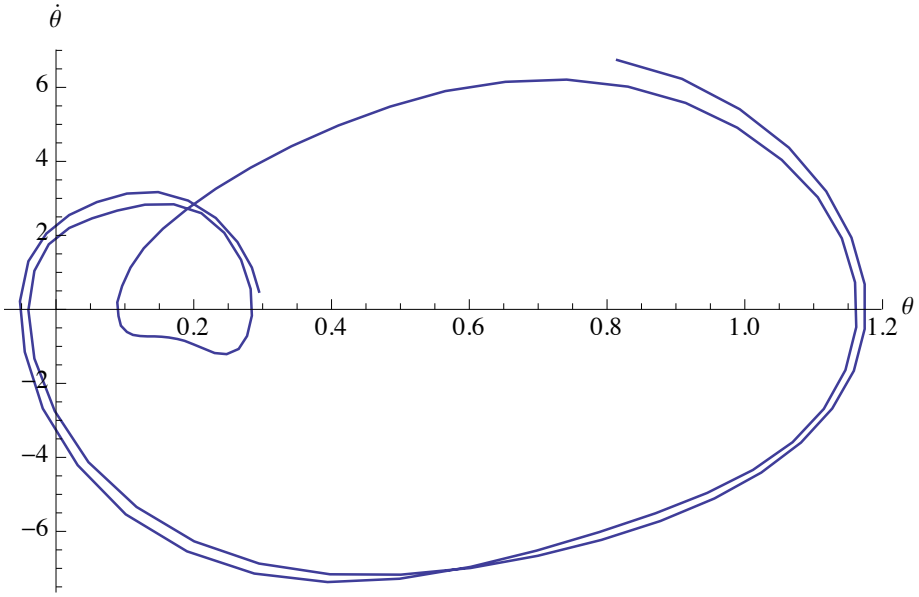

Figure 4.19: The phase-portrait of the gait cycle extracted from Winter [1] measurements.

The two orbit projections are in a qualitative agreement establishing the dynamic equivalence between the reconstructed and measured phase-spaces. Specifically, both phase-portraits show two loops; a large loop corresponding to the leg swing phase and a small loop corresponding to the heal strike-toe off phase of the human gait cycle.

Examination of the gait cycle orbits in figure 4.18 show significant cycle-on-cycle variability. There are various possible sources of this variation. Previous tests have shown that the accuracy of the direct knee angle measurement system is better than 0.3° Alwasel et al. [14] indicating that the contribution of measurement noise to the overall orbit variability is relatively small. A major source of variability is the input of the central nervous system

(CNS) to the gait cycle.

Winter [1] suggested that human gait approximates an inverted pendulum supporting a point mass at the center of body mass. Stabilizing this inherently unstable inverted pendulum requires continuous intra-cycle feedback by the CNS to the lower limb. Our finite dimensional model ignores the CNS contribution to the lower limb dynamics which appears as a cycle-on-cycle variation.

4.5.4 Physiological Experiment

Fatigue indices obtained from EMG signals reveal details about individual muscle experimental observable states that are not available from the fatigue indices obtained from force signals. For example in the 7.5–22.5, 1–29, and 0–30 exercises, the fatigue indices obtained from the EMG signals for the medial and lateral triceps, figures 4.12 and 4.13, show load sharing patterns between the muscles absent from the fatigue index obtained from the force signal, figure 4.11, which represents the state of the aggregate fatigue in the muscle group performing the elbow extension.

The lateral and medial triceps fatigue indices shown in figures 4.12 and 4.13, respectively, indicate that these muscles are highly active in elbow extension. The results show that the presence of a rest time allowance is an important factor in muscle fatigue. It was

found that the triceps muscles rapidly fatigued during the 7.5–22.5 exercise, where no rest time was allowed, compared to the of 0–30 and 1–29 exercises, where muscles were allowed to rest for about half the period of the cyclic exercise. This conclusion is consistent with the results of Rohmert [22, 23].

4.6 Conclusion

A novel application of PSW to track fatigue on multi-level biological signals was presented. Kinematic data, represented by the knee angle during fast-walking, and physiological data, represented by EMG and force from lateral and medial triceps and biceps muscles, were examined. The method assumes that fatigue is a slowly changing variable in the EMG signal. Thus, tracking the change in shape and position of the phase space through time leads to an estimation of the slowly variable changes. Hence, the method of time delay embedding was used to construct the muscle EMG phase-space. Then, the tracking procedure was carried out using the method of phase-space warping (PSW).

Results showed that the methods used are capable of identifying the slow change variable (fatigue) using kinematic, force, and EMG signals. The fatigue index based on Kinematic and force signals revealed information about the health state of the overall coupled dynamic system under test, the lower limb in this case. The fatigue indices based on EMG

signals, on the other hand, revealed information of the health states for each muscle.

It has been shown that time delay embedding and PSW methods can examine the function of the individual muscles. It has also been shown that load sharing patterns among different muscles can be identified using the fatigue metric.

The combination of time delay embedding and PSW is shown to provide a 'big picture' estimator of fatigue in the lower limb using the time-history of a single joint angle. Unlike state-of-the-art fatigue detection techniques described by Dong et al [166], which uses cumbersome sensors, this method can supply information about fatigue evolution outside a laboratory environment. This opens doors to applications such as tracking the physical state of athletes during competitions, workers in a plant, and patients undergoing in-home rehabilitation.

The findings show that while fatigue indices derived from non-invasive methods, and kinematic and force measurements, provide an overall estimate for the state of the muscle group, fatigue indices obtained from more invasive measurement methods, e.g., EMG signals, provide a more detailed evaluation of the state of individual muscles. As a result, the latter indices can be used to study muscle participation in motion and load sharing patterns.

Chapter 5

Experience, Productivity, and Musculoskeletal Injury Among Masonry Workers

5.1 Objectives and Methodology

Different data collection methods were tested for use in non-structured environments in chapter three. Fatigue level analysis was also tested in chapter four. While promising, the use of the tested techniques in non-structured environments, worksites, needs further

study. An example of highly repetitive, highly physical, and non-structured environments is masonry work, which the subject of the following chapters.

The masonry workforce is composed of two classes: apprentices and journeymen. In Ontario, Canada the masonry apprenticeship program lasts for three years before a mason is examined to become a journeymen. Currently, a low retention rate prevails among masons in the first five years with the same employer combined with an aging workers' population [11, 12]. Moreover, workers with less than five years of experience have higher rates of musculoskeletal injuries compared to journeymen with more than five years of experience.

Throughout the first five years, masons gain proficiency, productivity, and ergonomic safety. This chapter examines the hypothesis that journeymen with more than five years of experience are more productive and ergonomically safer than less experienced groups. Previous studies have used a similar approach to examine the relationships among safety, efficiency, and experience in sports studies [167, 168] and material handling [99, 101, 102].

Twenty-one right-hand dominant participants were recruited through the Brick and Stone Mason (Apprenticeship) program, School of Trades & Apprenticeship, Conestoga College, Waterloo, ON. Participants were recruited into four groups: 5 novices, 4 apprentices with one year experience, 7 apprentices with 3 years experience, and 5 journeymen with more than five years of experience. Table 5.1 shows the participants' demographics.

Table 5.1: Participants demographics

# of participants	Experience (years)	Height(SD)	Weight (SD)	Skill
5	0	176.6 (8.41)	83.8 (7.6)	Novice
4	1	174.7 (8.73)	80.75 (15)	Apprentice
7	3	179.7 (4.7)	93.4 (4.75)	Apprentice
5	>5	176.8 (8.84)	85.6 (10.5)	Journeymen
21	Average	177.3 (7.17)	86.85(9.98)	–

The study received ethics approval from Offices of Research Ethics at the University of Waterloo and Conestoga College. It took place at the masonry workshop, Conestoga College. Upon arrival to the site, each participant was briefed on the experiment and instructed to build a 12×6 block wall. No other instructions were given to the participants.

5.1.1 Task

A lead wall, shown in figure 5.1, was built prior to the experiment. Participants used this 27-blocks-laid frame to complete the wall. As shown in figure 5.1, the participant performed the task of laying blocks only. Mixing mortar and bringing blocks was done by a helper. All participants brought their trowels except the novice group where trowels were given to them. A total of 45 blocks were laid to complete the wall. In the beginning, the blocks were placed $\simeq$ 60cm away from the lead wall, arranged in three piles, each pile 5 courses high. Two panels of mortar were placed alongside the blocks. The work space was controlled, thus, spurious factors such as working on scaffolding and clutters were not

considered.

Figure 5.1: Lead wall built to guide participants.

5.1.2 Instrumentation and test setup

Motion detection was conducted using a body area network sensors suite [2, 169] and video cameras. The suite consists of 17 sensors placed at each body segment including the head. Each sensor is composed of a tri-axial accelerometer, a tri-axial gyroscope, and a magnetometer. Data from the suite are extracted as BVH files that contain local 3D coordinates of body joints with the hip joint center serving as the origin of the local

coordinate system.

Three camcorders were set up around the wall to capture the task on video. This video was used to segment the data in the processing phase. The blocks used are standard Concrete Masonry Units (CMU) weighing 10kg with dimensions of $390 \times 190 \times 100$mm.

5.1.3 Data collection and processing

Once the motion suite was calibrated, the participant was asked to start building the wall. They started by placing an alignment wire to help align the course. Motion and video data were collected continuously until the participant declared the wall ready. Data collection was then terminated. On average, the novice group completed the wall in 74 minutes, the one-year group in 48.5 minutes, the three-years group in 41 minutes, and the journeymen group in 25.5 minutes.

Biomechanical analysis

Motion data was segmented into blocks resulting in 45 ".BVH" files for each participant Each file starts when the participant is standing before the block and ends when the block is finally laid on the wall. Forces on the hands were manually added to those files. The ".BVH" files were converted into ".loc" input files for 3D Static Strength Prediction

Program (3D SSPP) [91].

The software was used to carry out full body biomechanical analysis based on the static strength prediction model described by Chaffin et al. [170]. It uses body anthropometric parameters, body joint angles, and external forces applied on the body to predict three dimensional joint forces and moments. Upon identification of whether the worker is using one or two hands, it was deployed to calculate the joints' loads and moments listed in table 5.2. The structure of input and output data is shown in figure 5.2.

Productivity analysis

Masonry jobs are paid by the number of blocks laid per day. Since the experiment presented in this paper controls for that by tasking participants with building the same wall, productivity was defined as the time a mason requires to build the wall. Timing was set to start at picking up the first block and ends by laying the last block. Combining biomechanical and productivity analyses for workers with varying levels of experience provides insight into whether workers are gaining in proficiency and productivity in tandem with ergonomic safety.

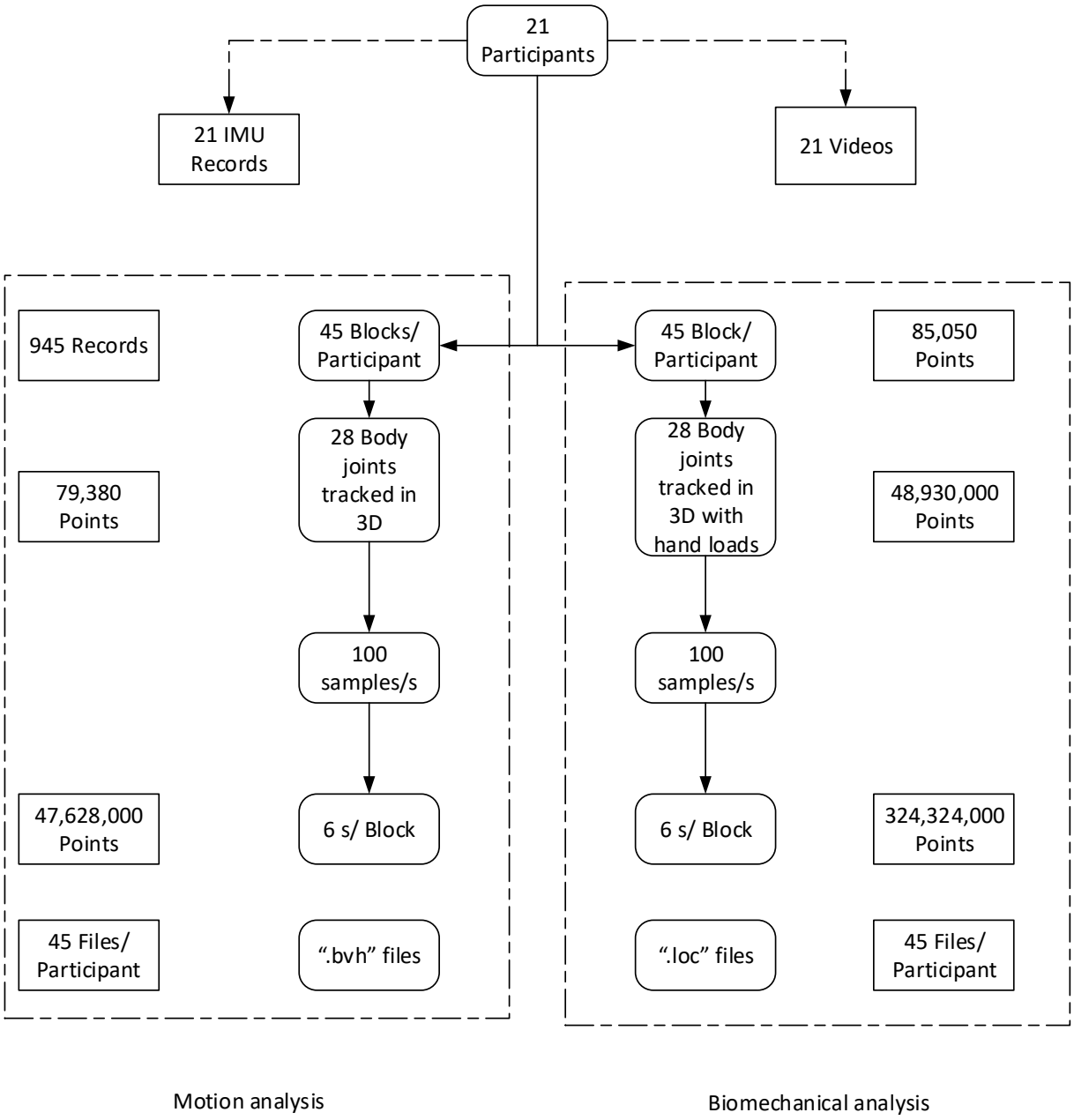

Figure 5.2: Dataset structure.

5.2 Results

Using 3D SSPP to analyze the data collected provides a vast amount of in-depth information. The results are divided into two sets: joint moments and joint compression forces. In this chapter, only the major joints, highlighted in bold text, in table 5.2 are reported and highlighted in figure 5.3. These joints are typically considered in biomechanical analysis of the human body [140, 171]. The magnitudes of joint moments and forces are used to study the effects of experience. The normalized joint moments and compression forces are used to study the effects of course height.

Joint forces and moments allow for quantification of load levels at each joint. Comparing these forces and moments to epidemiologically and biomechanically verified limits set by National Institute for Occupational Safety and Health (NIOSH) allow for risk assessment [33, 43, 172].

5.2.1 Experience vs. Loads

Lower back (L4-L5) joint compression forces are shown in figure 5.4, each curve represents the average compression force for each group. At the first course, the group with three years of experience showed high values of compression with an average $\simeq 6000\ N$. The three remaining groups showed relatively similar values. As they are laying the second course,

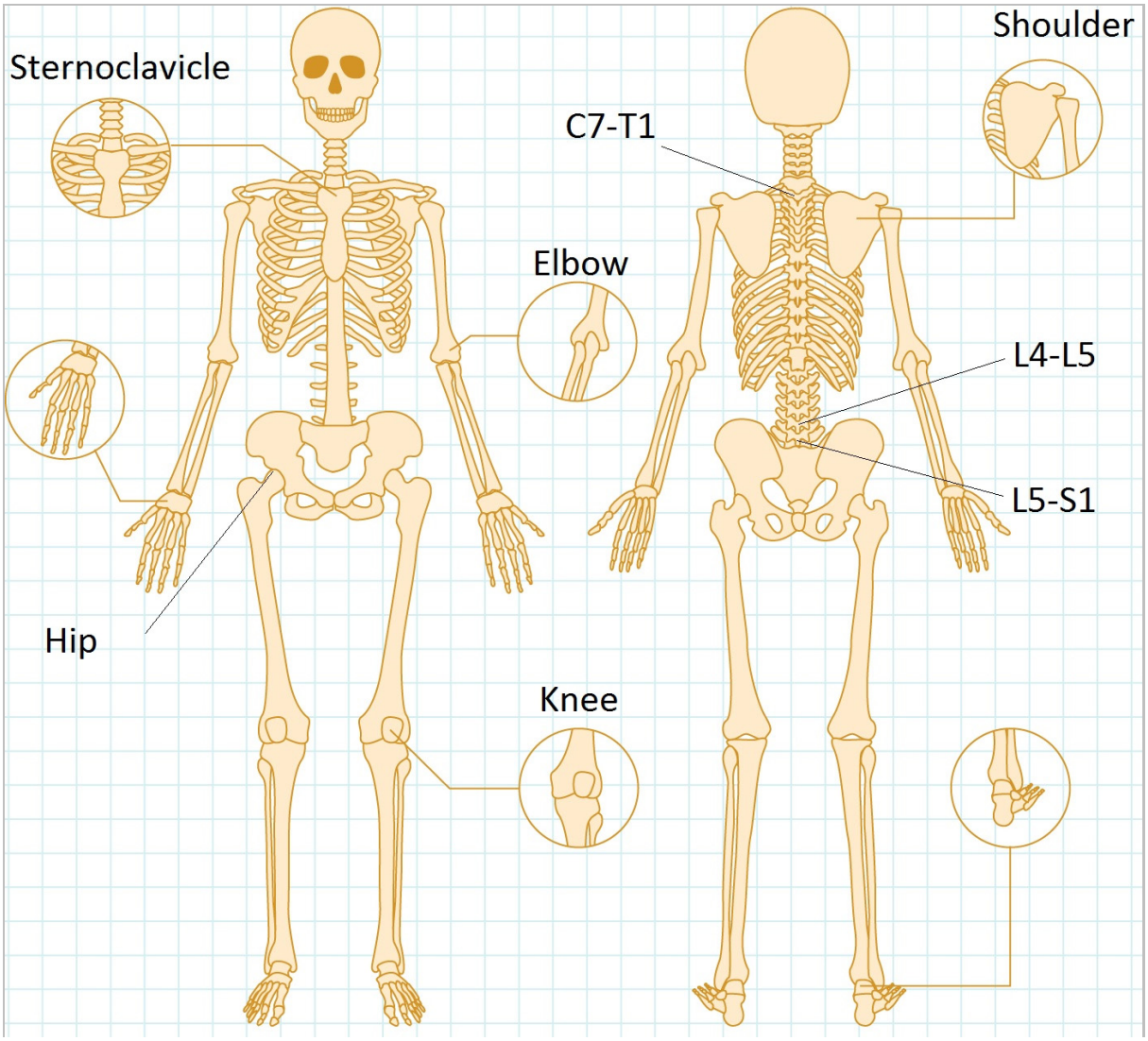

Figure 5.3: Major body joints (Designed by Freepik).

all groups showed lower values of compression force compared to first course. However, the drop in the 3 years of experience group was significantly higher than the other group, 20% compared to 10%. The third course had the lowest values of compression across all groups,

Table 5.2: Joints included in the biomechanical analysis

Joint	Parameter	Anatomical location
L5-S1	**XYZ Force**	**Low back**
L4-L5	**XYZ Force**	**Low back**
Wrist	XYZ Force	Radial to Carpal
Elbow	XYZ Force	Humerus to Radius and Ulna
Shoulder	XYZ Force	Clavicle to humerus
C7-T1	XYZ Force	Cervical to thoracic
SCJ	XYZ Force	Sternum to clavicle
Hip	XYZ Force	Femur to acetabulum
Knee	XYZ Force	Femur to tibia and fibula
Ankle	XYZ Force	Tibia and fibula to talus
L5-S1	**XYZ Moment**	**Low back**
Wrist	XYZ Moment	Radial to Carpal
Elbow	**XYZ Moment**	**Humerus to Radius and Ulna**
Shoulder	**XYZ Moment**	**Clavicle to humerus**
C7-T1	XYZ Moment	Cervical to thoracic
SCJ	**XYZ Moment**	**Sternum to clavicle**
Hip	**XYZ Moment**	**Femur to acetabulum**
Knee	**XYZ Moment**	**Femur to tibia and fibula**
Ankle	XYZ Moment	Tibia and fibula to talus

moreover, the three years group showed lower forces compared to one year group. Gradual increase from this minimum is observed across all groups for the fourth and fifth course. Lower back (L5-S1) joint compression forces show similar patterns to those observed for L4-L5 but at a reduced level.

Lower back (L5-S1) joint moments are shown in figure 5.5. Similar patterns to those observed for joint compression, figure 5.4, hold for the (L5-S1) joint moments. Furthermore the Sternoclavicular joint moment showed similar patterns to L5-S1 moment but with a

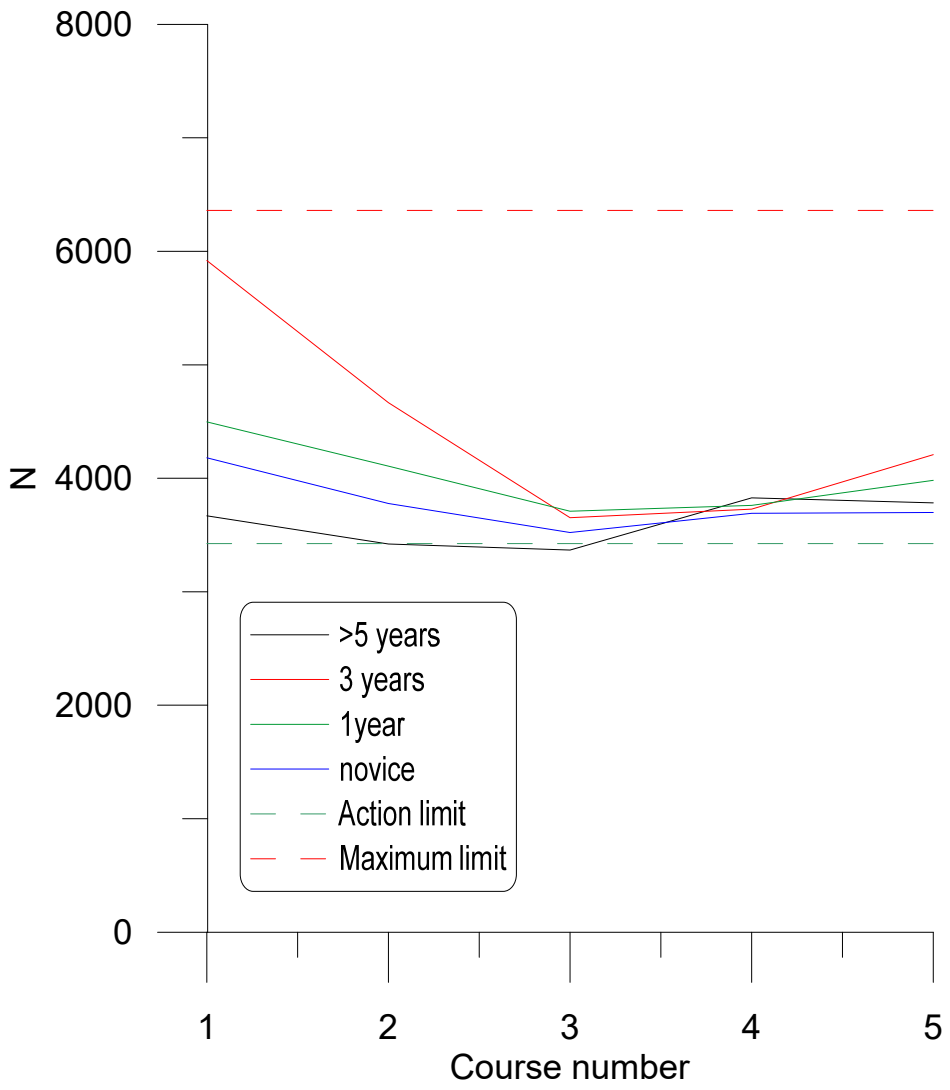

Figure 5.4: L4-L5 joint compression force

drop of $\simeq 10\%$.

The moments of the left and right shoulder joints are shown in figure 5.6. The group with three years of experience has the highest moments followed by the group with 1

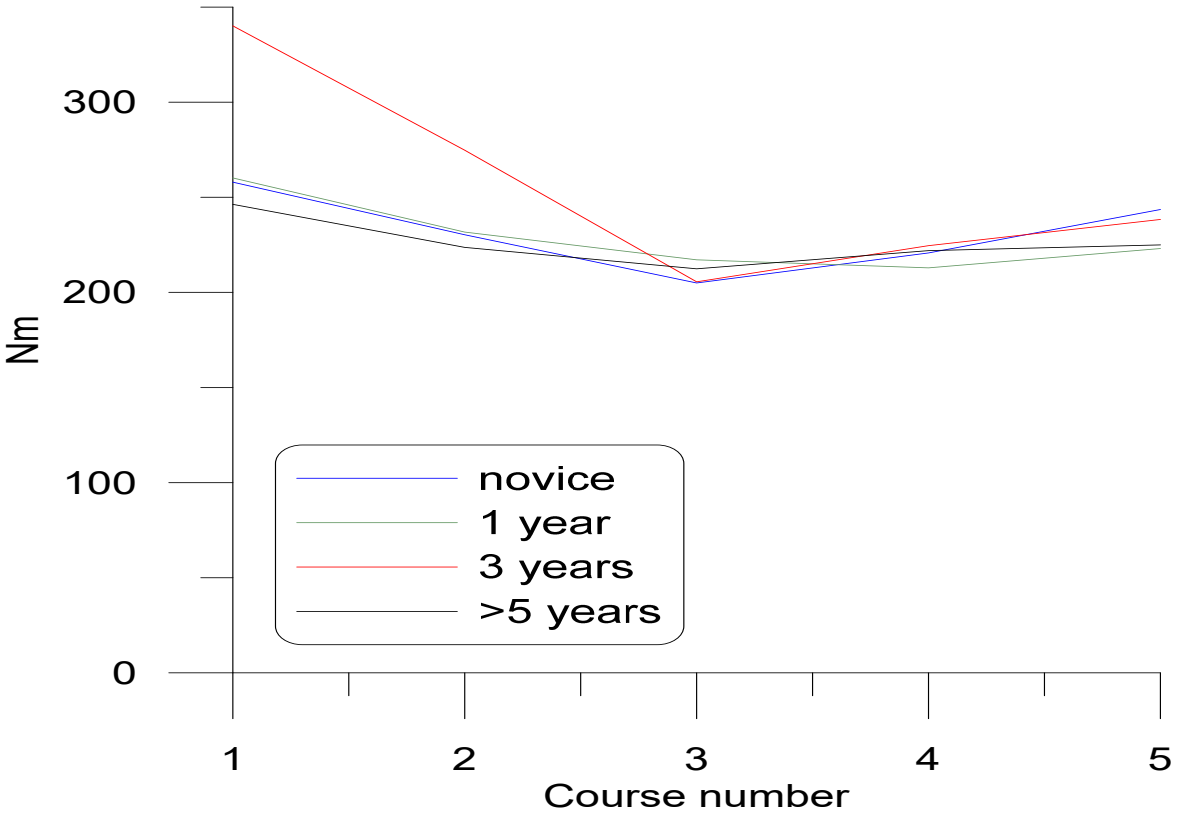

Figure 5.5: L5-S1 Joint moment

year and then novice and experts for both joint joints and throughout the five courses. Furthermore, the non-dominant left shoulder joint experienced higher moments compared to the right.

Left and right elbow joint moments are shown in figure 5.7. Elbow joints moment demonstrated similar patterns to those observed for the shoulder. The dominant hand has less spread among different experience groups than the non-dominant hand. Moreover, the expert group appears more successful in balancing loads between left and right sides.

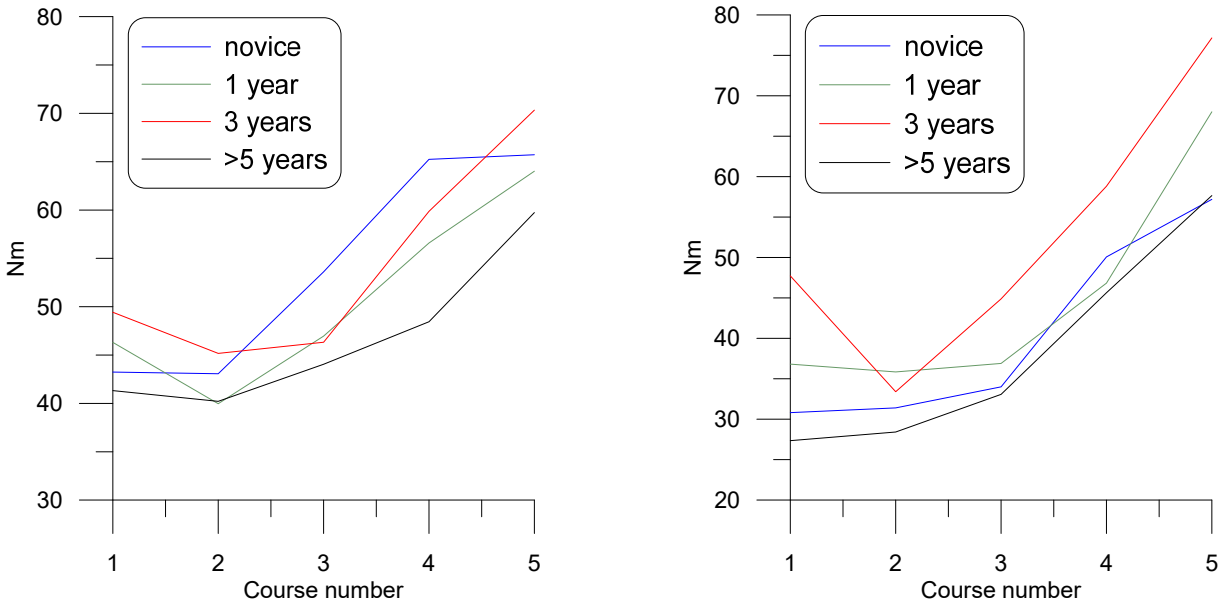

Figure 5.6: Left and right shoulder joint moment

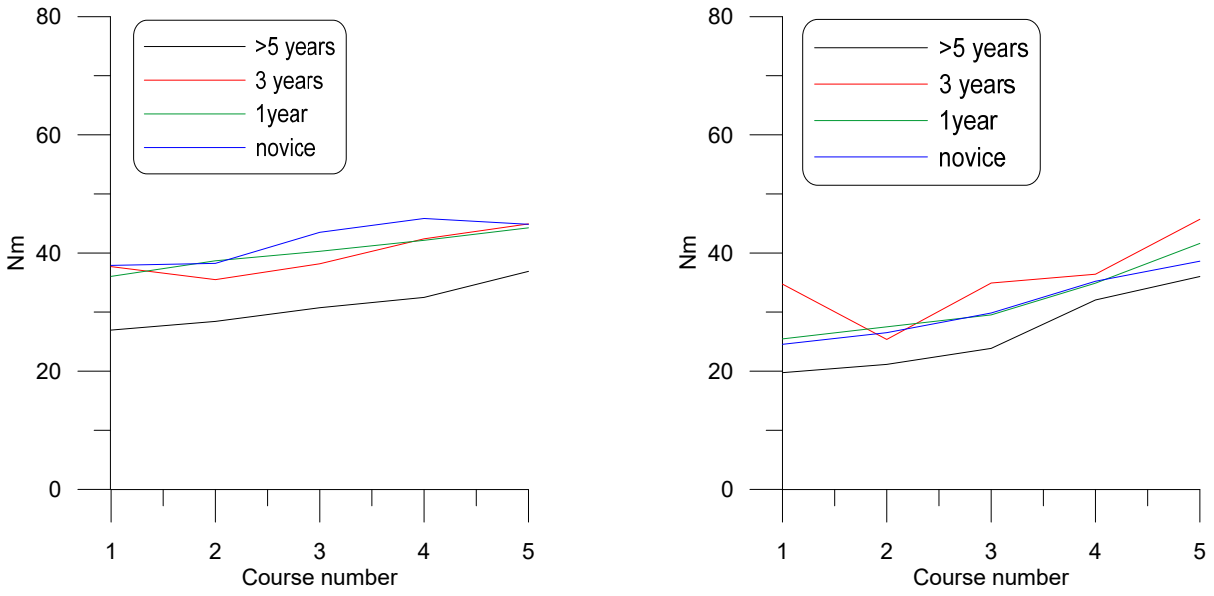

Figure 5.7: Left and right elbow joint moment

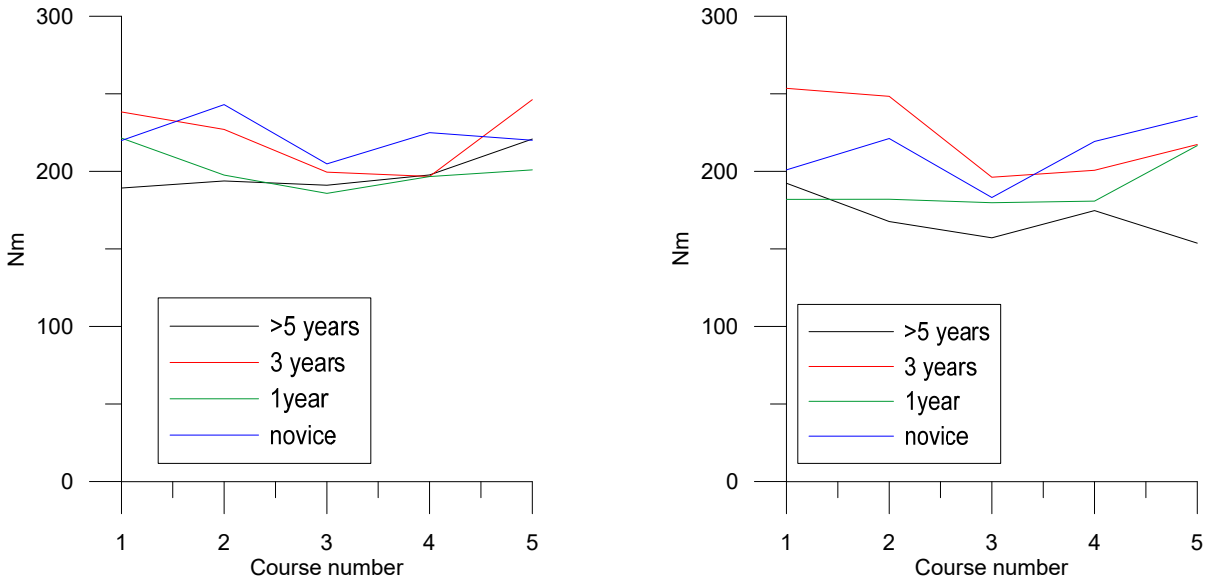

Figure 5.8: Left and right hip joint moment

Figure 5.8 shows the left and right hip joints moments. The lower limbs carry most of the load in lifting and material handling. The three years and novice groups have the highest hip joint moments in both sides across all courses. The expert group has the least values of moment among all groups in both hips. Moreover, the variation between experience groups is more apparent on the dominant side.

Knee joint moments experienced by the novice group were the highest among all four group across the courses as shown in figure 5.9. The experts' group have the lowest knee joint moments consistently.

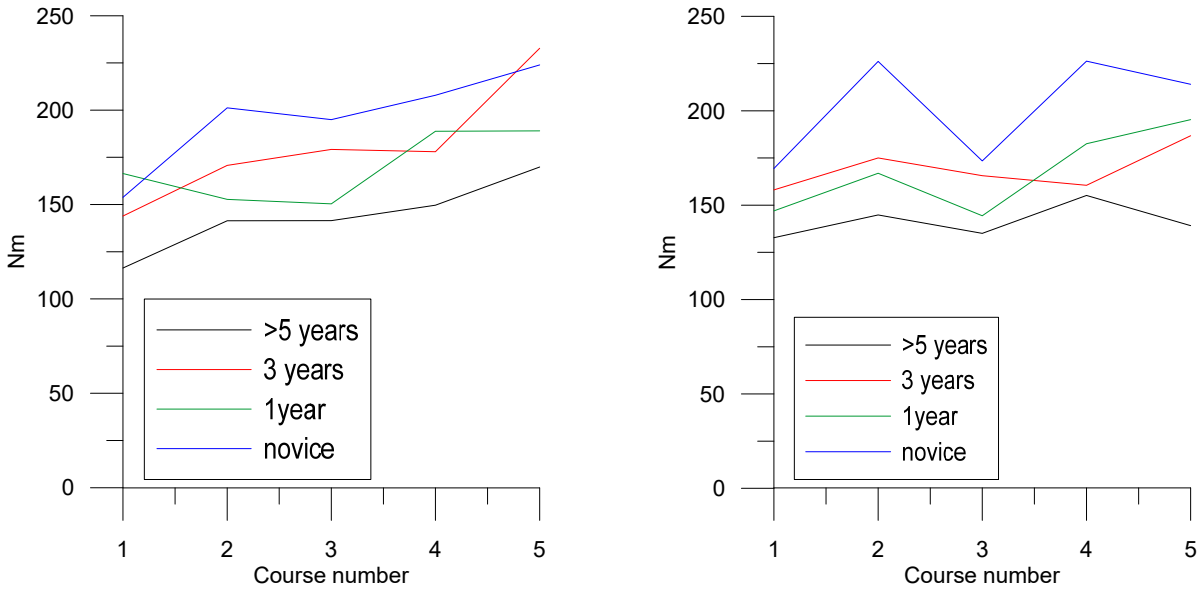

Figure 5.9: Left and right knee joint moment

5.2.2 Course height vs. Load

The four groups L4-L5 joint compression forces are shown in figure 5.10 normalized with respect to each group's average for all blocks. This representation provides an indication of the forces exerted for each course height compared to average exerted force. The first course required from $100 - 130\%$ more than the average block. On the other hand, the second and third courses required compression forces below average. The same force level pattern is seen in the L5-S1 joint.

The normalized L5-S1 joint moment is shown in figure 5.11. Similar to the low back compression force the first course required above average joint moment at $110 - 135\%$ and

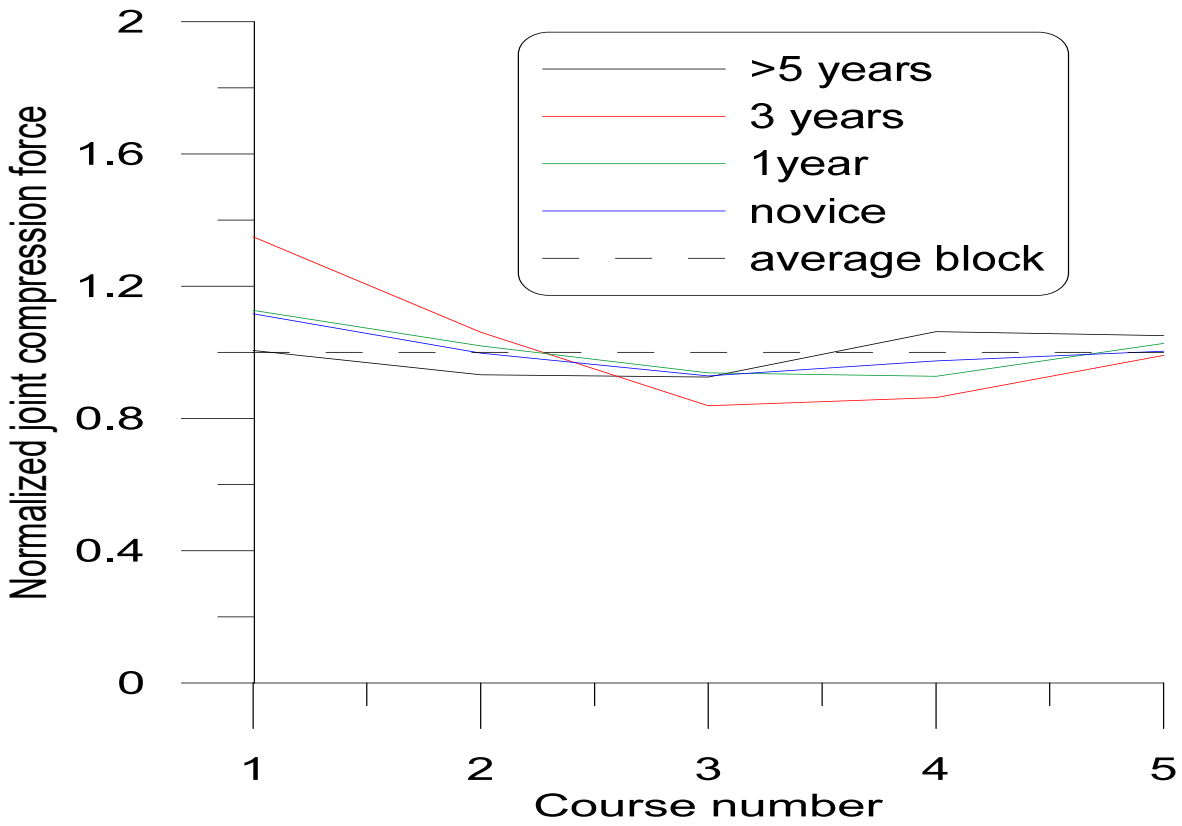

Figure 5.10: L4-L5 Normalized joint compression forces

$115-135\%$ of the average block. Third and the fourth course required below average joint moment at $80-95\%$ and $85-100\%$. Moreover, Sternoclavicular joint moment followed the same pattern as low back compression and moment.

The left and right shoulder joint moment requirements for the first three courses were below average at $75-105\%$. The fifth course required significantly above average joint moments at $125-225\%$ as shown in figure 5.12. Moreover, the expert group showed significantly higher joint moments in the non-dominant side at the upper courses compared

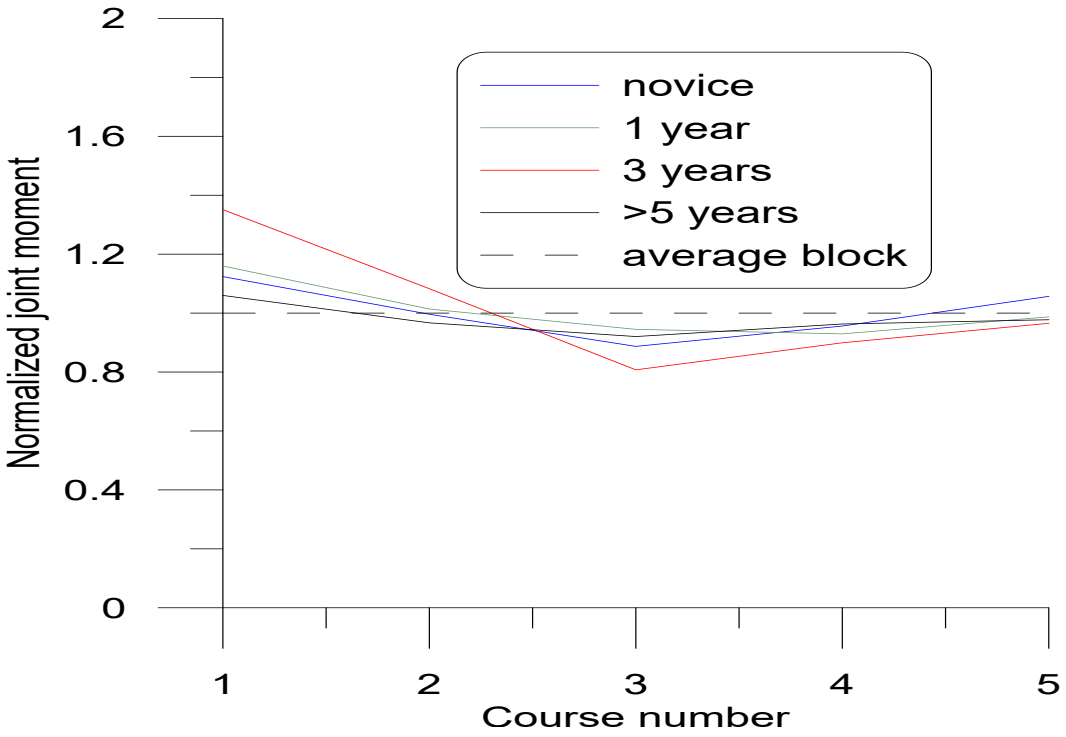

Figure 5.11: L5-S1 Normalized joint moment

to all groups.

The normalized elbow joint moment, shown in figure 5.13, showed lower moments in the first two courses, $70-90\%$ of the average, followed by increased values as the course gets higher. The fifth course required joint moments significantly above average for the dominant side at $120-200\%$. In contrast to the shoulder, the elbow joint moments of the dominant side showed more variation than the non-dominant side.

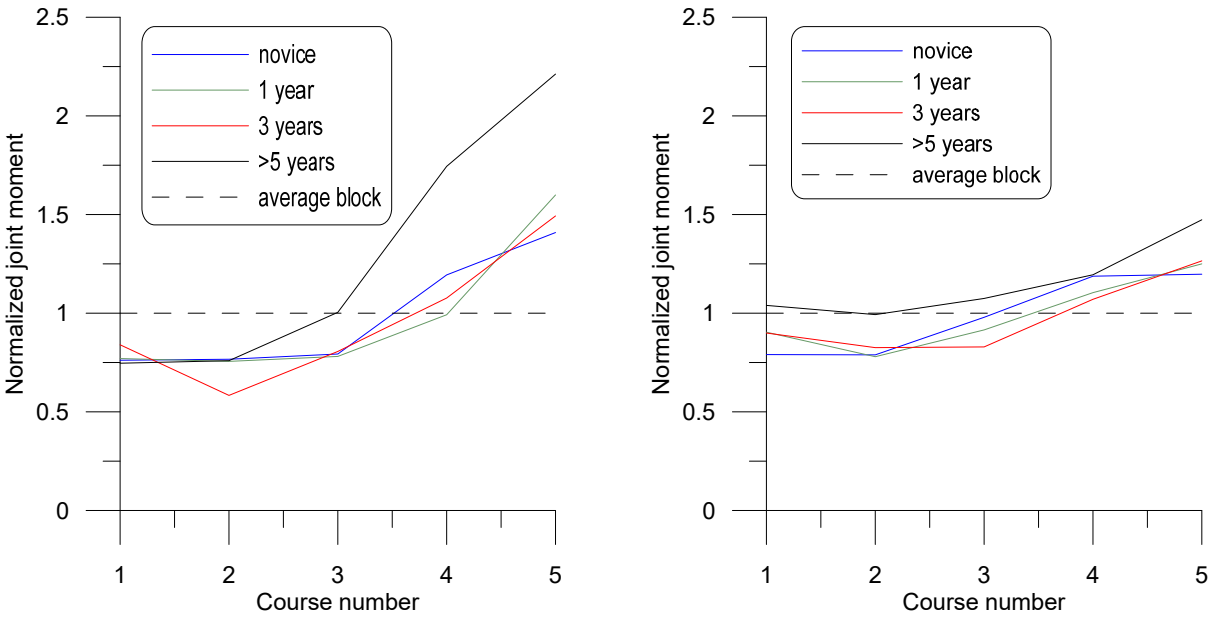

Figure 5.12: Left and right normalized shoulder joint moment

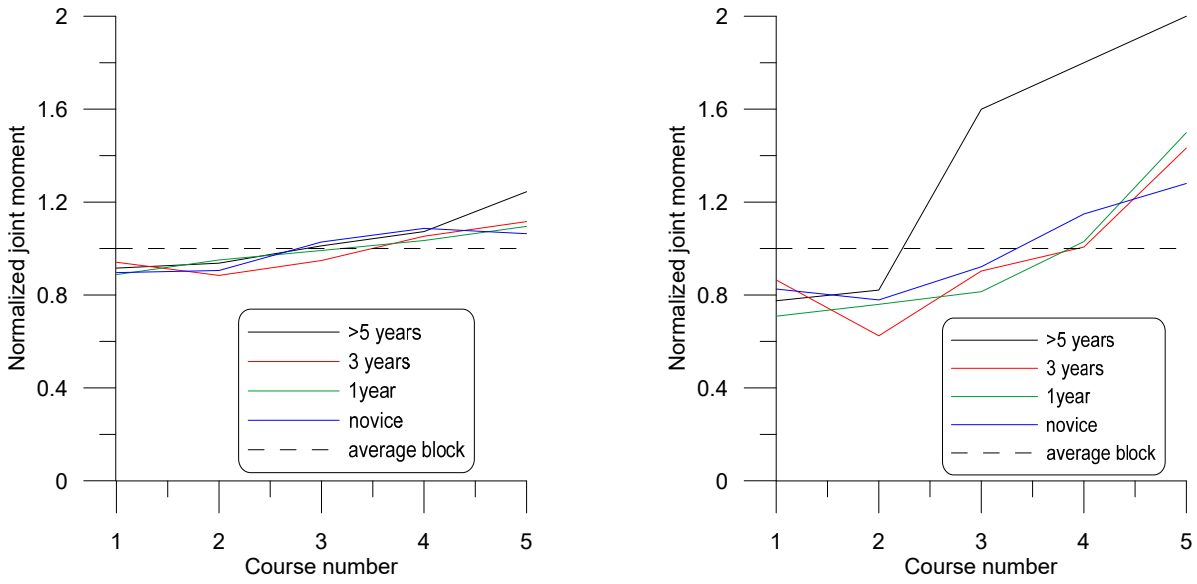

Figure 5.13: Normalized left and right elbow joint moment

The lower limb joints exhibited similar patterns. The hip joint moment, shown in figure 5.14, and knee joint moments in both sides showed small variations from average. However, the joint moment requirements were clearly below average at courses three and four.

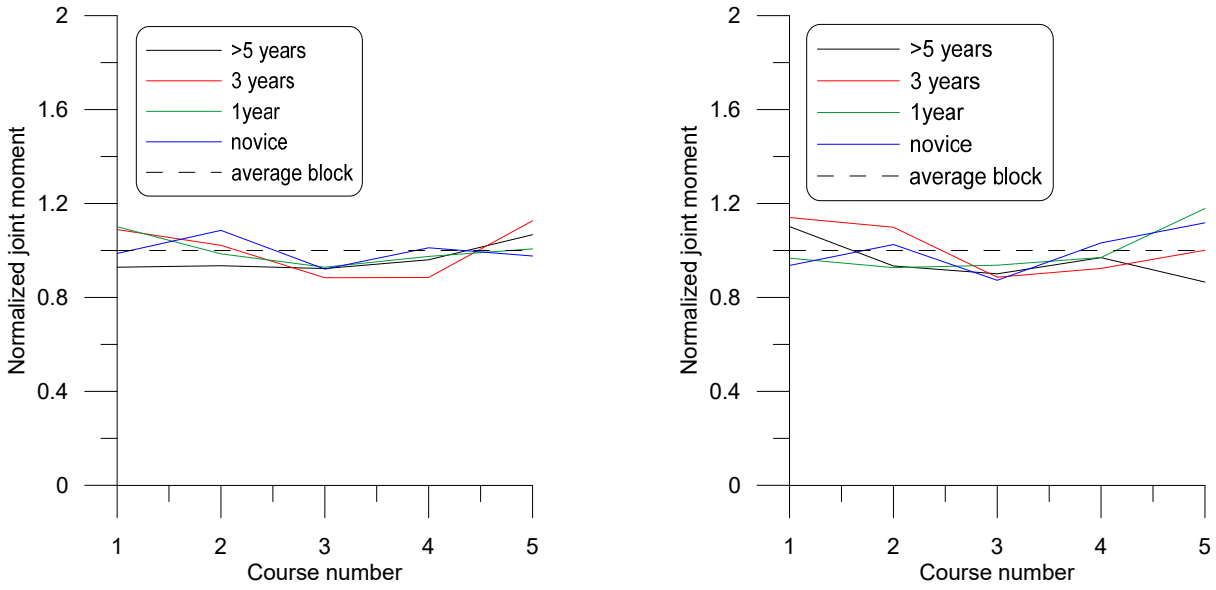

Figure 5.14: Normalized left and right hip joint moment

5.2.3 Productivity

Productivity is measured as the number of laid blocks per minute. The build quality was visually assessed at the end of each session, all walls were in an acceptable state by the end of the task. Novice group laid an average of 0.67 block per minute. The one-year

experienced apprentices laid an average of 0.99 blocks per minute. Apprentices with three years of experience laid an average of 1.23 blocks per minute. Journeymen group laid 1.8 blocks per minute. An association between experience and productivity is apparent from these results, as blocks laid per minute increase with experience.

Table 5.3: ANOVA analysis for biomechanical loads and moments

Group \ Parameter	L4/L5 Comp	L5/S1 Comp	L5/S1 Mom	SCJ Mom	L. Elbow Mom	R. Elbow Mom
Novice		∗			∗	⋆
1-Year		⋆			∗	∗
3-Years	∗	◦∗			∗	•∗
Journeymen	⋆	•⋆			•◦⋆	⋆◦
Group \ Parameter	**L. Shlder Mom**	**R. Shlder Mom**	**L. Hip Mom**	**R. Hip Mom**	**L. Knee Mom**	**R. Knee Mom**
Novice	∗	⋆		∗	◦∗	◦⋆∗
1-Year		⋆		⋆	•	•∗
3-Years	∗	•◦∗		◦∗	∗	•∗
Journeymen	•⋆	⋆		•⋆	•⋆	•◦⋆

•Significantly different from Novice group (p-value <0.05)
◦Significantly different from 1-Years group (p-value <0.05)
⋆Significantly different from 3-Years group (p-value <0.05)
∗Significantly different from Journeymen group (p-value <0.05)

5.3 Discussion

An initial goal of this effort is to determine the critical joints in body segments. Trunk segment analysis resulted in the tracking of four parameters, two compression forces and two joint moments. The results revealed that two of these parameters are enough to analyze trunk loads. It was found that the L5-S1 and L4-L5 joints experience the same force profile; however, the L4-L5 joint experiences higher compression forces. Thus, it is safe to use L4-L5 joint compression force to analyze low back forces. Similarly, the Sternoclavicular and L5-S1 joints moments exhibited the same behavior; however, the L5-S1 joint experienced higher moments, thus it can be used to analyze low back joint moment. Limb joints demonstrated differences among joints along the same dynamical link, such as shoulder and elbow. Moreover, differences were found between the dominant and non-dominant sides of the joint. Hence, all limb joints must be analyzed.

NIOSH equation for the design and evaluation of manual lifting tasks [43] recommends that the maximum carried load should not exceed 23kg because it will generate a disk compression force over the safe action limit (AL) set at 3.4kN. Compression forces lower than the action limit can be carried with low risk of injury by 99% of men and 75% of women [172]. However, only 1% of women and 25% of men are capable of carrying loads above the maximum permissible limit (MPL) of 6.4kN. The range between AL and MPL

is considered a high-risk zone for low back injuries, hence, workers should minimize the time spent in this region, if avoiding it prove unrealistic.

In the case of masonry, carried loads are lower than 23kg; however, the average low back compression forces shown in figure 5.4 indicate that workers consistently experience forces in excess of AL, which is in agreement with Faber et al. [97]. Although the compression forces do not exceed MPL, the risk of developing low back injuries is significant. Chaffin and Park [49] conclude that high stresses must be avoided in low back because they increase the risk of disc degeneration and that repetitive work at lower stresses is a potential hazard. Masonry work is repetitive, hence, lowering the stresses on the low back must be an objective to decrease the incidence rates of injury. In conclusion, while the loads carried by masons are safe, material handling techniques are not.

Comparing the four experience groups in figures 5.4 and 5.5, journeymen past the five years experience mark seem to adopt safer techniques and achieve the lowest compression forces and joint moments. In agreement with Plamondon et al. [102] and Plamondon et al. [101], novice workers experience similar low back joint compression forces and moments to those of journeymen. On the other hand, apprentices with three years of experience undergo elevated joint compression forces and moments compared to other groups. We note that lower joint moments indicate lower energy expenditure to complete a task.

Apprentices with three years of experience also undergo significantly higher shoulder

joint moments, figure 5.6, than journeymen. Novice workers exert higher moments in the non-dominant hand, which indicates that they are carrying the loads non-isometrically. Journeymen, on the other hand, have similar values for both shoulders. They are also the group with the least moments.

The elbow joint, figure 5.7, undergoes increased levels of moment with course height but lower values than the shoulder joint due to the shorter moment arm of the elbow joint. Journeymen experience significantly lower elbow joint moments compared to all groups which indicates that journeymen are shortening the moment arm further by carrying the loads closer to the body. Apprentices with three years of experience show the highest dominant arm joint moments among all groups.

Lower limbs joint moments show more variation among the experience groups compared to trunk and upper limbs, which indicates that experience affects the way masons load their hips and knees. Hip joint moments, figure 5.8, indicate that all groups maintain a similar level of activity in the non-dominant side while significant variations occur on the dominant side. The journeymen group has the least hip joint moment. On the other hand, the knee joint moment patterns, figure 5.9, show no clear distinction between the dominant and non-dominant sides.

In conclusion, apprentices with three years of experience underwent higher joint forces and moments than all other groups while journeymen experienced the least forces and

moments. The one-year apprentice group had the second highest loads followed by the novice group. It appears that journeymen have developed techniques to minimize energy expenditure and maximize safety.

The similarity between loads of expert and novice groups comes at the cost of lower novice productivity. Although novices work safely, they produce less than half the experts. A novice mason is not yet trained to handle blocks. Fear, anxiety, and inexperience make novices more careful in handling blocks than 1 and 3 years apprentices. This explains the safer method of work novices adopt compared to 1 and 3 years apprentices. However, it is important to note that novice techniques are not a desirable outcome.

We hypothesize that workers tend to prioritize safety early in their career. As their skills improve and they become more proficient and efficient, they do not maintain ergonomic safety. During the experiments, apprentice participants appeared to be in competition with their peers and more experienced mason to show that they can complete the task in a similar time frame. Verbal communications with participants showed that peer pressure on the job leads them to exert more effort to match the seniors' production level. In turn, it leads apprentices to manage loads in ergonomically unsafe manners increasing compression forces and joint moments.

The effect of course height was examined by normalizing each participant's joint compression forces and moments with respect to the participant's average across all 45 blocks.

This representation was adopted to elucidate variations in the body force profile across different courses. The lower back joints and the sternoclavicular joint showed similar patterns, figures 5.10 and 5.11, where the first course required masons to exert up to 35% more forces and moments except for the journeymen group who exerted average force and moments indicating that this group utilizes a squatting technique.

Shoulder and elbow joint moments increase with course height, figures 5.12 and 5.13, in tune with other studies that reported elevated muscles activity with the increase of work height [94, 173, 174] and associated shoulder injuries with elevated work height [19]. Moreover, the non-dominant shoulder joint moment showed significantly higher excursions away from average compared to the dominant side for the upper courses. This result is in agreement with Anton et al. [94] results who showed that non-dominant upper trapezius muscle exhibited $40 - 50\%$ more muscles activity compared to the dominant side for the higher courses.

The dominant side of the elbow showed significantly higher values compared to the non-dominant side. The load distribution between the dominant and non-dominant sides of the shoulder and elbow joints appear related to block carrying technique. Participants utilized the dominant arm to support the bottom of the block while guiding it using the non-dominant arm. This was most pronounced for journeymen as shown in figures 5.12 and 5.13.

Lower courses requirements were below average while higher courses were significantly above average which suggests a need to limit the work height to hip level. In particular, the fact that the normalized dominant elbow and non-dominant shoulder in journeymen showed larger excursions from average for the higher courses indicate that there work techniques were optimized for lower courses.

Knee and hip joint moments, figure 5.14, did not significantly change among all groups in all courses. This indicates that course height has limited effect on the lower limbs. Moreover, although it is not significantly different journeymen exerted less than average in almost all course except the fifth course.

In conclusion, journeymen do not only experience the minimum amount of forces and moments in the lower back, but they also maintain similar levels of forces across different courses. This indicates that journeymen are adopting techniques that offsets the effect of course height. Moreover, all groups were found to exert minimum forces and moments in the third course indicating that working above the knee and below hip level is the desirable.

The differences among the mean joints' loads in different experience groups were examined for statistical significance using analysis of variance (ANOVA) test. A confidence interval of 95% was used as a measure of statistical significance. The results are shown in table 5.3. The analysis confirms that experienced group is significantly different (p-value < 0.05) than at least one of the less experienced groups for all joint loads except for L5/S1

and SCJ moments. In particular, the L4/L5 joint compression forces in journeymen were significantly different from those of the 3-years group only. Furthermore, L5/S1 compression force in the journeymen group was significantly different from both novices and 3-years group.

As expected journeymen laid more blocks per minute than all other groups, followed by three-year apprentices. However, as the experience increases, figure 5.15, the increase in productivity is accompanied by an increase in three other parameters: the number of injuries reported, with the same employer, and low back joint compression and moment. While the increase in production is a desired outcome, the other three parameters are not. Ideally, it is desirable that apprentices gain proficiency, safety, and productivity over the course of their training while lowering joint loads and injury rates. However, this is not the case.

Instead, injury rate increase with experience reaching a peak apex at three-years experience, after that injury rate decreases [11, 12]. The increase in injury rate is accompanied by an increase in low back forces and moments up to three years experience which then decreases for journeymen. The relationship between experience and low back compression forces and moments takes an inverted U-shape following Yerkes and Dodson law [175]. It states that variation of stimulus on a subject is highly related to change in behavioral task performance, where the apex performance is achieved at the right amount of stim-

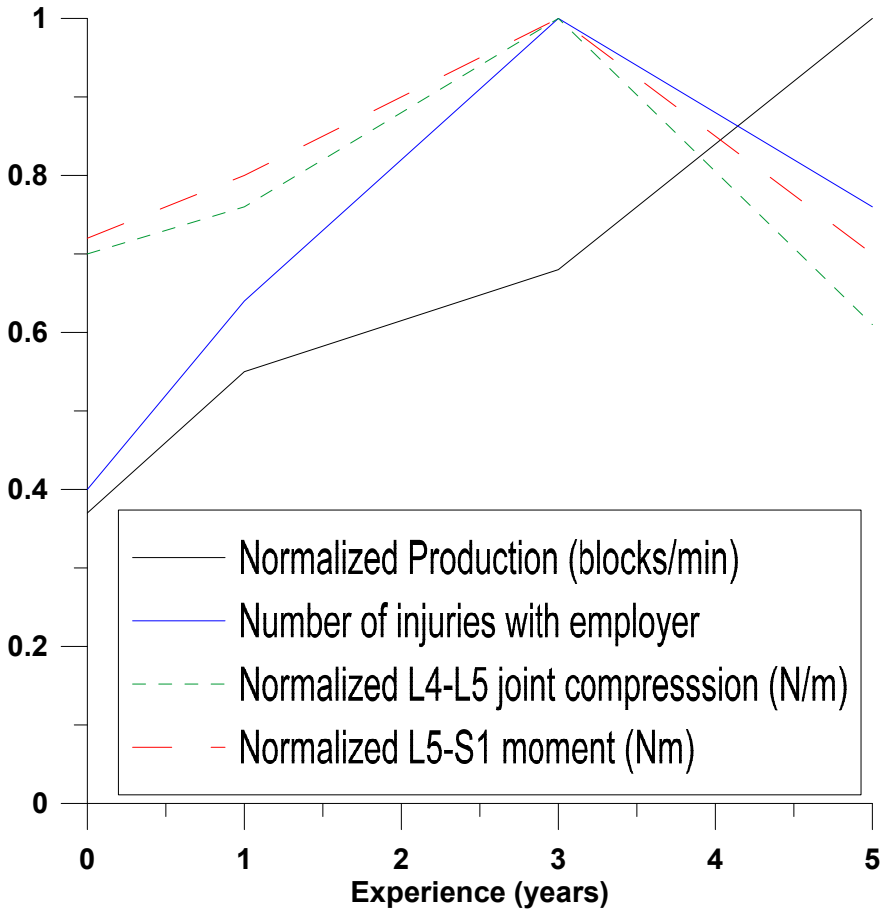

Figure 5.15: Productivity, injuries, and low back joint force and moment as functions of experience

ulus. Moreover, under or over stimulus lead to a decrease in performance. The stimulus of peer pressure on apprentices during their five-years training leads some apprentices to sacrifice ergonomic safety to achieve productivity and proficiency. Apprentices who survive this apex tend to learn, in the process, work techniques that allow them to cope with the stimulus and achieve the objective of increased productivity while maintaining ergonomic

safety. This supports the hypothesis that at the five years mark, journeymen adopt work techniques that decrease the forces on their body segment and increase productivity; hence they remain active on the job.

When masons first enter the workforce, they intuitively adopt postures that generate similar levels of joint forces and moments to journeymen. As a result, ergonomic safety levels for novices and journeymen are approximately the same. However, productivity is a key parameter in the industry and must be considered when designing interventions [176, 177]. Journeymen lay more than twice as much blocks per minute as novices. Although novice are working safe, their method of work is not an objective target. Apprentices who learn to mimic the journeymen group to work with minimal forces and moments will potentially achieve proficiency and ergonomic safety and, thereby, productivity and longevity in the workforce.

It is feasible to develop tools to automatically detect the ways journeymen perform their tasks and train novices how to mimic them. Current technology allow for online measurement of body segment inertial properties such as rotational acceleration and velocities. These parameters can be used to create classifiers that can detect, on-site, whether a novice is performing the job like a journeyman and alert them, if not.

5.4 Conclusion

A controlled experiment involving the building a 12×6 blocks wall was carried out to examine the relationships among masons' experience, safety, and productivity. Twenty-one participants distributed in four groups with different experience levels ranging from novice to more than five years of masonry work took part of the study. A combined biomechanical-productivity analysis was conducted to evaluate stresses on masons' major body joints and to assess productivity.

Results show that experience has a significant effect on productivity as journeymen laid more than twice the blocks per minute as novice masons. Novice and experienced journeymen bear lower joint forces and moments compared to one and three-years experience groups. Moreover, in agreement with Plamondon et al. [102] joint compression forces and moments were the lowest in journeymen group. Journeymen appear to develop a technique which allow them to be more productive and safe compared to other groups. The three-years experience group sustained the highest joint compression forces and moments. This correlates well with the U.S. Bureau of Labor Statistics [11] finding that workers with three-years experience with the same employer sustained the highest injury rate.

Unlike less experienced groups, journeymen appear to adopt a method of work that maintains similar joint forces and moments across all course heights. Furthermore, in

agreement with Faber et al. [97], the analysis on the effect of course height showed that working on the third course, approximately hip level, generated the least joint forces and moments among all experience groups. This suggests that improvements can be made in bricklaying systems to reduce stresses experienced by masons.

Comparing the performance of masons at all four experience levels suggests that workers who learn to manipulate blocks in an ergonomically safe and productive manner by the five years experience mark enjoy a long-term career. On the other hand, during their first five years workers gain proficiency and productivity at the cost of safety leading to increased rate of injury and lower retention rates.

There is potential for training apprentices to excel in all three aspects: proficiency, productivity, and ergonomic safety. This will help improve workers' welfare and retention rates. More studies are needed to develop those training methods and to extend the use of combined safety-productivity analysis in masonry and other trades. Furthermore, it is recommend to recruit of more participant with a view to improving the confidence level of the results.

Chapter 6

Identifying Safe and Productive Masons Using Machine Learning

This chapter describes the results of implementing machine learning algorithms to classify masons' kinematics based on their level-of-experience.

6.1 Machine learning applications for motion classification

On-site kinematic data collection allows researchers to implement automated systems to track workers' motion for training and safety. The use of machine learning algorithms and data analytics is on the rise for such applications. Machine learning and data mining techniques call for defining features that differentiate and separate actions from each other to create a classifier. The uniqueness of these features determines the accuracy of the classifier. The input to these classifiers is extracted from either IMU or image-based data collection methods.

Examples of using machine learning are found in the literature for various applications. Reddy et al. [178] used a decision tree and the discrete hidden Markov model (DHMM) to classify the transportation mode using GPS and acceleration data extracted from a smartphone. They achieved an accuracy of 93.6%. Akhavian and Behzadan [179] used acceleration data from a smartphone to perform activity classification of construction workers, such as sawing, hammering, and turning a wrench, in a controlled environment. They compared the use of artificial neural network (ANN), a decision tree, K-nearest neighbor, logistic regression, and support vector machine (SVM) classifiers. They demonstrated an ANN algorithm able to classify activities with an accuracy up to 97% [179].

Joshua and Varghese [78] used a wired accelerometer mounted on a masons' waist to perform masonry activity tracking. They were able to classify three activities: (1) fetch and spread mortar, (2) fetch and lay brick, and (3) filling joints with an accuracy up to 80%. Ryu et al. [84] used a wristband equipped with an accelerometer to perform activity classification in masonry work. They compared the use of K-nearest neighbor, multi-layer perceptron neural network, and support vector machine classifiers, and achieved an accuracy of more than 97% using a multi-layer perceptron neural network.

Machine learning and data analytics are also used in the other fields in order to classify actions. For instance, Namal et al. [180] used 12 accelerometers to detect, analyze, and classify soccer players gait. Senanayake et al. [181] used neural network to assess the rehabilitation process of the Anterior Cruciate Ligament (ACL) injury. Ahn et al. [182] used K-nearest neighbor, naive bayes, decision tree, and multi-layer perceptron classifiers to measure the operational efficiency of construction equipment using accelerometers. They achieved a classification accuracy of more than 93% for all classifiers except naive bayes.

SVM classifiers have been found efficient and accurate for classification, in general, and for binary classification, in particular [183]. SVM finds the boundaries among classes in the form of hyperplanes to separate various classes. They overcome the overfitting problem that typically encountered when using other classification techniques, such as artificial neural networks

Machine learning has been widely used in construction recently. The applications of machine learning and data analytics in construction settings tend to be activity recognition, automation, and productivity analysis. Unprecedented opportunities have materialized to create real-time classifiers for safety applications. To date, no study has explored the effect of experience on workers' motion kinematics and its relations to safety and productivity. However, studies that compare different levels of experience are found in sport and gaming literature [167, 168, 184–186]. Expert players are shown to have better motion execution skills [185]. Moreover, Karimi et al. [187] showed the importance of experienced workers in lowering the number of injuries in workplaces. Their analysis revealed that methods have to be developed to solve the shortage in craft workers to limit the number of injuries. Furthermore, in Chapter 5, it was shown that indeed journeymen workers are more productive and safe than novice and apprentices [17]. Thus, this chapter uses SVM to classify masonry work into (1) expert (safe and productive) and (2) inexpert (less safe and productive).

6.2 Methodology

The framework identifying expert vs. inexpert operations of masons is illustrated in figure 6.1. The proposed methodology for masons' classification consists of four steps: (1) data collection using an IMU-based sensor suit, (2) pre-processing to filter out noise and

prepare the dataset as input for generating the classification model, (3) pose codebook generation to represent activity sequences in a comparable form, and (4) training engine development to generate SVM supervised learning algorithm. The framework is used to categorize sequences, the process of laying a block, based on the level of expertise. The set of sequences comprising the building of a wall is termed an activity. Data collection is explained in Chapter 5.

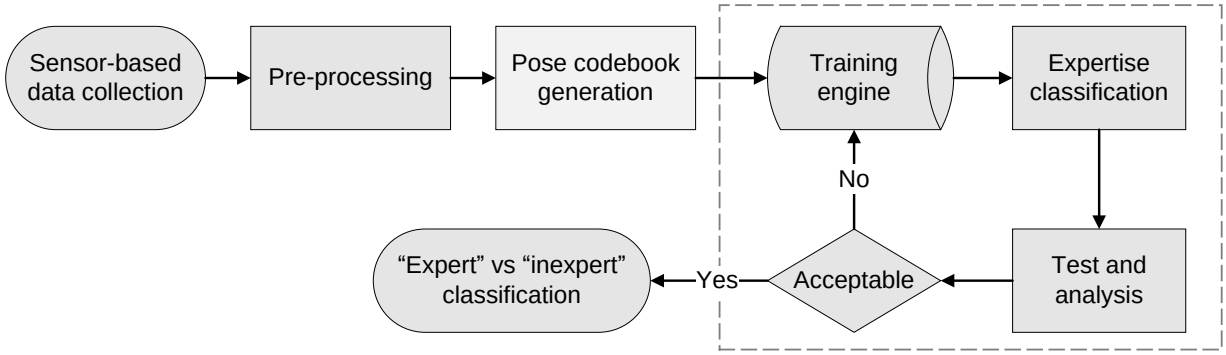

Figure 6.1: Overview of the proposed methodology for safety and productivity classification of masons.

6.2.1 Body Model

The data is exported from the suit to create a body skeleton estimate at discrete time increments using the algorithm described in Chapter 5. The sensor fusion scheme, therefore, allows the calculation of the position, velocity, acceleration, orientation, angular velocity and acceleration of each joint with respect to a global reference coordinate system. A

subset of body joints was selected, based on heuristic analysis to fully represent masonry activities and to decrease dimensionality, shown in figure 6.2.

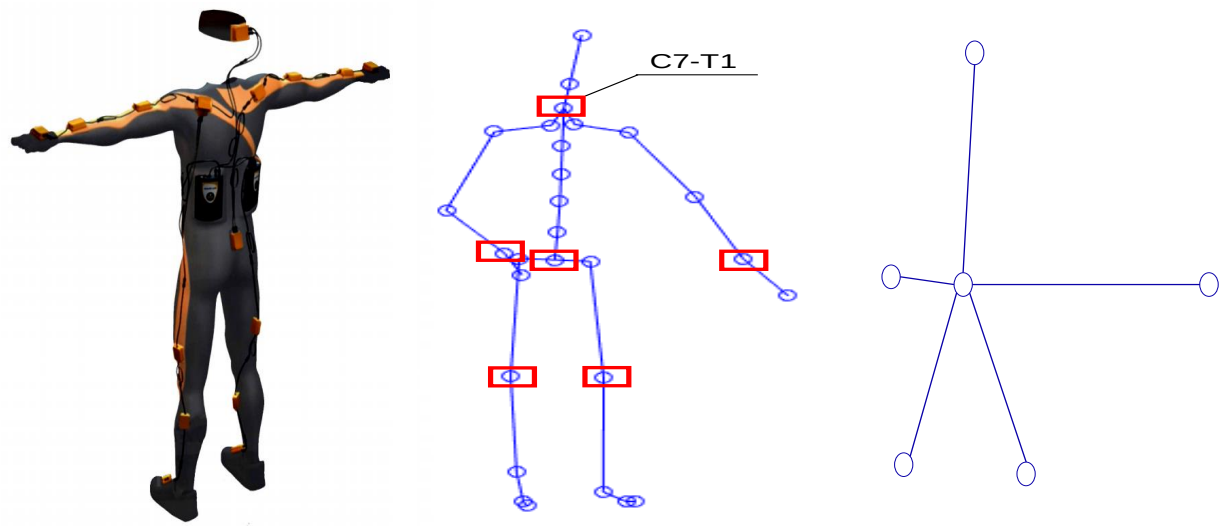

(a) IMU suit. (b) Full body model. (c) Simplified body model.

Figure 6.2: Sensor-based body suit for data collection [2].

The global reference coordinate system is a right-handed Cartesian coordinate system. The local joint coordinate systems follow the International Society of Biomechanics (ISB) standard [188, 189]. The classification methodology uses posture data from each sequence as its feature set and hands' force data to aid in isolating activity sequences relevant to bricklaying during the pre-processing and conversion of raw data to postures suitable for codebook generation and classifier training.

6.2.2 Pre-processing

A major challenge in the analysis of 3D motion data is the sheer variation in motion types and gestures that participants perform during a task. The pre-processing phase reduces the dimensionality of the dataset, converts joint absolute motion into relative motion to make activity sequences more comparable, and segments the dataset to include only data strictly belonging to bricklaying.

The sequence of joint position data collected by the motion suit represents the trajectory of joint features through space and time. This trajectory is approximated using a Kalman. It averages out irregularities due to sensor error (drift). To efficiently train the learning algorithm, the data dimensionality is reduced by selecting a representative subset of joint features, key joints. The selected key joints meaningfully capture worker posture (pose) at each frame, shown in figure 6.2c. Hand force data is used as an additional input feature to trigger start and end of activities. Segmentation is carried out by using the presence of non-zero hand force to indicate the beginning and end bricklaying. Thus, the pre-processing step prepares the data set for the codebook generation.

6.2.3 Pose Codebook Generation

The pose codebook is composed of the set of dominant poses, most frequent, within the entire activity dataset. These dominant poses are determined using the simplified key-joints data in the activity sequence. The simplified pose graph is comprised of the locations of the knee and wrist joint centers with respect to mid-hip point as shown in 6.3. This simplified stick figure is able to capture relevant masonry postures such as bending and kneeling. For illustration, a hypothetical example of codebook generation for an activity dataset is shown in figure 6.3. It consists of two steps: pose segmentation using k-means clustering and histogram creation as the codebook for activity representation. In figure 6.3, simplified poses are clustered into k clusters using k-means clustering approach. Blue poses are the original poses, while colored poses represent the cluster statistical centroids corresponding to the k bins of the histogram generated as the codebook.

Pose Segmentation

Each sequence is categorized into a number of clusters for segmenting various poses. In this analysis, k-means clustering [190] is used for pose segmentation. The number of clusters (k) used to segment poses identifies the number of dominant poses for the construction activity. For example, the dominant tasks in bricklaying include: walking, picking, carrying, placing, spreading mortar, etc. A typical example for pose segmentation using k-means clustering

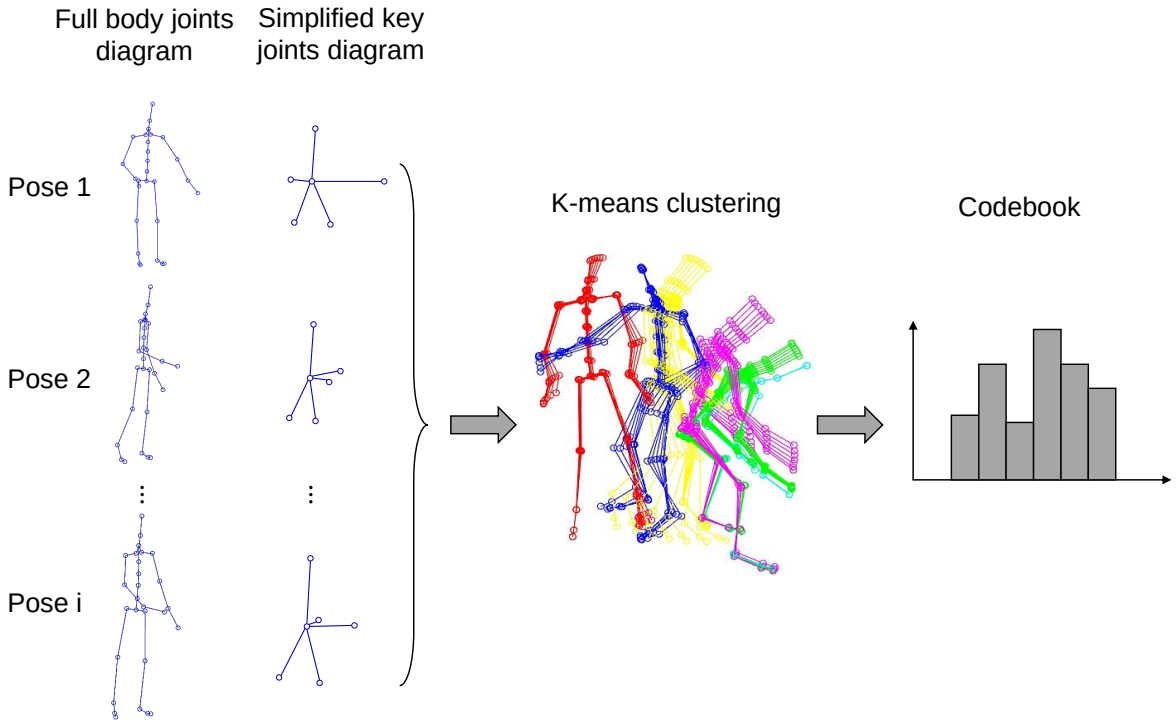

Figure 6.3: Codebook generation for a set of poses.

is shown in figure 6.3. In this example, the number of clusters is set to (k=6). While pose segmentation is carried out on the simplified key joints diagram, figure 6.3 is visualized using the full joint body diagram. Once clustering is performed, the statistical centroid of each cluster represents the exact dominant pose being segmented. Poses in figure 6.3 represent the centroid of the clusters that correspond to the dominant poses.

In the pose segmentation step, activity analysis resolution is directly related to the number of clusters. In other words, if more clusters, bins, are forced to be detected, the sequence will be represented by more dominant poses and it is analyzed more comprehen-

sively. This value is one of the effective variants on the final training results, which is further investigated in this analysis. The output of the pose segmentation step is fed as an input for the codebook generation step.

Histogram Creation

Once each frame is clustered and the dominant poses are segmented, a histogram is generated as the codebook for each sequence 6.3. The number of bins used for creating the codebook equals the number of dominant poses used in the previous step. Instead of representing a sequence with a volume or a trajectory, the algorithm represents it as a set of features extracted from the volume and the trajectory. 3D volumes are viewed as rigid objects; common patterns are extracted to represent them. For filling the bins in the histogram, each pose is assigned to its nearest dominant pose, centroid. This step is performed by calculating the Euclidean distance of each pose to each dominant pose in pose space. The pose is then assigned to the bin of its nearest centroid. This histogram is used as a codebook representing a sequence in terms of an arbitrary number of dominant poses. The pseudocode for codebook and sequence representation is summarized in 1. The histogram generated in this step is used to train a classifier. The training engine and its components are explained in the following section.

Input: Sequence $S = p$, where p are the measured poses.
Output: Codebook (H): histogram for sequence S representation.
Null $H \leftarrow \varnothing$
$k \leftarrow user$ input
Cluster: S into k clusters using k-means and Euclidean distance
Such that: $S = \bigcup_{i=1}^{k} S_i$ and $\bigcap_{i=1}^{k} S_i = \varnothing$
For $i = 1$ to k
Assign the clusters to bins: $H_i = ||S_i||$
Populate the histogram: $H = H \bigcup H_i$
End For
Report H

Algorithm 1: Codebook generation for sequence representation.

6.2.4 Training Engine

The codebook is the key metric for training a safety, productivity, and expertise classifier. The codebooks, one for each sequence, are imported as inputs to the training engine. As shown in figure 6.4, the training engine tested in this analysis includes the following sub-processes: (1) sampling and labeling, and (2) support vector machine (SVM) training.

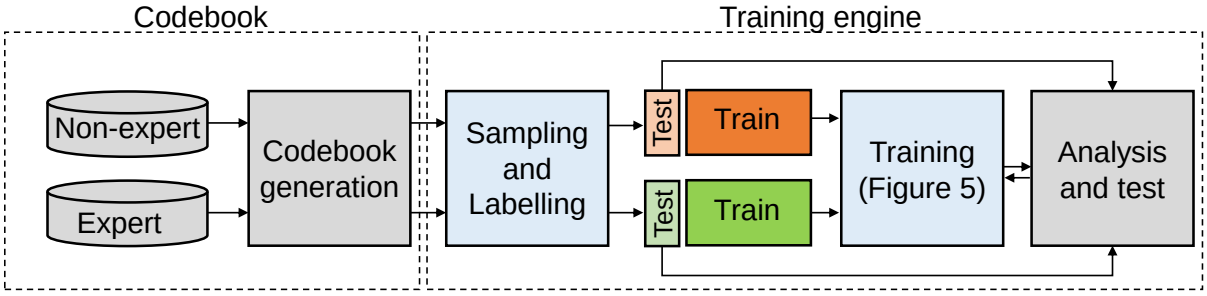

Figure 6.4: Overview of the training engine with the codebook inputs.

Sampling and Labeling

The sequences are grouped and labeled as expert and inexpert. Then, the data is sampled from these groups and a codebook is generated for each sample as illustrated in figure 6.4. Typically, a large proportion of the data (e.g. 70-80%) is sampled for training the classifier, while the remaining samples are used for testing the accuracy of the trained classifier.

Support Vector Machine (SVM) -based Classification

A hypothetical example of the SVM-based classification is shown in figure 6.5. In simple words, samples used for training are used to identify the separating boundary between the two classes (i.e. expert vs. inexpert). The testing samples are then used in order to measure the accuracy and the error of the trained classifier.

6.3 Results and Discussion

In order to measure the performance of the proposed framework for classifying the level of expertise, and to verify the effective variants on the classification results, a set of experiments was carried out. The proposed methodology for expertise classification was implemented in a MATLAB-based environment. Time-related aspects of the proposed

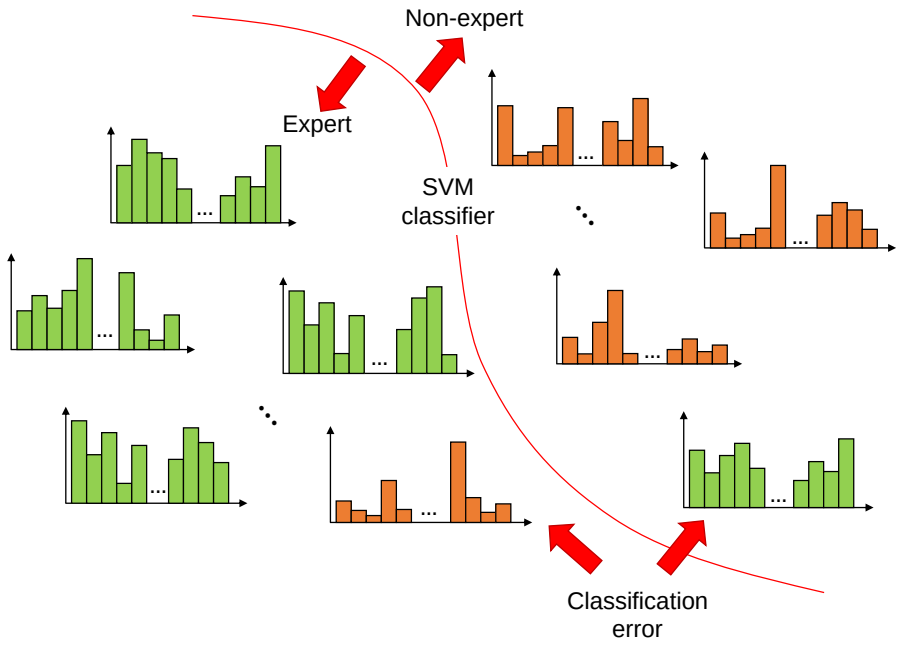

Figure 6.5: Overview of the training engine for a binary classification.

methodology were conducted on a machine with a 2.4×8 GHz processing unit and a 16 GB RAM.

6.3.1 Performance Metrics

Two parameters were used to verify the efficiency of the proposed methodology and to measure its performance: classification accuracy and processing time required for training. These metrics are investigated and compared under various circumstances.

6.3.2 Classifier Performance

At the training stage, we used annotated and labeled data consisting of sequences of body joint feature vectors which capture the frame-by-frame state of workers during bricklaying. These input sequence can vary in length. The joint feature vector comprises the set of key joints described in figure 6.2. Two scenarios were considered for the level of expertise classification. The structure and architecture of the training engine used in classification are illustrated in figure 6.6. Following a description of the two scenarios.

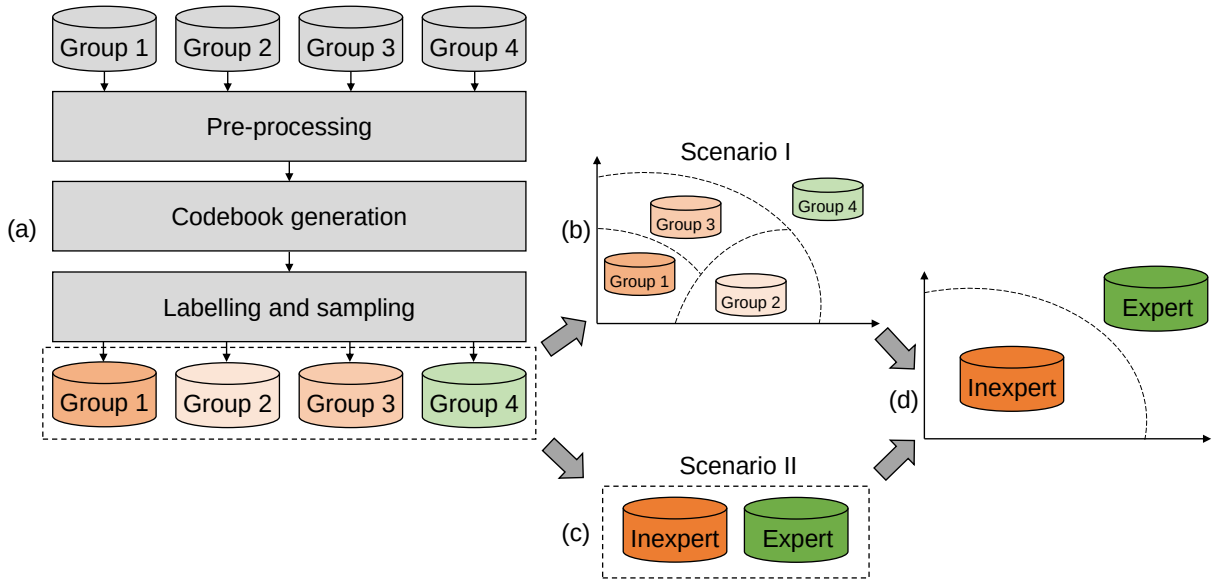

Figure 6.6: Database structure and architecture of the SVM-based classifier for the two scenarios.

Scenario 1: Multi-class Classification

A multi-class SVM classifier is trained for identifying the boundaries between the four groups as different classes. First, the preprocessed data is classified into four classes using a multi-class SVM-based classifier, shown in figure 6.6b. The first three classes are then merged into the inexpert class, and Class 4 is considered as the expert class as shown in figure 6.6d. Results of the classification step are then tested and analyzed in terms of accuracy and error.

Scenario 2: Merged Classifier

Group 1, 2, and 3 are merged and annotated as inexpert for binary classification. The groups are proportionally sampled and merged into the inexpert group, while Group 4 represents the expert group. A binary SVM-based classification is then performed to identify the boundary between the two classes. In this scenario, the classification results may be impacted by the uneven (imbalanced) sampling resulting from the skewed dataset of the expert vs. inexpert group. Results of the classification steps using the two scenarios explained here, are provided in table 6.1.

Table 6.1: Summary of the results using the two scenarios

Scenario	Number of clusters	Dataset % for training	SVM kernel	Accuracy (%)	Processing time (s)
I	50	70%	Linear	91.23	524
II	50	70%	Linear	92.04	13

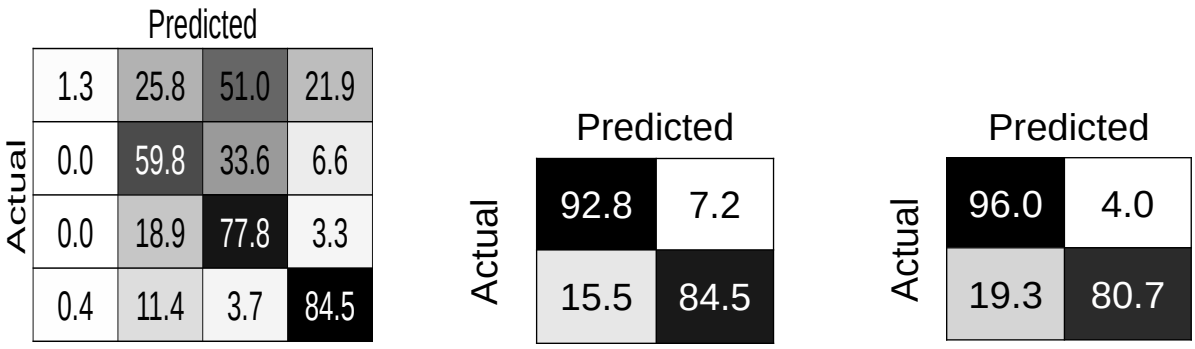

(a) Scenario I. (b) Scenario I. (c) Scenario II.

Figure 6.7: Confusion matrices for the classification scenarios.

As seen in table 6.1 and figure 6.7, both scenarios are similar in terms of the classification accuracy. However, Scenario 1 is computationally more expensive and requires longer processing time. Another notable observation is the poor classification results for the novice masons, Group 1, in training the SVM classifier, shown in figure 6.7a. The reason of the poor training is that the novice masons do not inherently follow a specific pattern, and this phenomenon results in a scattered pattern in their codebooks. Also, one of the novices had significant experience in other forms of physical labor. Therefore, the classifier is unsuccessful in identifying a distinctive boundary for such random and unstructured patterns.

To compare the classifiers' performance trained in Scenario 1, their receiver operating characteristic (ROC) curves are reported in figure 6.8. ROC is a measure for the trade-off between true and false-positive classification [191]. A ROC curve that passes throw the

point where the true positive rate is 1 and false positive rate is zero is considered ideal. The classifier trained for Group 4 outperforms the other classifiers. This is because of the distinctive pattern Group 4 adopts in performing tasks. On the other hand, ROC also confirms the poor performance of the classifier for the novice group due to their random and unstructured patterns, as previously discussed .

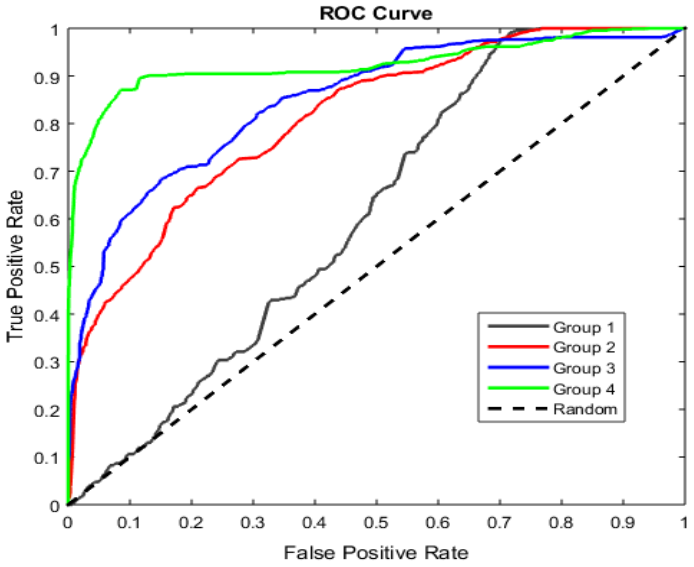

Figure 6.8: Receiver operating characteristic (ROC) curves for the classifiers trained in Scenario 1.

6.3.3 Effective Variants on Classification Results

Two parameters that affect the classification accuracy and processing time are evaluated: the number of clusters used for codebook generation is and the SVM kernel used for the

classification step. In both cases, the verification metrics are recorded for comparison. A summary of the results is presented.

Number of Clusters for Codebook Generation

The number of bins used for clustering is varied in a range between 10 to 100. The accuracy of the classifier and the required processing time for training and classification are reported in table 6.2. Confusion matrices are also reported in figure 6.9, in order to compare the performance of the SVM classifiers.

Table 6.2: Effect of number of clusters on the verification metrics for Scenario 2 and linear kernel for SVM classification.

Number of clusters (bins)	Accuracy of the classifier	Processing time (s)
10	84.79	2
25	85.55	4
50	92.04	13
75	92.63	26
100	92.11	32

As shown in table 6.2 and figure 6.9, 10 and 25 clusters achieve poor classification accuracy compared to 50, 75, and 100 clusters. Moreover, when the number of cluster is > 50 no significant difference in accuracy is observed. A larger number of clusters improves the accuracy of the classifier as a result of increasing the resolution of dominant poses in the sequences. On the other hand, the process of calculating more clusters (bins) is computationally expensive, since it requires calculating more cluster centroids and therefore more

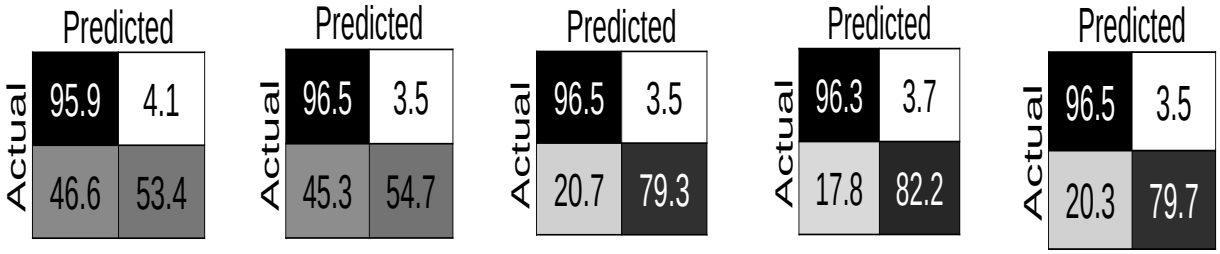

(a) 10. (b) 25. (c) 50. (d) 75. (e) 100.

Figure 6.9: Confusion matrices vs. number of clusters for Scenario 2 using a linear kernel.

distances for each step. In order to investigate the overall performance of the classifiers and the time-related aspects of the classification step, ROC curves and processing times for various numbers of clusters are shown in figure 6.10 and figure 12.

The use of 100 clusters for codebook generation offers the best performance, figure 6.10, among the numbers of clusters tested. Nonetheless, the use of 75, 50, and 25 clusters in classification offers similar performances with a slight decrease as the resolution of the activity representation decreases. However, the overall accuracy reported in figure 6.11 is slightly improved using 50 clusters compared to 75 clusters, 92.04% to 92.63%, while taking twice as much time for classification, 13 sec to 26 sec. To balance accuracy and computation cost, the default value for codebook generation was set to 50 bins.

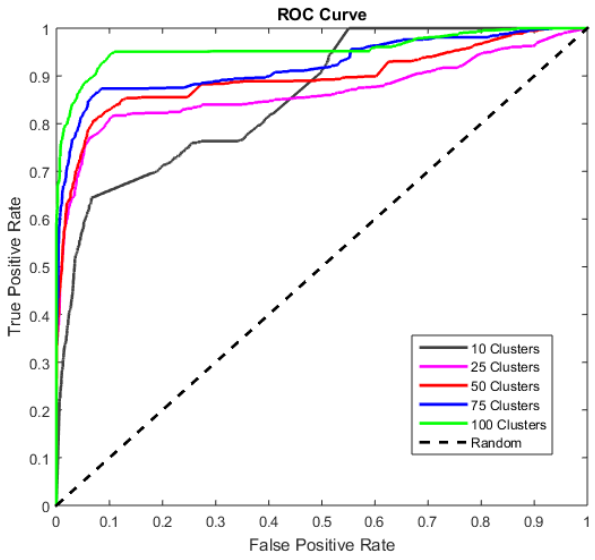

Figure 6.10: ROC curves vs. number of clusters of linear kernel.

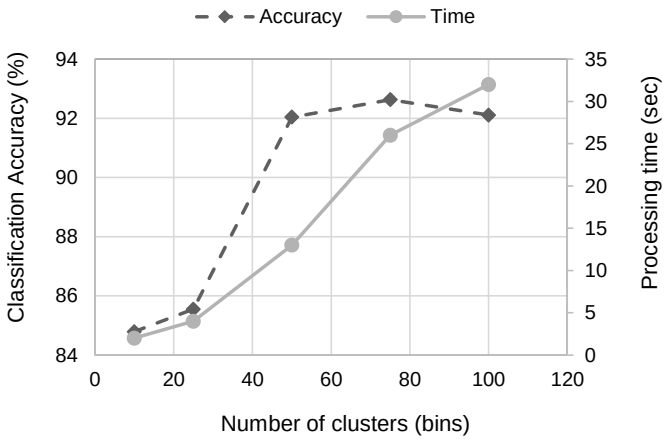

Figure 6.11: Classification accuracy vs. number of clusters vs. processing time of linear kernel.

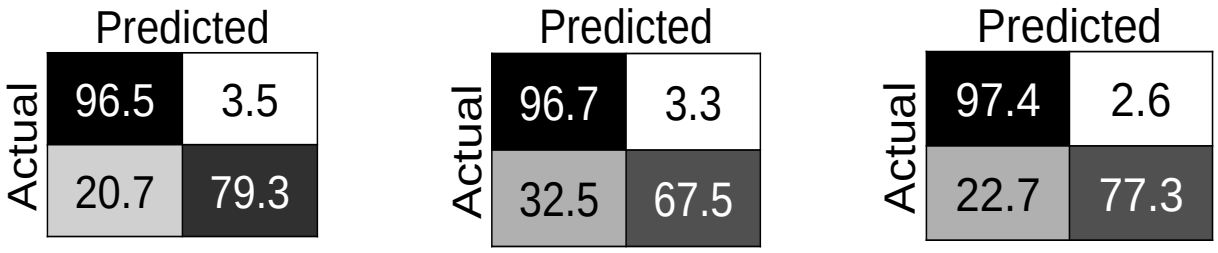

(a) Linear. (b) Gaussian. (c) Polynomial.

Figure 6.12: Confusion matrices for the classification with different kernels.

Effect of Kernels vs. Accuracy

For refining and tuning the classifier, three kernels were used in the SVM-based classification step: linear, Gaussian, and polynomial. Verification metrics are recorded and listed in table 6.3 for comparison of the kernels' performance. Confusion matrices are shown in 6.12 and ROC curves are reported in figure 6.13.

Table 6.3: Verification metrics for the three SVM kernel used for classification, Scenario 2 with 50 clusters.

SVM kernel used for classification	Accuracy of the classifier	Processing time (sec)
Linear	92.04	13
Gaussian	89.07	8
Polynomial	92.11	276

Figures 6.12 and 6.13 and table 6.3, the linear and polynomial kernels outperform the Gaussian kernel in overall accuracy. However, the required processing time for classification using a polynomial kernel is 276 sec, which is significantly higher than that for the linear kernel, 13 sec.

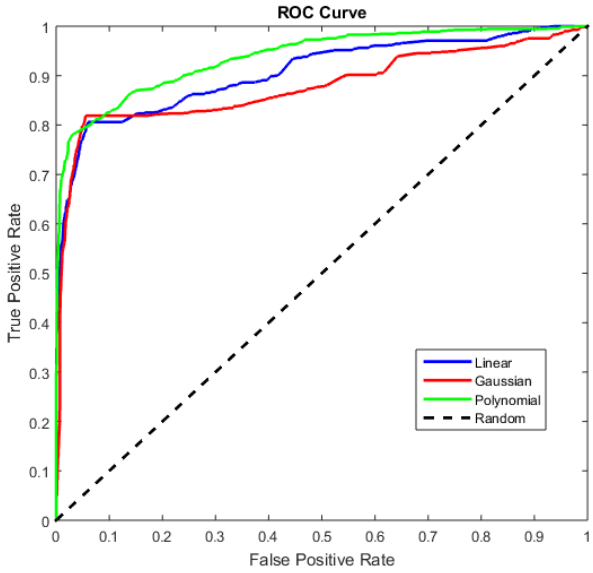

Figure 6.13: ROC curves vs. kernel.

Moreover, figure 6.13 signifies that the Gaussian kernel is less accurate than linear and polynomial kernels for classifying the masons, and the latter two kernels are similar in terms of overall accuracy. However, taking into account processing time table 6.3, the linear kernel appears to be the most effective choice for this classification.

6.4 Expert vs. Inexpert Poses

Classification histogram results showed that expert masons work in a structured fashion compared to inexpert masons as manifested by using fewer bins in the histogram shown in figure 6.14. The use of fewer bins indicates that experts move in an efficient way

that minimizes their energy expenditure compared to novices and apprentices. Moreover, inexpert masons have frequent poses that filled all bins. Keeping in mind that expert masons laid twice the number of blocks per minute as novices, the histograms indicate that inexpert masons are frequently taking poses that are not productive and potentially unsafe.

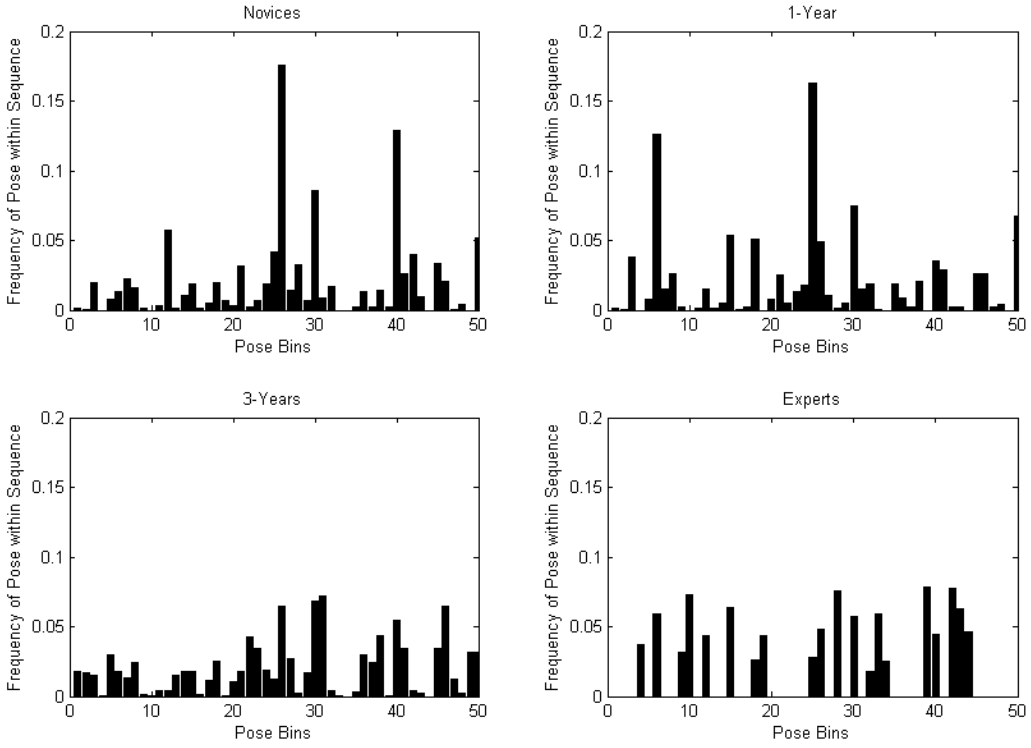

Figure 6.14: Frequency of dominant poses in all experience groups.

The dominant pose in each experience category is shown in 6.15. Expert poses represent the masons carrying a block close to the torso which decreases the loads on the lower back.

Further, poses assumed by experts tend to shift of most load carrying to the hips. The 3-year apprentice group is found to bend their back more than expert workers, which increases their lower back moment.

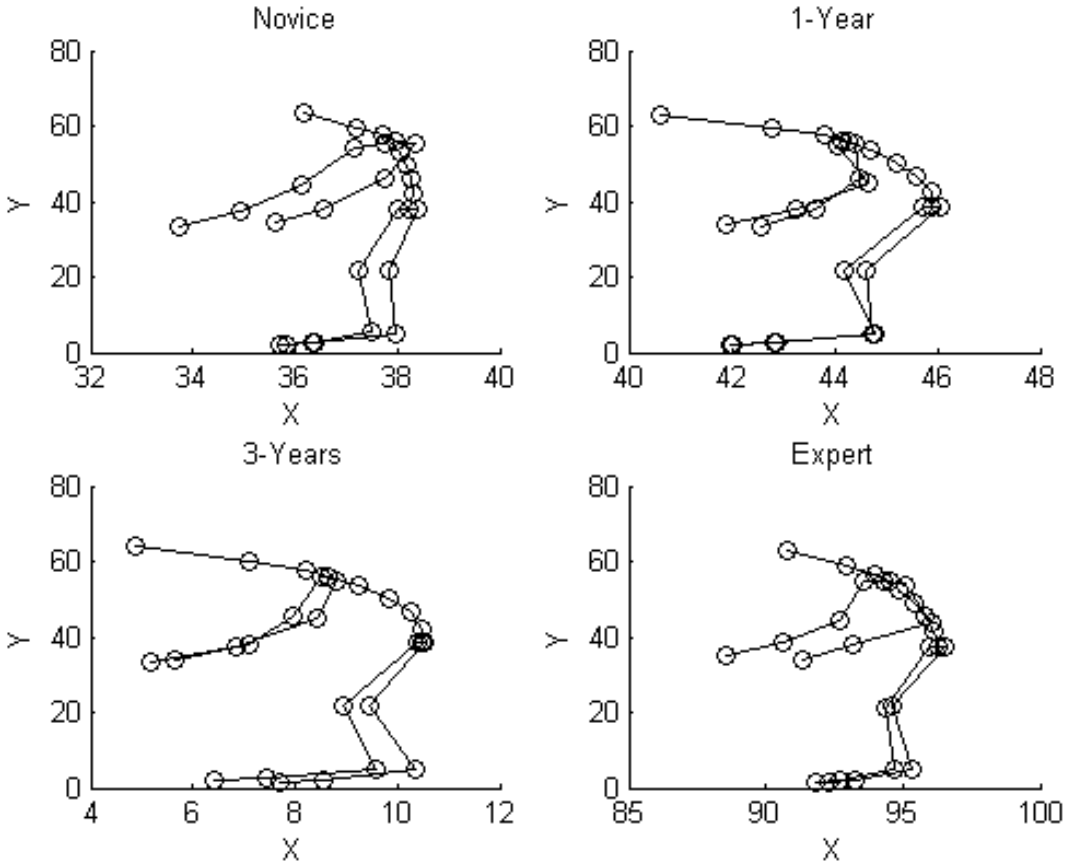

Figure 6.15: Frequency of dominant poses in all experience groups.

Since it has been shown in Chapter 5 that on average expert masons bear lower joint forces and moments than inexpert masons and produce more blocks per minute, these histograms can be used as guides to potentially alert masons whenever they perform a pose

that is not typically performed by an expert mason. With the use of simple IMUs on body segments, ergonomists can assess whether a task is conducted along the lines of an expert mason. Trade-specific expert pose histograms have to be generated to allow users to create an active learning system that can be used by workers to be informed when they perform inexpert posture. A full-list of all dominant posture is shown in figures 7.10, 7.11, 7.12, and 7.13.

6.5 Conclusion

This chapter reports on the use of a support vector machine (SVM) supervised machine learning algorithm to classify masonry workers' kinematics based on level-of-expertise. Chapter 5 established the link between expertise and improved safety and productivity. Understanding why experts are safer and more productive is the next step in this research. The classifier helps in that analysis by identifying sets of poses that result in safer and more productive work. A full-scale experiment involving masons was carried out. Twenty-one masons with varying levels of expertise were recruited into four groups: (1) novice (no related experience), (2) one-year of experience, (3) three-years of experience, and (4) more than 5 years of experience. Each participant built a 72-blocks, 6-course high, concrete masonry unit wall. Data collection was conducted using an inertial measurement unit

(IMU) suit with 17 trackers. Three video-cameras recorded all data collection sessions.

The kinematic data obtained from the IMU suit was comprised of 28 joint center locations and the corresponding joint angles, constituting a full human body model. These joint center locations were transformed from the global reference frame to a local reference frame located at the mid-point of the hip joints. A subset of body joints was selected to form a simplified model representative of masonry activities. The simplified model removes data unrelated to masonry activities. Using the video records, the kinematics data was manually augmented with hand force data and segmented to remove data unrelated to masonry activities. Data was clustered using different numbers of k-means clusters to identify the dominant postures masons assumed during the experiment. A histogram was then created to represent the frequency of each dominant posture in each sequence.

The segmented data was sampled and labeled into expert and inexpert groups for the SVM classifier training. For each group, 70% of the data was used as a training set and the remaining 30% comprised the test set. Accuracy and processing time were used as performance metrics in this study. Two classification scenarios were implemented: multi-class SVM and binary SVM. Furthermore, three SVM kernels were compared: linear, Gaussian, and polynomial.

Results show that a clear distinction exists between expert and inexpert masons motion patterns. SVM classifiers were able to identify these differences with reasonable accuracy.

The k value used in the k-means clustering was shown to have a direct relationship with the classification accuracy and computational cost. The optimal number of clusters was found to be $k = 50$, as it offers a sufficiently accurate classification and a reasonably acceptable processing time. Furthermore, the Gaussian kernel was found to perform less accurately than the linear and polynomial kernels, which had approximately similar accuracies. Therefore, the linear kernel was determined to have the most suitable balance between the accuracy and computational cost. These results show that an objective difference exists between expert and inexpert masons' kinematics that can be classified using a subset of the human posture model.

Future work includes exploring the classification performance and whether it can be further enhanced with larger numbers of participants. Furthermore, it is worth exploring the direct use of IMU raw acceleration data and whether it can enhance the classification framework. A potential application is an extension of this study's experimental design and methodology into other construction trades. The study results show a potential for using SVM classifiers on experienced workers' motion to identify safe and productive motion patterns that can then be used to train apprentice and novice workers.

Chapter 7

Conclusions, Recommendations, and Future Work

This thesis investigated the use of human body kinematics to improve workers' ergonomics with an emphasis on the masonry trade. It reported the findings of four studies: (1) a comparison of motion capture techniques, (2) a novel application of time delay embedding, (3) a biomechanical analysis of masonry work, and (4) an application of machine learning algorithms to identify masons' level-of-experience.

7.1 Direct and Indirect Motion Measurement Techniques

Two categories of motion capture techniques were compared for accuracy and usability in non-structured environments: (1) direct (electrogoniometers) and (2) indirect (vision-based). Two participants took part in this study. They performed static and dynamic tasks. The accuracy of each technique was compared to a state-of-the-art motion capture technique (Optotrak™) in terms of mean and standard deviation of absolute errors; as well as maximum and minimum errors.

The results indicate that direct measurement techniques offer higher measurement accuracy for dynamic and static postures, which can be summarized as ± 3 deg in planar motions compared to ± 10 deg for vision-based techniques. Furthermore, vision-based techniques require preparation of the environment, such as direct line-of-sight to subject and lighting conditions. These requirements are not needed for direct measurement techniques. However, direct measurement techniques become cumbersome when used for more than one degree-of-freedom.

7.2 Fatigue Detection

A novel application of time-delay embedding and phase-space warping (PSW) was deployed to detect fatigue in the lower limbs. Ten participants took part in this study. Knee flexion angle data were collected using an electrogoniometer and upper arm muscle EMG, and force data were collected using surface electrodes and force transducers. The method compares the muscle state (fatigue) to a local map of its healthy state and over time.

Results show that the PSW is capable of detecting muscle fatigue at all three signal levels: (1) kinematics, (2) force, and (3) EMG. Moreover, it showed that muscle loading patterns can be investigated using PSW. The findings show that while fatigue indices derived from non-invasive methods, kinematic and force measurements, provide an overall estimate for the state of the muscle group, fatigue indices obtained from more invasive measurement methods, EMG signals, provide a more detailed evaluation of the state of individual muscles. As a result, the latter indices can be used to study muscle participation in motion and load sharing patterns.

7.3 Relationships Among Experience, Safety, and Productivity of Workers

A combined biomechanical-productivity analysis was conducted using IMUs and vision-based motion capture techniques on masonry workers. Twenty-one subjects were classified into four masonry experience categories. Each participant laid a 12×6 blocks wall.

Results show that journeymen laid more than twice the blocks per minute as novice masons. Novice and experienced journeymen bore lower joint forces and moments compared to the one-year and three-years experience groups. Moreover, the three-years experience group sustained the highest joint compression forces and moments. This correlates well with the U.S. Bureau of Labor Statistics [11] finding that workers with three-years experience with the same employer sustained the highest injury rates. Journeymen appear to adopt a method of work that maintains similar joint forces and moments across all course heights. Furthermore, working on the third course, at approximately hip level, generated the least joint forces and moments across all experience groups.

7.4 Identifying Safe and Productive Work Using Machine Learning

A classifier was built using support vector machine (SVM) supervised machine learning algorithms applied to data collected using IMUs to capture the motion of masonry workers. Twenty-one subjects were grouped in four categories based on their masonry experience level. Each participant laid a 12×6 blocks wall.

Results show that a clear distinction exists between expert and inexpert masons' motion patterns. The k value used in the k-means clustering was shown to have a direct relationship with the classification accuracy and computational cost. The optimal number of clusters was found to be $k = 50$. Furthermore, the Gaussian kernel was found to perform less accurately than linear and polynomial kernels, which had approximately similar accuracies. Therefore, the linear kernel was determined to have the most suitable balance between accuracy and computational cost. These results show that an objective difference exists between expert and inexpert masons' kinematics that can be classified using a subset of the human posture model.

7.5 Future Work

The thesis findings justify exploration of sensor fusion techniques to combine direct and indirect motion capture systems. Just like a magnetometer functions in Inertial Measurement Units (IMUs), direct measurement techniques can be selectively used to overcome line-of-sight issues within an indirect-measurement framework.

The findings also recommend the use of PSW for applications such as rehabilitation to access hidden information about the full kinematic chain using a single kinematic signal. This approach can overcome the cumbersomeness of other techniques that require excessive subject preparation. The use of PSW can be applied to study muscle synergy to better understand the effect of fatigue of muscle recruitment using kinematic signals.

Furthermore, findings show the potential for training apprentices to excel in all three aspects: proficiency, productivity, and ergonomic safety. This will help improve workers' welfare and retention rates. More studies are needed to develop those training methods and to extend the use of combined safety-productivity analysis in masonry and other trades. The biomechanical analysis conducted in this thesis is static analysis, further dynamic analysis should be carried out to better understand the effect of motion patterns on body joint's forces and moments.

Future work should also investigate the performance of workers' classifiers and whether

they can be enhanced with larger numbers of participants. Furthermore, it should explore direct use of IMU's raw acceleration data in classification and whether it can enhance the classification framework. A potential application is an extension of this study experimental design and methodology into other construction trades. The thesis results show a potential for using SVM classifiers on experienced workers' motion in other trades to identify safe and productive motion patterns that can then be used to train apprentice and novice workers. Furthermore, the SVM training can be expanded to include all data and not only bricklaying activity.

7.6 Publications of this thesis

In this section, the publications resulting from this thesis work are listed.

7.6.1 Journal Papers

1. Abdullatif Alwasel, Marcus Yung, Eihab M. Abdel-Rahman, and Richard P. Wells. Fatigue Detection Using Phase-Space Warping. *Journal of Biomechanical Engineering*, 139 (3) 2017.

2. Abdullatif Alwasel, Eihab Abdel-Rahman, Carl T. Haas, and SangHyun Lee. Experince, Productivity, and Musculoskeletal Injuries Among Masonry Workers. *Journal*

of Construction Engineering and Management, 2017.

3. JoonOh Seo, Abdullatif Alwasel, Eihab Abdel-Rahman, Carl T. Haas, and SangHyun Lee. A Comparative Study of Motion Capture Approaches for Ergonomic Evaluation during Construction Tasks. *Robotica*, (Submitted) 2016.

4. Abdullatif Alwasel, Ali Sabet, Mohammad Nahangi, Carl T. Haas, and Eihab Abdel-Rahman. Identifying Safe and Productive Masons Using Machine Learning. *Automation in Construction*, (Submitted), 2017.

7.6.2 Conference Papers

1. Abdullatif Alwasel, Carl T. Haas, and Eihab Abdel-Rahman. Level-of-expertise classification for identifying safe and productive masons. Abstract (Accepted) to International Workshop on Computing for Civil Engineering (IWCCE) Seattle, WA, USA, from June 25^{th} - June 27^{th}, 2017.

2. Abdullatif Alwasel, Mohammad Nahangi, Carl T. Haas, and Eihab Abdel-Rahman. Improving Health and Productivity of Construction Workers: A New Toolkit" Abstract (Accepted) to the 13^{th} Canadian Masonry Symposium, Halifax, Canada, June 4^{th} -June 7^{th}, 2017.

3. Abdullatif Alwasel, Eihab M. Abdel-Rahman, and Carl T. Haas. A Technique to Detect Fatigue in the Lower Limbs. In *Volume 8: 26th Conference on Mechanical Vibration and Noise*, Buffalo, NY, Aug 2014.

4. Abdullatif Alwasel, Karim Elrayes, Eihab Abdel-Rahman, and Carl T. Haas. A human body posture sensor for monitoring and diagnosing MSD risk factors. In *ISARC 2013 - 30th International Symposium on Automation and Robotics in Construction and Mining*, Held in Conjunction with the 23rd World Mining Congress, pages 531-539, 2013.

APPENDICES

Appendix: A

Participants

The study recruited participants from 4 different masonry experience levels, table 7.1. The hypothesis is that masons with more than five years of experience are performing the job have adopted a technique of work that minimize their exposure to MSDs risk factors which led to maximizing their work-life expectancy.

Furthermore, workers learn to mitigate the painful work gradually with experience, this learning process can be shown if the workers from different experience groups are monitored. Hence, novice masons were recruited as baseline, 1 & 2 years experienced workers to show progress, and experts to compare and learn the way they work.

Group Number	Group Experience	Number of Participants
1	No experience	5
2	1 Year	4
3	3 Years	7
4	>5 Years	5

Table 7.1: Participants distribution in groups

Recruitment Process

This study was reviewed and approved by the office of research ethics in University of Waterloo, Waterloo, Canada and was assigned to ORE#: 20023. The study took place inside the workshop in masonry building at Conestoga College (Waterloo Campus).

Participants were recruited by contacting the chair of trades and apprenticeship program in Conestoga college and brick and stone program coordinator. For the first three groups, the instructor posted an advertisement for the study around the masonry building. The advertisement stated that a research group from the University of Waterloo is looking for participants to take part in a bricklaying study, and that the study is looking for participants with different experience levels. The reason this advertisement was posted in masonry building is that the brick & stone program in Conestoga college is a three year program. The first students have no experience in bricklaying, the second year students have one year experience, and by the end of third year students have 3 years of experience which matches the requirements of our participants. The fourth group participants were

approached by the instructor and agreed to take part in the study.

Participants Anthropometry

Participants' anthropometrics were collected before each participant started the experiment. Anthropometric data collected were: gender, height (in centimeters), and weight (in kilograms).Anthropometric data are shown in table 7.2. The average height of participant was 177.61 cm with a standard deviation of ±7.42. The average weight of participant was 88.44 kg with a standard deviation of ±9.69. Although no gender requirement was posted to potential participants, all participants were males.

Participants Coding System

Participants are identified in this guide by their sequence and group number. No names were collected to maintain participants privacy.

The convention used in the identification is also used in data files names for ease use. For example, a file with a title (1_1) indicates that it belongs to the first novice participant.

Participant Group	Participant Number	Gender	Height	Weight
1	1	Male	170	83
1	2	Male	189	93
1	3	Male	176	85
1	4	Male	180	86
1	5	Male	168	72
2	1	Male	175	76
2	2	Male	169	74
2	3	Male	168	103
2	4	Male	187	95
3	1	Male	180	94
3	2	Male	183	96
3	3	Male	170	86
3	4	Male	185	95
3	5	Male	180	90
3	6	Male	180	101
3	7	Male	180	92
4	1	Male	168	73
4	2	Male	189	98
4	3	Male	183	85
4	4	Male	171	78
4	5	Male	173	94

Table 7.2: Participants anthropometric data

Methodology

The methodology of this study was designed to target the hypothesis that a healthy experienced mason has adopted a technique of work that can be extracted and taught to novice workers to increase their work-life expectancy. Moreover, current masonry working conditions can be altered to increase safety and decrease accumulative stresses on masons body. Therefore, participants were not provided with any instructions on how to perform

the work.

Participants came to the workshop, where the data collection took place, and were provided with information about the study. The information included what research teams are involved, why is this study being conducted, and where this study was reviewed and approved. Then, participants signed the form indicating their consent to participate.

The participant then put the xsens motion capture suite with 19 trackers on the body. Following this, a calibration session for the suit began. The calibration consisted of 3 parts: participant stood straight with their arms parallel to their body for 5 seconds as shown in fig 7.1.

The second calibration part was a T-pose where the participant stood straight and spread their arms in a T shape as shown in fig 7.2 for 5 second while the system was collecting data and relating each tracker.

The third calibration part was done by asking the participant to stand still and put their hands together with the palms touching each other and then start making a figure 8 shape in the space as shown in fig 7.3

Once the calibration is done, participant was asked to prepare themselves and build the wall. Each participant came with their own trowel and work gloves. At least three cameras were used in conjunction with the motion suit to record the participant while

Figure 7.1: Standing pose calibration

working. One camera was placed on each side of the wall parallel to the participant with a lateral point of view (side view), another camera was recording the participant from the back side.

Figure 7.2: T-pose calibration

The Wall

The task conducted by participant is building a wall that is 12 blocks wide and 6 courses high. The blocks used in building the wall were a standard CMU with dimension of $390 \times 190 \times 100$mm. The weight of the CMU is 10 kg.

The leads for the wall were built prior to the participant coming to the site, as shown in fig7.4. The participant started with placing a fine robe (alignment wire) to indicate the height of the course for alignment purposes.

All material that a mason needs to build a wall are brought to the participant by a journeyman. The blocks are placed $\simeq$ 60cm from the leads. The blocks are placed in three groups along the length of the wall. Two panels of mortar were also placed along the wall

Figure 7.3: Waiving pose calibration

between the piles of blocks.

Once the wall built, the motion suit was stopped collecting data and the video cameras stopped recording. The suit was removed and the session finished.

Figure 7.4: Lead wall

Data Storage and Handling

Two types of raw data was obtained: motion and videogrammetry. The video data was saved as ".avi" files that run on most video programs. The motion data was saved as ".mvnx" files, which is a type of files that only works with the xsens software called "MVN studio".

Each session recorded by the xsens motion suit is stored in one ".mvnx" file. This file contains the types of data shown in table 7.3. Depending on the application, certain information can be exported from the ".mvnx" file into one of the following file formats: ASCII (XML), C3D, and BVH.

Data	Type
Displacement	Linear
Velocity	Linear
Acceleration	Linear
Displacement	Angular
Velocity	Angular
Acceleration	Angular
Orientation	Quaternions/Matrix/Euler angles
Earth magnetic field	3D
Relative joint angles	3D Anatomical
Body center of mass	coordinates

Table 7.3: Types of output data from xsens motion suit

Data Analysis

This section* discusses how the data was exported and available file formats and naming conventions. It also discusses how different results were obtained.

Export files

First, for each session, the ".mvnx" file was exported using "MVN studio" into ".BVH" file. The ".BVH" file contains all the data in table 7.3. The exportation procedure is:

1. Open the ".mvnx" file using "MVN studio".

2. Go to file → Export → Export file, as shown in fig 7.5.

3. In the opened box select the file format required from the exporter and click export,

as shown in fig 7.6.

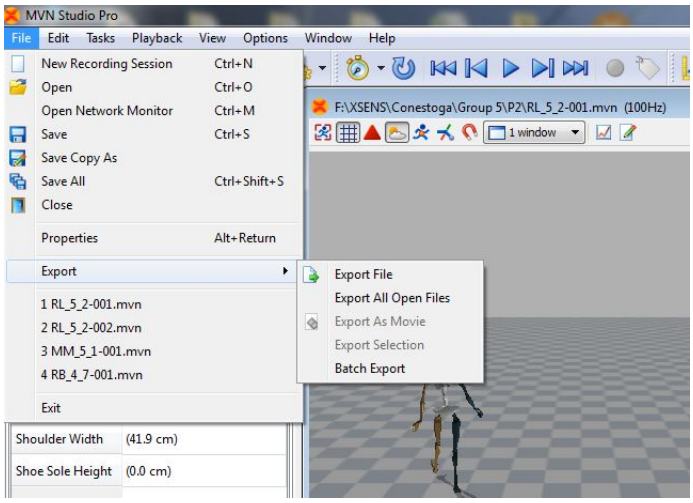

Figure 7.5: Export a file

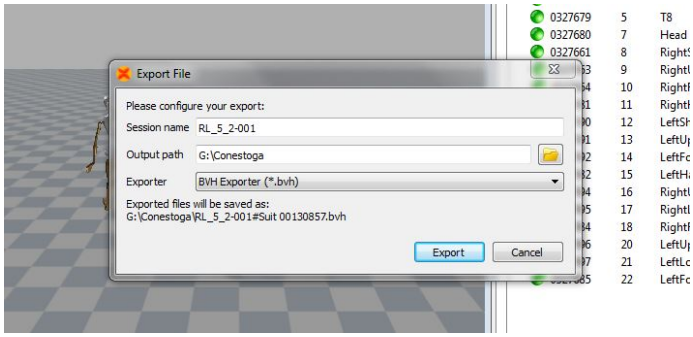

Figure 7.6: Choose extension of exported file

Data collection frame rate was set to 100 frames/s, however, this frame rate can be changed during file exportation. To change this rate you have to:

1. Go to Options tab.

2. Select Preferences.

3. Select Exporter → extension that you want to manipulate.

4. change the exporter frame skip for downsampling and units if needed, as shown in fig 7.7

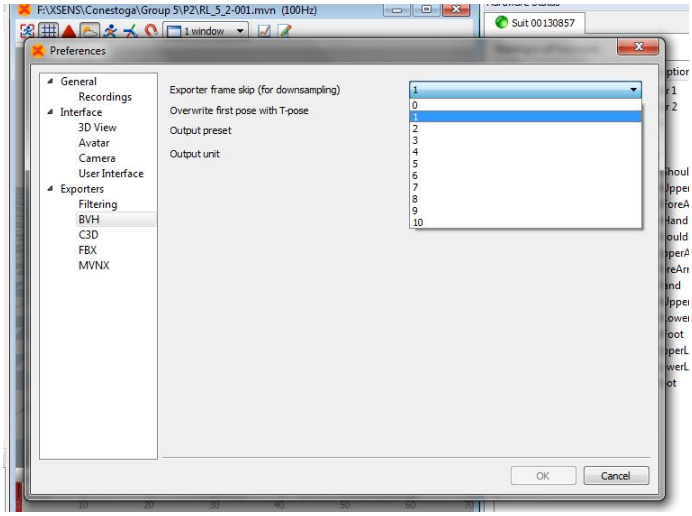

Figure 7.7: Change the sampling rate for the exported file

BVH format

"BVH" stands for Biovision Hierarchy. It is a file format used initially by animation movie industry to create characters. This format divides the data into two sections: header, describes the initial pose, hierarchy, and initial pose; the second section is a data section containing the motion data frame by frame. The hierarchy is divided into several "root"

describing the segments of the body, each root starts with a keyword “OFFSET” that carry information about the offset of the “child” ROOT from its “parents”. The offset will be given in X,Y, and Z directions. The file also carries information about the location of joint centers under header “JOINTS”.

To interpret the data from a BVH file, a BVH viewer is used. However, in principle it is possible to calculate the position of the segments from the BVH file. To do so, a rotation matrix must be created from the local translation and rotational information into parent segment coordinate system. This rotation matrix has to be 3 rotation matrices; one for each axis.

In this study a BVH viewer called “BVHViewer”, which has the ability to export 3D joint information from the BVH files into “.txt” file, was used to view BVH files and export the 3D joint center information. A sample picture from the software is shown in fig 7.8. This “.txt” file is to be used in creating a file containing the motion data to be uploaded to “3DSSPP” program for analysis eventually. To create the “.txt” file containing the 3D joint locations from the “BVH” file you first opent he “BVH” file in the “BVH Viewer” software as shown in fig 7.8. Then click on the button labeled as “3D”, circled in the figure and choose where to save it.

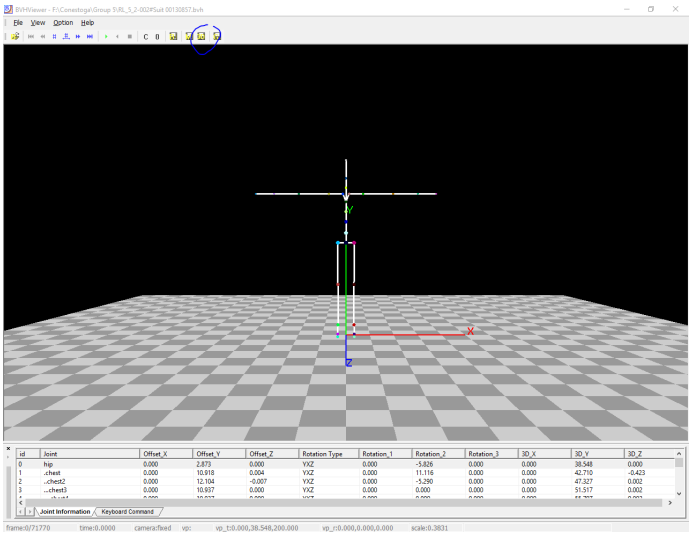

Figure 7.8: Creating 3D location file

Data segmentation

Segmenting the data is the most important task in this analysis, it must be consistent for the analysis to be reliable. Therefore, the data was segmented initially to four tasks tasks: lifting a block, walking/carrying the block, laying a block, and spreading mortar. However, for biomechanical analysis with 3DSSPP analysis, discussed in section 7.6.2, the motion were segmented by block. The block motion for biomechanical analysis starts from the frame where a participant is standing adjacent to a block and finishes when the participant lay the block on the wall. The key frame in this segmentation is the frame where the participant starts lifting the block, it is when the loads are applied in the analysis.

Creating ".loc" files for 3DSSPP

3D Static Strength Prediction Program (3DSSPP) is a software developed by University of Michigan research group to analyze the effect of loads on the body joints statically. It requires the user to input the joint center location information of the motion to be analyzed. In addition, the amount of force that the participant is carrying must be identified. The software requires the data for the input to be in a file with extension ".loc". To create this type of files, a Matlab code was written to convert the 3D joint center location file exported from BVH file into ".loc" file. This code exports a ".loc"a file consisting of 90 columns. the last six columns represent the force applied on the hands of the participant and their orientation.

To create this ".loc" file, first the ".txt" file containing the 3D joint center location must be opened using "Excel" software. Along with this guide document, is an ".xlsx" file titled " JointLocation(BVH)_format (including handloads)". The first row of this file contains the headers arranged according to the ".txt" file arrangement from BVH file. It contains 90 columns, of which the last six columns are empty, it must be filled with the forces (loads on hands in N). Of the last six columns, the first three are for the left hand and the last three for the right hand. In each hand, the first column is for the amount of load, the second for the vertical orientation, and the last is for the horizontal orientation, as

shown in table 7.4, in this example a 10N loan is applied to the left hand directed upwards ↑ and 10N load is applied to the right hand direct up to right ↗. In the second row in table 7.4, the same loads but oriented downwards as it should be direct in this experiment, so it becomes 10N ↓ and 10N ↙.

Left hand			Right hand		
N	Vertical °	Horizontal °	N	Vertical °	Horizontal °
10	90	0	10	0	45
10	-90	0	10	0	-45

Table 7.4: Joint location and hand loads for ".xlsx" file

Hand forces are determined from the video that was captured of the participants building the wall. The frame numbers from when the participant carried the block until he laid it on the wall were put as 98 N on the ".xlsx" file with $-90°$ vertically on both hands.

After completing the ".xlsx" file with hand forces, the file is to be saved as ".xls" file to be imported into Matlab for creating the ".loc" file. The Matlab code (found in appendix 7.6.2) will import the ".xls" file and process it to export a file with the same name but with ".loc" extension. This file is to be used by 3DSSPP.

3DSSPP analysis

The biomechanical analysis of the task was conducted using 3DSSPP. It contains information about the biomechanical and static strength capabilities of the employee in relation to

the physical demands of the work environment. Moreover, The strengths and capabilities in the software have a strong correlation the average population ($r = 0.8$).

3DSSPP default settings are set to calculated everything in English units, this must be changed to metric units. The analysis process starts with identifying the anthropometric information of the participant in the software. For each participant this anthropometric data are different so it has to be done every time. The anthropometric data changed from the software home screen by:

1. Task-Input → Set metric units.
2. Click on Anthropometry.
3. From the opened box → Set participant height (cm) and weight (kg), shown in fig 7.9.
4. Go to file → Click on set startup Task to current.

The last step mentioned above is to set the current anthropometric information throughout the session.

After setting up the session, the analysis can start by:

1. Go to Animation tab → Import Loc file.
2. From the box choose the ".loc" file to be imported.

After that, the report containing the biomechanical analysis can be accessed from "Report" tab. Moreover, the overall information can be exported as a ".txt" file by:

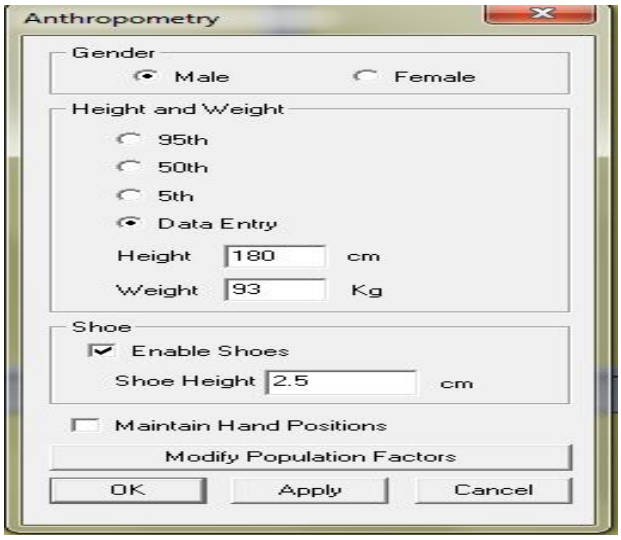

Figure 7.9: Setting anthropometry data for participant

1. Go to Report tab.

2. Click on Export output summary.

This ".txt" file containing the biomechanical analysis is to be pasted to Excel or any other graphing software to make a graphical representation of the results. Attached with this guide is an "Excel" file named "Results from 3DSSPP_format". This file is setup with its two rows arranged according to the format generated from the summary output of 3DSSPP, this way the results from 3DSSPP can be directly pasted on "Excel" for graph generation or further analysis.

Files Naming Convention

Since the experiment is conducted with 20 participants divided into four categories, the file naming convention was set accordingly. First, a folder called "Conestoga" contains all the data, it contains 4 folders: Group 1, 2, 3, and 4.

Each one of these folders contains folder named "p*" where * indicates the participant sequence number in this group. The sequence number indicates which participant performed the experiment first. For Example P1 indicates participant number 1 in this category.

Each folder "P*" contains several file with the same name but different extension. The file name is unique for each participant, the uniqueness is the name consists of three parts: participant initials, group number, and participant number. After these three parts, some of the files have three numbers following, which indicates the number of files coming from the ".mvnx" file from the suit. It comes in a "-00*" format where * indicates the file number. Table 7.5 lists all file extension types with their explanation.

Along with these files, are three folders names: Lay block, Report, and Results. Lay block folder contains the segmented data files for each block. The files are named according to their sequence from 1–45. Each block has two kinds of files: ".loc" file to be used in 3DSSPP and ".xls" file to be used in MATLAB to generate the ".loc" file.

Table 7.5: File extensions

Extension	Use with
mvna	initiation file from MVN studio
mvnx	data file from xsens original format
3d	any 3D software for manipulation
bvh	bvh viewer
c3d	another file type to manipulate 3d files
loc	3DSSPP
xls	MATLAB
xlsx	Excel to apply loads
txt	reports generated from 3DSSPP

Report folder contains files with same naming convention as lay block folder from 1–45. It contains the reports generated by 3DSSPP for each block. Results folder contains one ".xlsx" file called results, this file is where all the graphs are generated for all joints forces and moments. It consists of 52 sheets number from 1–45 and then each sheet named after its description. For example, sheet "back compression" contains the graphs of back compression for all blocks.

Matlab Code to create ".loc" file from a ".3D" file

```
1 (* ::Package:: *)
2
3 clear all;
```

```
close all;
clc

Rawdata=xlsread('JointLocation (BVH).xlsx');
Joints=Rawdata(:,1:84);
HandLoads=Rawdata(:,85:90);
%% inch to mm

Joints=Joints*25.4;
[n m]=size(Joints);

%% Translation

Hip=repmat(Joints(:,1:3),1,28);
Joints_T = Joints - Hip;

%% Rotation

% Matching coordinate systems between BVH and 3DSSPP
X=90;
Z=180;

RX=[1 0 0;0 cosd(X) -sind(X);0 sind(X) cosd(X)];
```

```
27 RZ=[cosd(Z) -sind(Z) 0;sind(Z) cosd(Z) 0;0 0 1];
28
29 Joints_R = zeros(n,m);
30
31 for i=1:28
32     Joints_R(:,3*(i-1)+1:3*(i-1)+3) = (RZ*RX*Joints_T (:,3*(i-1)+1:3*(i-1)
           +3)')';
33 end
34
35
36 % Rotation of torso to face front (+Y)
37
38 R_Hip = Joints_R(:,56:58);
39 L_Hip = Joints_R(:,70:72);
40
41 TorsoV=R_Hip - L_Hip;
42 TorsoV(:,3)=0;
43
44 Joints_converted = zeros(n,m);
45 Joints_converted=Joints_R;
46
47 %% Create Loc data
48
```

```
49 Loc = zeros(n,123);
50
51 % find forward vector
52
53 for i=1:n
54     Shoulder(i,:)=Joints_converted(i,28:30)-Joints_converted(i,43:45);
55     NecktoHead(i,:)=Joints_converted(i,22:24)-Joints_converted(i,16:18);
56     F_Vector(i,:)=cross(NecktoHead(i,:),Shoulder(i,:));
57     N_Vector(i)=norm(F_Vector(i,:));
58     U_Vector(i,:) = F_Vector (i,:)/N_Vector(i);
59 end
60
61 % find forearm vector
62 for i=1:n
63   LeftUA(i,:)=Joints_converted(i,49:51)-Joints_converted(i,46:48);% Vector
       from elbow to wrist(left)
64   U_LeftUA(i,:) = LeftUA (i,:)/norm(LeftUA(i,:));% Unit vector
65
66   RightUA(i,:)=Joints_converted(i,34:36)-Joints_converted(i,31:33);% Vector
       from elbow to wrist (right)
67   U_RightUA(i,:) = RightUA (i,:)/norm(RightUA(i,:));% Unit vector
68 end
69
```

```
70 Loc(:,10:12)=Joints_converted(:,19:21);% 10 - 12 Head origin !!
71 Loc(:,13:15)=Joints_converted(:,19:21)+100*U_Vector;% 13 - 15 Nasion !!
72 Loc(:,19:21)=Joints_converted(:,16:18);% 19 - 21 C7/T1
73 Loc(:,22:24)=Joints_converted(:,13:15)+100*U_Vector;% 22 - 24
       Sternoclavicular Joint!!
74 Loc(:,28:30)=Joints_converted(:,4:6);% 28 - 30 L5/S1
75 Loc(:,34:36)=Joints_converted(:,43:45);% 34 - 36 L. Shoulder
76 Loc(:,40:42)=Joints_converted(:,46:48);% 40 - 42 L. Elbow
77 Loc(:,46:48)=Joints_converted(:,49:51);% 46 - 48 L. Wrist
78 Loc(:,49:51)=Joints_converted(:,52:54);% 49 - 51 L. Grip Center  (virtual)
79 Loc(:,52:54)=Joints_converted(:,49:51)+100*U_LeftUA;% 52 - 54 L. Hand
80
81
82 Loc(:,55:57)=Joints_converted(:,28:30);% 55 - 57 R. Shoulder
83 Loc(:,61:63)=Joints_converted(:,31:33);% 61 - 63 R. Elbow
84 Loc(:,67:69)=Joints_converted(:,34:36);% 67 - 69 R. Wrist
85 Loc(:,70:72)=Joints_converted(:,37:39);% 70 - 72 R. Grip Center (virtual)
86 Loc(:,73:75)=Joints_converted(:,34:36)+100*U_RightUA;% 73 - 75 R. Hand
87
88 Loc(:,76:78)=Joints_converted(:,70:72);% 76 - 78 L. Hip
89 Loc(:,79:81)=Joints_converted(:,73:75);% 79 - 81 L. Kne
90 Loc(:,85:87)=Joints_converted(:,76:78);% 85 - 87 L. Ankle
91 Loc(:,91:93)=Joints_converted(:,79:81);% 91 - 93 L. Ball of Foot
```

```
92 Loc(:,97:99)=Joints_converted(:,55:57);% 97 - 99 R. Hip
93 Loc(:,100:102)=Joints_converted(:,58:60);% 100 - 102 R. Knee
94 Loc(:,106:108)=Joints_converted(:,61:63);% 106 - 108 R. Ankle
95 Loc(:,112:114)=Joints_converted(:,64:66);% 112 - 114 R. Ball of Foot
96
97 Loc(:,118:123)=HandLoads;
98
99 save('test9.loc','Loc','-ascii')
```

Appendix: B

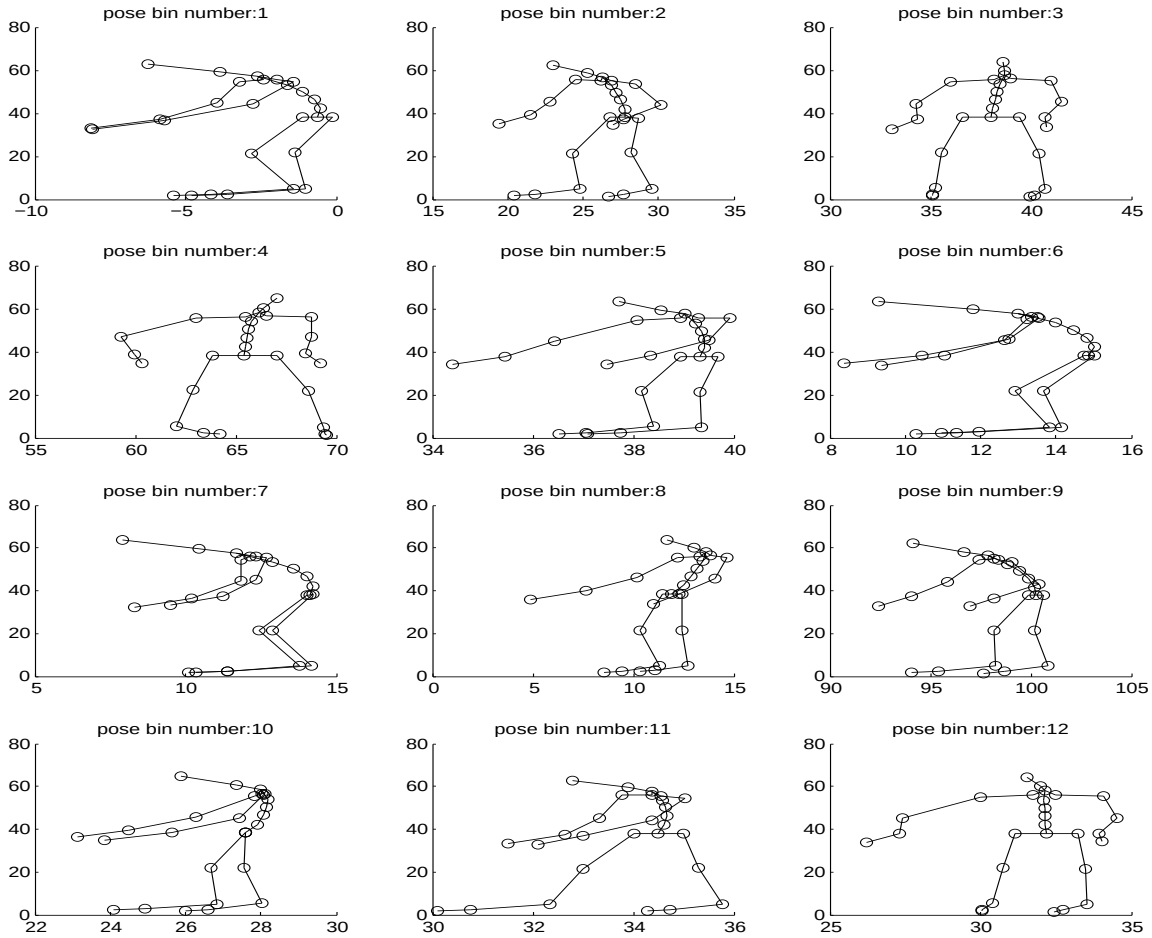

Figure 7.10: Frequent poses from 1- 12

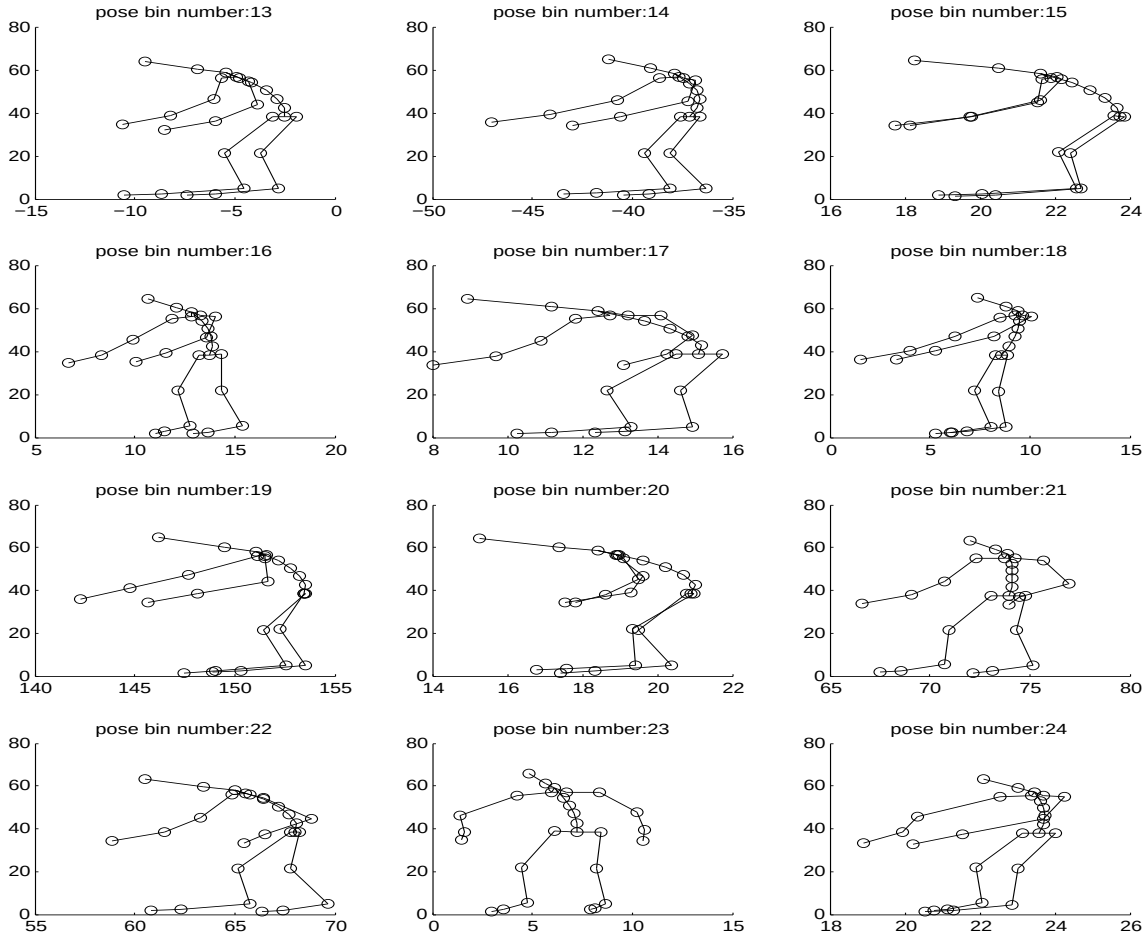

Figure 7.11: Frequent poses from 13- 24

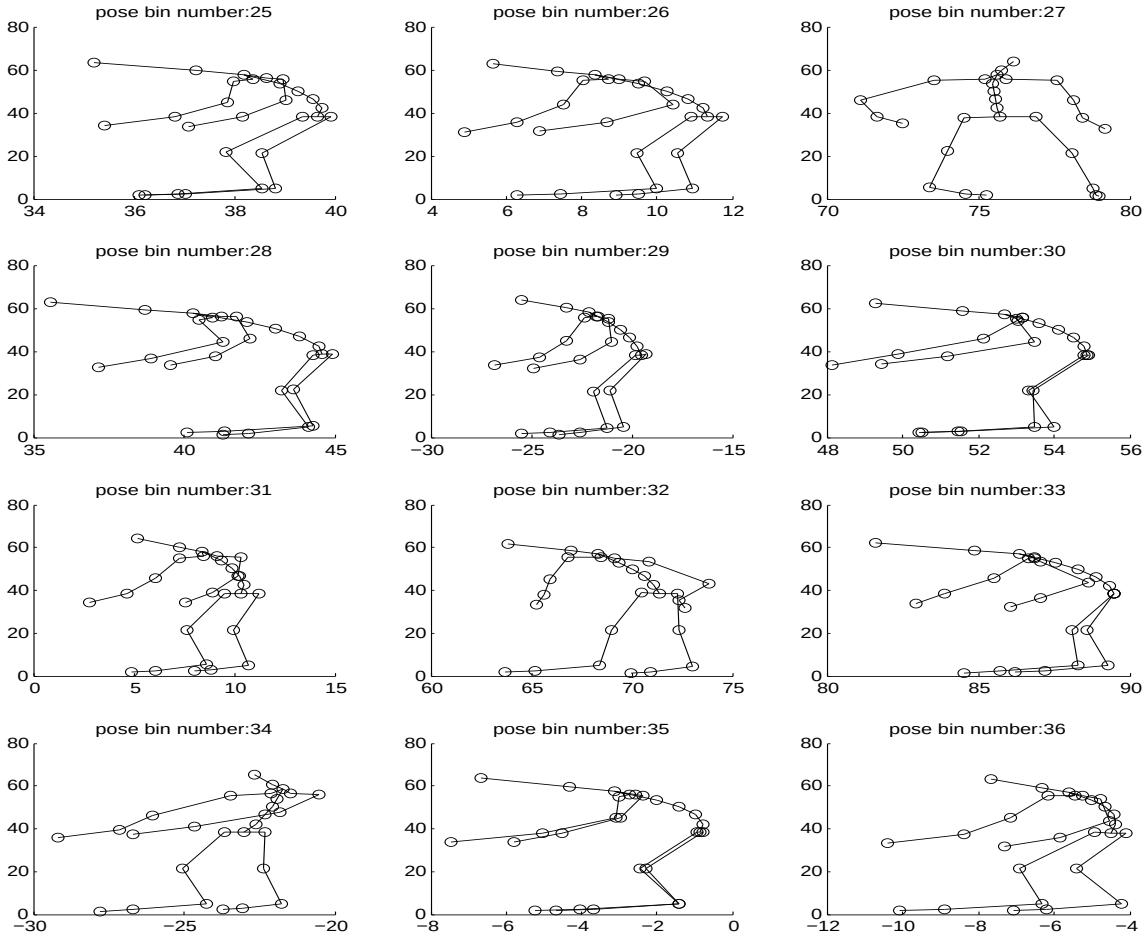

Figure 7.12: Frequent poses from 25- 37

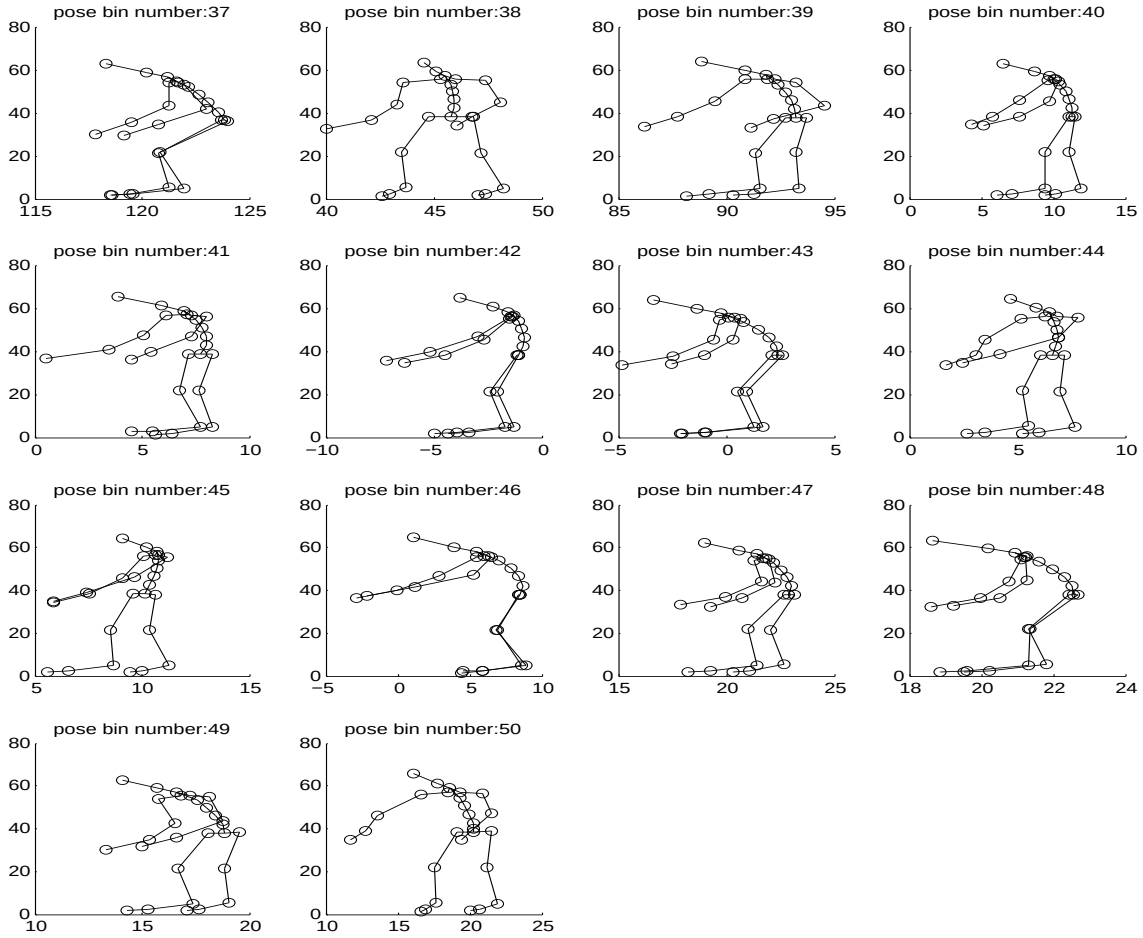

Figure 7.13: Frequent poses from 38- 50

References

[1] D. A. Winter, "Biomechanical Movement Synergies," in *Biomechanics and Motor Control of Human Movement*, 4th ed. Hoboken, NJ, USA: John Wiley & Sons, Inc., 2009, ch. Biomechani, pp. 281–295. [Online]. Available: http://doi.wiley.com/10.1002/9780470549148.ch11

[2] Xsens, "Xsens," 2016. [Online]. Available: https://www.xsens.com/

[3] V. Arndt, D. Rothenbacher, U. Daniel, B. Zschenderlein, S. Schuberth, and H. Brenner, "Construction work and risk of occupational disability: a ten year follow up of 14,474 male workers." *Occupational and environmental medicine*, vol. 62, no. 8, pp. 559–66, aug 2005. [Online]. Available: http://www.ncbi.nlm.nih.gov/pubmed/16046609

[4] Statistics Canada, "Canada Year Book 2012," Satistics Canada, Tech. Rep., 2012.

[Online]. Available: http://www.statcan.gc.ca/pub/11-402-x/11-402-x2012000-eng.htm

[5] F. Edition, "The Construction Chart Book," Center for Construction Research and Training (CPWR), Tech. Rep. April, 2013.

[6] A. S. Hanna, J. S. Russell, E. V. Nordheim, and M. J. Bruggink, "Impact of Change Orders on Labor Efficiency for Electrical Construction," *Journal of Construction Engineering and Management*, vol. 125, no. 4, pp. 224–232, aug 1999.

[7] S. Kumar, "Theories of musculoskeletal injury causation," *Ergonomics*, vol. 44, no. 1, pp. 17–47, jan 2001.

[8] Y. Wang, P. M. Goodrum, C. T. Haas, and R. W. Glover, "Craft Training Issues in American Industrial and Commercial Construction," *Journal of Construction Engineering and Management*, vol. 134, no. 10, pp. 795–803, oct 2008. [Online]. Available: http://ascelibrary.org/doi/10.1061/{%}28ASCE{%}290733-9364{%}282008{%}29134{%}3A10{%}28795{%}29

[9] D. Denis, M. St-Vincent, D. Imbeau, C. Jetté, and I. Nastasia, "Intervention practices in musculoskeletal disorder prevention: A critical literature review," *Applied Ergonomics*, vol. 39, no. 1, pp. 1–14, jan 2008.

[10] P. Entzel, J. Albers, and L. Welch, "Best practices for preventing musculoskeletal disorders in masonry: Stakeholder perspectives," *Applied Ergonomics*, vol. 38, no. 5, pp. 557–566, 2007.

[11] U.S. Bureau of Labor Statistics, "Nonfatal occupational injuries and illnesses requiring days away from work, 2014," U.S. Bureau of Labor Statistics, Tech. Rep. 202, 2015.

[12] Statistics Canada, "The Canadian Population in 2011: Age and Sex," 2011.

[13] J. Seo, A. Alwasel, S. Lee, E. Abdel-Rahman, and C. Haas, "A Comparative Study of In-field Motion Capture Approaches for Body Kinematics Measurement in Construction," *Robotica*, vol. Submitted, 2016.

[14] A. Alwasel, K. Elrayes, E. Abdel-Rahman, and C. T. Haas, "A human body posture sensor for monitoring and diagnosing MSD risk factors," in *ISARC 2013 - 30th International Symposium on Automation and Robotics in Construction and Mining, Held in Conjunction with the 23rd World Mining Congress*, 2013, pp. 531–539.

[15] A. Alwasel, M. Yung, E. Abdel-Rahman, R. P. Wells, and C. T. Haas, "Fatigue Detection Using Phase-Space Warping," *Journal of Biomechanical Engineering*, vol. 139, no. 3, pp. 031 001–031 001–9, jan 2016. [Online]. Available: http://biomechanical.asmedigitalcollection.asme.org/article.aspx?doi=10.1115/1.4035367

[16] A. A. Alwasel, E. M. Abdel-Rahman, and C. T. Haas, "A Technique to Detect Fatigue in the Lower Limbs," in *Volume 8: 26th Conference on Mechanical Vibration and Noise*, vol. 8. Buffalo, NY: ASME, aug 2014, p. V008T11A005.

[17] A. Alwasel, E. M. Abdel-Rahman, C. T. Haas, and S. Lee, "Experience, Productivity, and Musculoskeletal Injury among Masonry Workers," *Journal of Construction Engineering and Management*, vol. In Press, p. 05017003, feb 2017. [Online]. Available: http://ascelibrary.org/doi/10.1061/{%}28ASCE{%}29CO.1943-7862.0001308

[18] A. Alwasel, A. Sabet, M. Nahangi, C. T. Haas, and E. Abdel-Rahman, "Identifying Safe and Productive Masons Using Machine Learning," *Automation in Construction*, vol. Submitted, 2016.

[19] National Institute for Occupational Safety and Health, "Musculoskeletal Disorders and Workplace Factors: A Critical Review of Epidemiologic Evidence for Work-Related Musculoskeletal Disorders of the Neck, Upper Extremity, and Low Back," National Institute for Occupational Safety and Health (NIOSH), Cincinnati, OH., Tech. Rep., 1997.

[20] A. Hauke, J. Flintrop, E. Brun, and R. Rugulies, "The impact of work-related psychosocial stressors on the onset of musculoskeletal disorders in specific body regions:

A review and meta-analysis of 54 longitudinal studies," *Work & Stress*, vol. 25, no. 3, pp. 243 – 256, 2011.

[21] M. Collins, "Genetic risk factors for soft-tissue injuries 101: a practical summary to help clinicians understand the role of genetics and 'personalised medicine'," *British Journal of Sports Medicine*, vol. 44, no. 13, pp. 915–917, oct 2010.

[22] W. Rohmert, "Determination of relaxation periods in industrial operations, Part 1," *Work Study and Management*, vol. 8, no. 11, pp. 500–505, 1964.

[23] ——, "Determination of relaxation periods in industrial operations, Part 2," *Work Study and Management*, vol. 8, no. 11, pp. 550 – 556, 1964.

[24] B.-t. Karsh, F. B. P. Moro, and M. J. Smith, "The efficacy of workplace ergonomic interventions to control musculoskeletal disorders: A critical analysis of the peer-reviewed literature," *Theoretical Issues in Ergonomics Science*, vol. 2, no. 1, pp. 23–96, jan 2001. [Online]. Available: http://www.tandfonline.com/doi/abs/10.1080/14639220152644533

[25] W. Rohmert, "Problems in determining rest allowances Part 1: Use of modern methods to evaluate stress and strain in static muscular work," *Applied Ergonomics*, vol. 4, no. 2, pp. 91–95, 1973.

[26] A. Alwasel, K. Elrayes, E. Abdel-Rahman, and C. Hass, "Reducing shoulder injuries among construction workers," *Gerontechnology*, vol. 11, no. 2, pp. 3–7, jun 2012.

[27] J.-m. Billette and T. Janz, "Injuries in Canada : Insights from the Canadian Community Health Survey," *Statistics Canada Catalogue*, vol. 82, no. 624, pp. 1–16, 2011. [Online]. Available: http://www.statcan.gc.ca/pub/82-624-x/2011001/article/11506-eng.pdf

[28] WHO, "Healthy workplaces : a model for action for employers, workers, policy-makers and practitioners," World Health Organization, Geneva, Tech. Rep., 2010.

[29] A. Kosny, E. MacEachen, M. Lifshen, P. Smith, G. J. Jafri, C. Neilson, D. Pugliese, and J. Shields, "Delicate dances: immigrant workers' experiences of injury reporting and claim filing." *Ethnicity & health*, vol. 17, no. 3, pp. 267–90, jan 2012. [Online]. Available: http://www.ncbi.nlm.nih.gov/pubmed/21970445

[30] N. Warren, "Work stress and musculoskeletal disorder etiology: The relative roles of psychosocial and physical risk factors." *Work: A Journal of Prevention, Assessment and Rehabilitation*, vol. 17, no. 3, pp. 221–234, jan 2001. [Online]. Available: http://www.ncbi.nlm.nih.gov/pubmed/12441601

[31] Steering Committee for the Workshop on Work-Related Musculoskeletal Injuries: The Research Base in National Research Council, *Work-Related Musculoskeletal*

Disorders. Washington, D.C.: National Academies Press, mar 1999. [Online]. Available: http://www.nap.edu/catalog/6431

[32] T. Waters and V. Putz-Anderson, "Scientific support documentation for the Revised 1991 NIOSH Lifting Equation," *National Institute for Occupational Safety and Health*, 1991.

[33] National Institute for Occupational Safety and Health (NIOSH), "Work practices guide for manual lifting," *US Department of Health and Human Services*, vol. 199, 1981.

[34] Statistics Canada, "Work Absence Rates," 2011. [Online]. Available: http://www.statcan.gc.ca/pub/71-211-x/71-211-x2012000-eng.pdf

[35] P. C. Coyte, C. V. Asche, R. Croxford, and B. Chan, "The Economic Cost of Musculoskeletal Disorders in Canada," *Arthritis & Rheumatism*, vol. 11, no. 5, pp. 315–325, 1998. [Online]. Available: http://onlinelibrary.wiley.com/doi/10.1002/art.1790110503/abstract

[36] A. Alwasel, "A Monitoring System to Reduce Shoulder Injury Among Construction Workers," Masters, University of Waterloo, 2011. [Online]. Available: http://uwspace.uwaterloo.ca/handle/10012/6390

[37] P. Corso, E. Finkelstein, T. Miller, I. Fiebelkorn, and E. Zaloshnja, "Incidence and lifetime costs of injuries in the United States," *Inj Prev*, vol. 12, no. 4, pp. 212–218, aug 2006.

[38] D. I. Nelson, M. Concha-Barrientos, T. Driscoll, K. Steenland, M. Fingerhut, L. Punnett, A. Pruss-Ustun, J. Leigh, and C. Corvalan, "The global burden of selected occupational diseases and injury risks: Methodology and summary," *American Journal of Industrial Medicine*, vol. 48, no. 6, pp. 400–418, 2005. [Online]. Available: http://onlinelibrary.wiley.com/doi/10.1002/ajim.20211/abstract

[39] S. Lahiri, P. Markkanen, and C. Levenstein, "The Cost Effectiveness of Occupational Health Interventions : Preventing Occupational Back Pain," *American Journal of Industrial Medicine*, vol. 48, no. 6, pp. 515–529, 2005.

[40] A. Morgan and S. Chow, "The economic impact of implementing and ergonomic plan," *Nursing Economics*, vol. 25, no. 3, pp. 150–155, 2007.

[41] Golden Gate Bridge Highway and Transportation District, "Golden Gate Bridge." [Online]. Available: http://goldengatebridge.org/research/SafetyFirst.php

[42] Performance Assessment Committee, "2014 Safety Report," Construction Industry Institute, Tech. Rep., 2015.

[43] T. R. Waters, V. Putz-Anderson, A. Garg, and L. J. Fine, "Revised NIOSH equation for the design and evaluation of manual lifting tasks," *Ergonomics*, vol. 36, no. 7, pp. 749–776, jul 1993. [Online]. Available: http://www.tandfonline.com/doi/abs/10.1080/00140139308967940

[44] C. S. Moriguchi, L. Carnaz, L. C. Miranda Júnior, R. W. Marklin, and H. J. C. Gil Coury, "Are posture data from simulated tasks representative of field conditions? Case study for overhead electric utility workers," *Ergonomics*, vol. 55, no. 11, pp. 1382–94, jan 2012. [Online]. Available: http://www.ncbi.nlm.nih.gov/pubmed/22897569

[45] D. C. Cole, N. Theberge, S. M. Dixon, I. Rivilis, W. P. Neumann, and R. Wells, "Reflecting on a program of participatory ergonomics interventions: A multiple case study," *Work*, vol. 34, no. 2, pp. 161–178, jan 2009. [Online]. Available: http://www.ncbi.nlm.nih.gov/pubmed/20037229

[46] W. Guth and I. MacMillan, "Strategy implementation versus middle management self-interest," *Strategic Management Journal*, vol. 7, no. 4, pp. 313–327, 2006. [Online]. Available: http://onlinelibrary.wiley.com/doi/10.1002/smj.4250070403/abstract

[47] J. A. Hess, L. Kincl, T. Amasay, and P. Wolfe, "Ergonomic evaluation of masons

laying concrete masonry units and autoclaved aerated concrete," *Applied Ergonomics*, vol. 41, no. 3, pp. 477–483, may 2010.

[48] M. Jakob, F. Liebers, and S. Behrendt, "The effects of working height and manipulated weights on subjective strain, body posture and muscular activity of milking parlor operatives - Laboratory study," *Applied Ergonomics*, vol. 43, no. 4, pp. 753–761, 2012. [Online]. Available: http://dx.doi.org/10.1016/j.apergo.2011.11.009

[49] D. B. Chaffin and K. S. Park, "A Longitudinal Study of Low-Back Pain as Associated with Occupational Weight Lifting Factors," *American Industrial Hygiene Association Journal*, vol. 34, no. 12, pp. 513–525, dec 1973. [Online]. Available: http://www.tandfonline.com/doi/abs/10.1080/0002889738506892

[50] G. David, V. Woods, G. Li, and P. Buckle, "The development of the Quick Exposure Check (QEC) for assessing exposure to risk factors for work-related musculoskeletal disorders," *Applied Ergonomics*, vol. 39, no. 1, pp. 57–69, 2008.

[51] L. McAtamney and E. Nigel Corlett, "RULA: a survey method for the investigation of work-related upper limb disorders." *Applied ergonomics*, vol. 24, no. 2, pp. 91–9, apr 1993. [Online]. Available: http://www.ncbi.nlm.nih.gov/pubmed/15676903

[52] B. Buchholz, V. Paquet, L. Punnett, D. Lee, and S. Moir, "PATH: A work sampling-

based approach to ergonomic job analysis for construction and other non-repetitive work," *Applied Ergonomics*, vol. 27, no. 3, pp. 177–187, jun 1996.

[53] O. Karhu, P. Kansi, and I. Kuorinka, "Correcting working postures in industry: A practical method for analysis." *Applied ergonomics*, vol. 8, no. 4, pp. 199–201, dec 1977. [Online]. Available: http://www.ncbi.nlm.nih.gov/pubmed/15677243

[54] O. Karhu, R. Härkönen, P. Sorvali, and P. Vepsäläinen, "Observing working postures in industry: Examples of OWAS application." *Applied ergonomics*, vol. 12, no. 1, pp. 13–17, 1981.

[55] A. Stroupe, T. Huntsberger, A. Okon, H. Aghazarian, and M. Robinson, "Behavior-based multi-robot collaboration for autonomous construction tasks," in *2005 IEEE/RSJ International Conference on Intelligent Robots and Systems*, no. August 2016. IEEE, 2005, pp. 1495–1500. [Online]. Available: http://ieeexplore.ieee.org/lpdocs/epic03/wrapper.htm?arnumber=1545269

[56] J. Seo, R. Starbuck, S. Han, S. Lee, and T. J. Armstrong, "Motion Data-Driven Biomechanical Analysis during Construction Tasks on Sites," *Journal of Computing in Civil Engineering*, vol. 29, no. 4, 2014.

[57] E. Valero, A. Sivanathan, F. Bosché, and M. Abdel-Wahab, "Musculoskeletal disor-

ders in construction: A review and a novel system for activity tracking with body area network," *Applied Ergonomics*, vol. 54, pp. 120–130, 2016.

[58] S. J. Ray and J. Teizer, "Real-time construction worker posture analysis for ergonomics training," *Advanced Engineering Informatics*, vol. 26, no. 2, pp. 439–455, 2012.

[59] S. Han, S. Lee, and F. Peña-Mora, "Vision-Based Detection of Unsafe Actions of a Construction Worker: Case Study of Ladder Climbing," *Journal of Computing in Civil Engineering*, vol. 27, no. 6, pp. 635–644, nov 2013.

[60] S. Han, M. Achar, S. Lee, and F. Peña-Mora, "Empirical assessment of a RGB-D sensor on motion capture and action recognition for construction worker monitoring," *Visualization in Engineering*, vol. 1, no. 1, p. 6, 2013. [Online]. Available: http://viejournal.springeropen.com/articles/10.1186/2213-7459-1-6

[61] J. Seo, S. Lee, T. Armstrong, and S. Han, "Dynamic Biomechanical Simulation for Identifying Risk Factors for Work-related Musculoskeletal Disorders During Construction Tasks," in *30th International Symposium on Automation and Robotics in Construction*, 2013.

[62] A. Khosrowpour, J. C. Niebles, and M. Golparvar-Fard, "Vision-based workface as-

sessment using depth images for activity analysis of interior construction operations," *Automation in Construction*, vol. 48, pp. 74–87, 2014.

[63] C. Plagemann, V. Ganapathi, D. Koller, and S. Thrun, "Real-time identification and localization of body parts from depth images," *Proceedings - IEEE International Conference on Robotics and Automation*, pp. 3108–3113, 2010.

[64] M. W. Lee and I. Cohen, "A model-based approach for estimating human 3D poses in static images," *IEEE Transactions on Pattern Analysis and Machine Intelligence*, vol. 28, no. 6, pp. 905–916, 2006.

[65] M. Siddiqui and G. Medioni, "Human pose estimation from a single view point, real-time range sensor," *Proceedings of Computer Vision and Pattern Recognition (CVPR)*, pp. 1–8, 2010.

[66] S. Akhtar, A. R. Ahmad, and E. M. Abdel-Rahman, "A metaheuristic bat-inspired algorithm for full body human pose estimation," in *Proceedings of the 2012 9th Conference on Computer and Robot Vision, CRV 2012*. IEEE, may 2012, pp. 369–375.

[67] J. Shotton, T. Sharp, A. Kipman, A. Fitzgibbon, M. Finocchio, A. Blake, M. Cook, and R. Moore, "Real-time human pose recognition in parts from single depth images," *Communications of the ACM*, vol. 56, no. 1, p. 116, jan 2013.

[68] J. I. Woodfill, G. Gordon, and R. Buck, "Tyzx DeepSea High Speed Stereo Vision System," in *Proceedings of the Conference on Computer Vision and Pattern Recognition Workshop*, 2004, pp. 4–8.

[69] S. Han, S. Lee, and F. Peña-Mora, "Vision-Based Detection of Unsafe Actions of a Construction Worker: Case Study of Ladder Climbing," *Journal of Computing in Civil Engineering*, vol. 27, no. 6, pp. 635–644, nov 2013.

[70] D. Côrrea and A. Balbinot, "Accelerometry for the motion analysis of the lateral plane of the human body during gait," *Health and Technology*, vol. 1, no. 1, pp. 35–46, jul 2011.

[71] A. Krüger and J. Edelmann-Nusser, "Biomechanical analysis in freestyle snowboarding: application of a full-body inertial measurement system and a bilateral insole measurement system," *Sports Technology*, vol. 2, no. 1-2, pp. 17–23, apr 2009.

[72] J. F. S. Lin and D. Kulić, "Human pose recovery using wireless inertial measurement units," *Physiological Measurement*, vol. 33, no. 12, pp. 2099–2115, dec 2012.

[73] B. Najafi, K. Aminian, F. Loew, Y. Blanc, and P. a. Robert, "Measurement of stand-sit and sit-stand transitions using a miniature gyroscope and its application in fall risk evaluation in the elderly." *IEEE transactions on bio-medical engineering*, vol. 49, no. 8, pp. 843–51, aug 2002.

[74] B. Najafi, K. Aminian, A. Paraschiv-Ionescu, F. Loew, C. J. Büla, and P. Robert, "Ambulatory system for human motion analysis using a kinematic sensor: Monitoring of daily physical activity in the elderly," *IEEE Transactions on Biomedical Engineering*, vol. 50, no. 6, pp. 711–723, 2003.

[75] A. Sabatini, "Quaternion-based extended Kalman filter for determining orientation by inertial and magnetic sensing," *Biomedical Engineering, IEEE Transactions on*, vol. 53, no. 7, pp. 1346–1356, 2006.

[76] Y. Z. Chong, "Full body wearable instrumented motion analysis system," in *3rd International Conference on Bioinformatics and Biomedical Engineering, iCBBE 2009*. IEEE, 2009, pp. 1–4.

[77] A. Peddi, L. Huan, Y. Bai, and S. Kim, "Development of Human Pose Analyzing Algorithms for the Determination of Construction Productivity in Real-Time," in *Construction Research Congress*. Reston, VA: American Society of Civil Engineers, apr 2009, pp. 11–20.

[78] L. Joshua and K. Varghese, "Accelerometer-Based Activity Recognition in Construction," *Journal of Computing in Civil Engineering*, vol. 25, no. 5, pp. 370–379, sep 2011.

[79] ——, "Video annotation framework for accelerometer placement in worker activity recognition studies," in *IAARC, Seoul, Korea*, 2011, pp. 317–322.

[80] ——, "Classification of bricklaying activities in work sampling categories using accelerometers," in *Construction Research Congress 2012*, 2012, pp. 2300–2309.

[81] ——, "Selection of Accelerometer Location on Bricklayers Using Decision Trees," *Computer-Aided Civil and Infrastructure Engineering*, vol. 28, no. 5, pp. 372–388, may 2013.

[82] T. Cheng, J. Teizer, G. C. Migliaccio, and U. C. Gatti, "Automated task-level activity analysis through fusion of real time location sensors and worker's thoracic posture data," *Automation in Construction*, vol. 29, pp. 24–39, 2013.

[83] S. Kim and M. a. Nussbaum, "Performance evaluation of a wearable inertial motion capture system for capturing physical exposures during manual material handling tasks." *Ergonomics*, vol. 56, no. 2, pp. 314–26, 2013.

[84] J. Ryu, J. Seo, M. Liu, S. Lee, and C. T. Haas, "Action Recognition Using a Wristband-Type Activity Tracker: Case Study of Masonry Work," in *Construction Research Congress*. Reston, VA: American Society of Civil Engineers, 2016, pp. 790–799.

[85] G. Migliaccio, J. Teizer, T. Cheng, and U. Gatti, "Automatic Identification of Unsafe Bending Behavior of Construction Workers using Real-time Location Sensing and Physiological Status Monitoring," in *Construction Research Congress 2012*, 2012, pp. 633–642.

[86] U. C. Gatti, S. Schneider, and G. C. Migliaccio, "Physiological condition monitoring of construction workers," *Automation in Construction*, vol. 44, pp. 227–233, 2014.

[87] W. Lee and G. C. Migliaccio, "Field Use of Physiological Status Monitoring (PSM) to Identify Construction Workers' Physiologically Acceptable Bounds and Heart Rate Zones," in *Computing in Civil and Building Engineering (2014)*. Reston, VA: American Society of Civil Engineers, 2014, pp. 1037–1044.

[88] B. Esmaeili and M. R. Hallowell, "Diffusion of Safety Innovations in the Construction Industry," *Journal of Construction Engineering and Management*, vol. 138, no. 8, pp. 955–963, aug 2012.

[89] A. Sivanathan, F. Bosche, M. Abdel-Wahab, and T. Lim, "Towards a Cyber-Physical Gaming System for Training in the Construction and Engineering Industry," in *ASME International Design Engineering Technical Conferences & Computers and Information in Engineering Conference*, Buffalo, NY, 2014, pp. 1–9.

[90] A. Golabchi, S. Han, J. Seo, S. Han, S. Lee, and M. Al-Hussein, "An Automated

Biomechanical Simulation Approach to Ergonomic Job Analysis for Workplace Design," *Journal of Construction Engineering and Management*, vol. 141, no. 8, p. 04015020, 2015.

[91] the Center for Ergonomics, "3DSSPP Software." [Online]. Available: http://c4e.engin.umich.edu/tools-services/3dsspp-software/

[92] S. L. Delp, F. C. Anderson, A. S. Arnold, P. Loan, A. Habib, C. T. John, E. Guendelman, and D. G. Thelen, "OpenSim: Open-source software to create and analyze dynamic simulations of movement," *IEEE Transactions on Biomedical Engineering*, vol. 54, no. 11, pp. 1940–1950, 2007.

[93] D. M. Kramer, P. L. Bigelow, N. Carlan, R. P. Wells, E. Garritano, P. Vi, and M. Plawinski, "Searching for needles in a haystack: identifying innovations to prevent MSDs in the construction sector." *Applied ergonomics*, vol. 41, no. 4, pp. 577–84, jul 2010. [Online]. Available: http://www.ncbi.nlm.nih.gov/pubmed/20170903

[94] D. Anton, J. C. Rosecrance, F. Gerr, L. a. Merlino, and T. M. Cook, "Effect of concrete block weight and wall height on electromyographic activity and heart rate of masons," *Ergonomics*, vol. 48, no. 10, pp. 1314–1330, aug 2005. [Online]. Available: http://www.tandfonline.com/doi/abs/10.1080/00140130500274168

[95] E. Attaianese and G. Duca, "The human component of sustainability: A study

for assessing "human performances" of energy efficient construction blocks," *Work*, vol. 41, no. SUPPL.1, pp. 2141–2146, 2012.

[96] J. S. Boschman, H. F. Van Der Molen, J. K. Sluiter, and M. H. W. Frings-Dresen, "Occupational demands and health effects for bricklayes and construction supervisors: A systematic review," *American Journal of Industrial Medicine*, vol. 54, no. 1, pp. 55–77, jan 2011.

[97] G. S. Faber, I. Kingma, P. P. F. M. Kuijer, H. F. van der Molen, M. J. M. Hoozemans, M. H. W. Frings-Dresen, and J. H. van Dieën, "Working height, block mass and one- vs. two-handed block handling: the contribution to low back and shoulder loading during masonry work." *Ergonomics*, vol. 52, no. 9, pp. 1104–1118, 2009.

[98] J. Hess, M. Weinstein, and L. Welch, "Ergonomic best practices in masonry: regional differences, benefits, barriers, and recommendations for dissemination." *Journal of occupational and environmental hygiene*, vol. 7, no. 8, pp. 446–55, 2010. [Online]. Available: http://www.ncbi.nlm.nih.gov/pubmed/20521196

[99] M. J. Hoozemans, I. Kingma, W. H. de Vries, and J. H. van Dieën, "Effect of lifting height and load mass on low back loading," *Ergonomics*, vol. 51, no. 7, pp. 1053–1063, jul 2008. [Online]. Available: http://www.tandfonline.com/doi/abs/10.1080/00140130801958642

[100] P. Kivi and M. Mattila, "Analysis and improvement of work postures in the building industry: application of the computerised OWAS method." *Applied ergonomics*, vol. 22, no. 1, pp. 43–48, 1991.

[101] A. Plamondon, C. Larivière, A. Delisle, D. Denis, and D. Gagnon, "Relative importance of expertise, lifting height and weight lifted on posture and lumbar external loading during a transfer task in manual material handling," *Ergonomics*, vol. 55, no. 1, pp. 87–102, jan 2012. [Online]. Available: http://www.tandfonline.com/doi/abs/10.1080/00140139.2011.634031

[102] A. Plamondon, D. Denis, A. Delisle, C. Lariviere, and E. Salazar, "Biomechanical differences between expert and novice workers in a manual material handling task." *Ergonomics*, vol. 53, no. 10, pp. 1239–53, oct 2010. [Online]. Available: http://www.ncbi.nlm.nih.gov/pubmed/20865607

[103] R. Poppe, "A survey on vision-based human action recognition," *Image and Vision Computing*, vol. 28, no. 6, pp. 976–990, 2010. [Online]. Available: http://dx.doi.org/10.1016/j.imavis.2009.11.014

[104] R. Starbuck, J. Seo, S. Han, and S. Lee, "A Stereo Vision-based Approach to Markerless Motion Capture for On-Site Kinematic Modeling of Construction Worker Tasks,"

in *The 15th International Conference on Computing in Civil and Building Engineering (ICCCBE).*, Orlando, FL, 2014, p. 1094.

[105] S. Knoop, S. Vacek, and R. Dillmann, "Sensor fusion for 3D human body tracking with an articulated 3D body model," *International Conference on Robotics and Automation*, no. May, pp. 1686–1691, 2006. [Online]. Available: http://ieeexplore.ieee.org/lpdocs/epic03/wrapper.htm?arnumber=1641949

[106] S. Han and S. Lee, "A vision-based motion capture and recognition framework for behavior-based safety management," *Automation in Construction*, vol. 35, pp. 131–141, nov 2013.

[107] M. Liu, S. Han, and S. Lee, "Tracking-based 3D human skeleton extraction from stereo video camera toward an on-site safety and ergonomic analysis," *Construction Innovation*, vol. 16, no. 3, pp. 348–367, jul 2016. [Online]. Available: http://www.emeraldinsight.com/doi/10.1108/CI-10-2015-0054

[108] N. Rafibakhsh, J. Gong, M. K. Siddiqui, C. Gordon, and H. F. Lee, "Analysis of XBOX Kinect Sensor Data for Use on Construction Sites : Depth Accuracy and Sensor Interference Assessment," in *Construction Research Congress 2012*, 2012, pp. 848–857. [Online]. Available: http://ascelibrary.org/doi/abs/10.1061/9780784412329.086

[109] Z. Zhang, "Microsoft Kinect Sensor and Its Effect," *IEEE Multimedia*, vol. 19, no. 2, pp. 4–10, feb 2012. [Online]. Available: http://ieeexplore.ieee.org/document/6190806/

[110] Seunghun Jin, Junguk Cho, Xuan Dai Pham, Kyoung Mu Lee, Sung-Kee Park, Munsang Kim, and Jae Wook Jeon, "FPGA Design and Implementation of a Real-Time Stereo Vision System," *IEEE Transactions on Circuits and Systems for Video Technology*, vol. 20, no. 1, pp. 15–26, jan 2010. [Online]. Available: http://ieeexplore.ieee.org/document/5159427/

[111] C. Shan, T. Tan, and Y. Wei, "Real-time hand tracking using a mean shift embedded particle filter," *Pattern Recognition*, vol. 40, no. 7, pp. 1958–1970, 2007.

[112] C. Liu, J. Yuen, S. Member, and A. Torralba, "SIFT Flow : Dense Correspondence across Scenes and its Applications," *IEEE Transactions on Pattern Analysis and Machine Intelligence*, vol. 33, no. 5, pp. 1–17, may 2011.

[113] J. R. R. Uijlings, A. W. M. Smeulders, and R. J. H. Scha, "Real-time visual concept classification," *IEEE Transactions on Multimedia*, vol. 12, no. 7, pp. 665–681, 2010.

[114] H. Bay, A. Ess, T. Tuytelaars, and L. Van Gool, "Speeded-Up Robust Features (SURF)," *Computer Vision and Image Understanding*, vol. 110, no. 3, pp.

346–359, jun 2008. [Online]. Available: http://linkinghub.elsevier.com/retrieve/pii/S1077314207001555

[115] R. Hartley and A. Zisserman, *Multiple view geometry in computer vision*, 2nd ed. Cambridge, UK: Cambridge University Press, 2003.

[116] Z. Zhang, "A flexible new technique for camera calibration," *IEEE Transactions on Pattern Analysis and Machine Intelligence*, vol. 22, no. 11, pp. 1330–1334, 2000. [Online]. Available: http://ieeexplore.ieee.org/document/888718/

[117] M. Tousignant, L. de Bellefeuille, S. O'Donoughue, and S. Grahovac, "Criterion validity of the cervical range of motion (CROM) goniometer for cervical flexion and extension." *Spine*, vol. 25, no. 3, pp. 324–330, 2000.

[118] T. Yamada, Y. Hayamizu, Y. Yamamoto, Y. Yomogida, A. Izadi-Najafabadi, D. N. Futaba, and K. Hata, "A stretchable carbon nanotube strain sensor for human-motion detection." *Nature nanotechnology*, vol. 6, no. 5, pp. 296–301, 2011. [Online]. Available: http://dx.doi.org/10.1038/nnano.2011.36

[119] P. H. Veltink, H. B. J. Bussmann, W. De Vries, W. L. J. Martens, and R. C. Van Lummel, "Detection of static and dynamic activities using uniaxial accelerometers," *IEEE Transactions on Rehabilitation Engineering*, vol. 4, no. 4, pp. 375–385, 1996.

[120] M. Yung, P. L. Bigelow, D. M. Hastings, and R. P. Wells, "Detecting within- and between-day manifestations of neuromuscular fatigue at work: an exploratory study," *Ergonomics*, vol. 57, no. 10, pp. 1562–73, jan 2014. [Online]. Available: http://www.ncbi.nlm.nih.gov/pubmed/24998392

[121] C. De Luca, "The Use of Surafce Electromyography in Biomechanics," *Journal of applied biomechanics*, vol. 13, pp. 135–163, 1997.

[122] J. V. Trontelj, J. Jabre, and M. Mihelin, "Needle and Wire Detection Techniques," in *Electromyography: Physiology, Engineering, and Noninvasive Applications*. John Wiley & Sons, Inc., 2004, pp. 27–46.

[123] C. J. De Luca, "Use of the surface EMG signal for performance evaluation of back muscles," *Muscle and Nerve*, vol. 16, no. 2, pp. 210–216, 1993.

[124] B. Gerdle, B. Larsson, and S. Karlsson, "Criterion validation of surface EMG variables as fatigue indicators using peak torque: A study of repetitive maximum isokinetic knee extensions," *Journal of Electromyography and Kinesiology*, vol. 10, no. 4, pp. 225–232, 2000.

[125] N.-T. Tsai, P. W. McClure, and A. R. Karduna, "Effects of muscle fatigue on 3-dimensional scapular kinematics11No commercial party having a direct financial interest in the results of the research supporting this article has or will confer a

benefit upon the author(s) or upon any organization with whi," *Archives of Physical Medicine and Rehabilitation*, vol. 84, no. 7, pp. 1000–1005, 2003. [Online]. Available: http://linkinghub.elsevier.com/retrieve/pii/S0003999303001278

[126] D. D. Ebaugh, P. W. McClure, and A. R. Karduna, "Effects of shoulder muscle fatigue caused by repetitive overhead activities on scapulothoracic and glenohumeral kinematics," *Journal of Electromyography and Kinesiology*, vol. 16, no. 3, pp. 224–235, 2006. [Online]. Available: http://linkinghub.elsevier.com/retrieve/pii/S1050641105000805

[127] R. R. Bini, F. Diefenthaeler, and C. B. Mota, "Fatigue effects on the coordinative pattern during cycling: Kinetics and kinematics evaluation," *Journal of Electromyography and Kinesiology*, vol. 20, no. 1, pp. 102–107, feb 2010. [Online]. Available: http://www.ncbi.nlm.nih.gov/pubmed/19028111

[128] Bourns, "EM14 - 14 mm Rotary Optical Encoder w/Switch," 2011. [Online]. Available: http://www.bourns.com/pdfs/em14.pdf

[129] A. Savitzky and M. J. E. Golay, "Smoothing and Differentiation of Data by Simplified Least Squares Procedures," *Analytical Chemistry*, vol. 36, no. 8, pp. 1627–1639, 1964.

[130] P. Esser, H. Dawes, J. Collett, and K. Howells, "IMU: Inertial sensing of vertical CoM movement," *Journal of Biomechanics*, vol. 42, no. 10, pp. 1578–1581, 2009.

[131] M. Y. Kim, S. M. Ayaz, J. Park, and Y. Roh, "Adaptive 3D sensing system based on variable magnification using stereo vision and structured light," *Optics and Lasers in Engineering*, vol. 55, pp. 113–127, apr 2014.

[132] P. Rowe, C. Myles, S. Hillmann, and M. Hazlewood, "Validation of Flexible Electrogoniometry as a Measure of Joint Kinematics," *Physiotherapy*, vol. 87, no. 9, pp. 479–488, 2001. [Online]. Available: http://www.sciencedirect.com/science/article/pii/S0031940605606955

[133] G. Li and P. Buckle, "Current techniques for assessing physical exposure to work-related musculoskeletal risks, with emphasis on posture-based methods," *Ergonomics*, vol. 42, no. 5, pp. 674–695, may 1999. [Online]. Available: http://www.tandfonline.com/doi/abs/10.1080/001401399185388

[134] S. Hignett and L. McAtamney, "Rapid entire body assessment (REBA)." *Applied ergonomics*, vol. 31, no. 2, pp. 201–5, apr 2000. [Online]. Available: http://www.ncbi.nlm.nih.gov/pubmed/10711982

[135] W. Laurig, F. M. Kühn, and K. C. Schoo, "An approach to assessing motor workload in assembly tasks by the use of predetermined-motion-time systems," *Applied Ergonomics*, vol. 16, no. 2, pp. 119–125, 1985.

[136] Å. Kolbom and J. Persson, "Work technique and its consequences for musculoskeletal

disorders," *Ergonomics*, vol. 30, no. 2, pp. 273–279, feb 1987. [Online]. Available: http://www.tandfonline.com/doi/abs/10.1080/00140138708969706

[137] Å. Kilbom, "Repetitive work of the upper extremity: Part II – The scientific basis (knowledge base) for the guide," *International Journal of Industrial Ergonomics*, vol. 14, no. 1-2, pp. 59–86, aug 1994. [Online]. Available: http://linkinghub.elsevier.com/retrieve/pii/016981419490006X

[138] R. Radwin, W. Marras, and S. Lavender, "Biomechanical aspects of work-related musculoskeletal disorders," *Theoretical Issues in Ergonomics Science*, vol. 2, no. 2, pp. 153–217, 2002.

[139] C. DB, A. GB, and M. BJ, *Occupational Biomechanics (copy 2)*, 4th ed. Wiley-Interscience Publication., 1999, vol. 3rd.

[140] D. B. Chaffin and M. Erig, "Three-Dimensional Biomechanical Static Strength Prediction Model Sensitivity to Postural and Anthropometric Inaccuracies," *IIE Transactions*, vol. 23, no. 3, pp. 215–227, sep 1991.

[141] A. Fraser and H. Swinney, "Independent Coordinates for Strange Attractors from Mutual Information," *Physical review A*, vol. 33, no. 2, 1986.

[142] T. Buzug and G. Pfister, "Optimal delay time and embedding dimension for

delay-time coordinates by analysis of the global static and local dynamical behavior of strange attractors," *Physical Review A*, vol. 45, no. 10, pp. 7073–7084, 1992. [Online]. Available: http://pra.aps.org/abstract/PRA/v45/i10/p7073{_}1

[143] M. Kennel, R. Brown, and H. Abarbanel, "Determining Embedding Dimension for Phase-Space Reconstruction Using a Geometrical Construction," *Physical review A*, vol. 45, no. 6, pp. 3403–3411, 1992.

[144] D. Chelidze, J. P. Cusumano, and A. Chatterjee, "A Dynamical Systems Approach to Damage Evolution Tracking, Part 1: Description and Experimental Application," *Journal of Vibration and Acoustics*, vol. 124, no. 2, p. 250, 2002. [Online]. Available: http://vibrationacoustics.asmedigitalcollection.asme.org/article.aspx?articleid=1470412

[145] ——, "A Dynamical Systems Approach to Damage Evolution Tracking, Part 1: Description and Experimental Application," *Journal of Vibration and Acoustics*, vol. 124, no. 2, p. 250, 2002. [Online]. Available: http://vibrationacoustics.asmedigitalcollection.asme.org/article.aspx?articleid=1470413

[146] D. Chelidze and J. P. Cusumano, "Phase space warping: nonlinear time-series analysis for slowly drifting systems." *Philosophical transactions. Series A,*

Mathematical, physical, and engineering sciences, vol. 364, no. 1846, pp. 2495–2513, sep 2006. [Online]. Available: http://www.ncbi.nlm.nih.gov/pubmed/16893800

[147] J. B. Dingwell, D. F. Napolitano, and D. Chelidze, "A nonlinear approach to tracking slow-time-scale changes in movement kinematics," *Journal of Biomechanics*, vol. 40, no. 7, pp. 1629–1634, jan 2007.

[148] D. B. Segala, D. H. Gates, J. B. Dingwell, and D. Chelidze, "Nonlinear smooth orthogonal decomposition of kinematic features of sawing reconstructs muscle fatigue evolution as indicated by electromyography." *Journal of biomechanical engineering*, vol. 133, no. 3, p. 031009, mar 2011. [Online]. Available: http://www.ncbi.nlm.nih.gov/pubmed/21303185

[149] M. A. Sanjari, A. R. Arshi, M. Parnianpour, and S. Seyed-Mohseni, "Local state space temporal fluctuations: a methodology to reveal changes during a fatiguing repetitive task." *Journal of biomechanical engineering*, vol. 132, no. 10, oct 2010. [Online]. Available: http://www.ncbi.nlm.nih.gov/pubmed/20887012

[150] M. Yung, S. E. Mathiassen, and R. P. Wells, "Variation of force amplitude and its effects on local fatigue," *European journal of applied physiology*, vol. 112, no. 11, pp. 3865–79, nov 2012. [Online]. Available: http://www.ncbi.nlm.nih.gov/pubmed/22407330

[151] M. a. Nussbaum, L. L. Clark, M. a. Lanza, and K. M. Rice, "Fatigue and endurance limits during intermittent overhead work," *American Industrial Hygiene Association Journal*, vol. 62, no. 4, pp. 446–56, 2001. [Online]. Available: http://www.ncbi.nlm.nih.gov/pubmed/11549138

[152] S. Mathiassen, "The Influence of Exercise/Rest Schedule on the Physiological and Psychophysical Response to Isometric Shoulder-Neck Exercise," *European Journal of Applied Physiology and Occupational Physiology*, vol. 67, pp. 528–539, 1993. [Online]. Available: http://link.springer.com/article/10.1007/BF00241650

[153] S. E. Mathiassen and E. Åhsberg, "Prediction of Shoulder Flexion Endurance from Personal Factors," *International Journal of Industrial Ergonomics*, vol. 24, 1999. [Online]. Available: http://www.sciencedirect.com/science/article/pii/S0169814198000390

[154] S. S. Ulin, T. J. Armstrong, S. H. Snook, and W. M. Keyserling, "Perceived exertion and discomfort associated with driving screws at various work locations and at different work frequencies." *Ergonomics*, vol. 36, no. 7, pp. 833–46, jul 1993. [Online]. Available: http://www.ncbi.nlm.nih.gov/pubmed/8339721

[155] L. W. O'Sullivan and T. J. Gallwey, "Forearm torque strengths and discomfort

profiles in pronation and supination," *Ergonomics*, vol. 48, no. 6, pp. 703–21, may 2005. [Online]. Available: http://www.ncbi.nlm.nih.gov/pubmed/16087504

[156] A. Moore and R. Wells, "Effect of cycle time and duty cycle on psychophysically determined acceptable levels in a highly repetitive task," *Ergonomics*, vol. 48, no. 7, pp. 859–73, jun 2005. [Online]. Available: http://www.ncbi.nlm.nih.gov/pubmed/16076742

[157] M. Yung, "Variation of Force Amplitude and its Effects on Muscle Fatigue," Master of Science, University of Waterloo, 2011. [Online]. Available: https://uwspace.uwaterloo.ca/handle/10012/5746

[158] R. Westgaard and J. Winkel, "Guidelines for occupational musculoskeletal load as a basis for intervention: a critical review," *Applied Ergonomics*, vol. 27, no. 2, pp. 79–88, 1996. [Online]. Available: http://linkinghub.elsevier.com/retrieve/pii/0003687095000623

[159] K. N. An, F. C. Hui, B. F. Morrey, R. L. Linscheid, and E. Y. Chao, "Muscles across the elbow joint: A biomechanical analysis," *Journal of Biomechanics*, vol. 14, no. 10, pp. 659–669, jan 1981. [Online]. Available: http://linkinghub.elsevier.com/retrieve/pii/0021929081900488

[160] F. Buchthal and H. Schmalbruch, "Contraction Times and Fibre Types in Intact

Human Muscle," *Acta Physiologica Scandinavica*, vol. 79, no. 4, pp. 435–452, aug 1970. [Online]. Available: http://www.ncbi.nlm.nih.gov/pubmed/5472111

[161] D. A. Winter, "Muscle Mechanics," in *Biomechanics and Motor Control of Human Movement*. Hoboken, NJ, USA: John Wiley & Sons, Inc., 2009, pp. 224–249. [Online]. Available: http://doi.wiley.com/10.1002/9780470549148.ch9

[162] K. E. Hagbarth, J. Jessop, G. Eklund, and E. U. Wallin, "The Piper Rhythm-A Phenomenon Related to Muscle Resonance Characteristics?" *Acta physiologica Scandinavica*, vol. 117, no. 2, pp. 263–71, feb 1983. [Online]. Available: http://www.ncbi.nlm.nih.gov/pubmed/6869036

[163] P. Brown, "Cortical drives to human muscle: The Piper and related rhythms," *Progress in Neurobiology*, vol. 60, no. 1, pp. 97–108, jan 2000. [Online]. Available: http://www.ncbi.nlm.nih.gov/pubmed/10622378

[164] J. B. Dingwell and J. P. Cusumano, "Nonlinear time series analysis of normal and pathological human walking," *Chaos: An Interdisciplinary Journal of Nonlinear Science*, vol. 10, no. 4, p. 848, 2000.

[165] J. B. Dingwell and L. C. Marin, "Kinematic variability and local dynamic stability of upper body motions when walking at different speeds," *Journal of Biomechanics*, vol. 39, no. 3, pp. 444–452, 2006.

[166] H. Dong, I. Ugalde, N. Figueroa, and A. El Saddik, "Towards whole body fatigue assessment of human movement: a fatigue-tracking system based on combined sEMG and accelerometer signals." *Sensors (Basel, Switzerland)*, vol. 14, no. 2, pp. 2052–2070, jan 2014.

[167] M. Sim and J. U. Kim, "Differences between experts and novices in kinematics and accuracy of golf putting," *Human Movement Science*, vol. 29, no. 6, pp. 932–946, 2010. [Online]. Available: http://dx.doi.org/10.1016/j.humov.2010.07.014

[168] G. Fleisig, R. Nicholls, B. Elliott, and R. Escamilla, "Kinematics Used by World Class Tennis Players to Produce High-Velocity Serves," *Sports Biomechanics*, vol. 2, no. 1, pp. 51–64, jan 2003. [Online]. Available: http://www.tandfonline.com/doi/abs/10.1080/14763140308522807

[169] Noitm Ltd, "PERCEPTION NEURON." [Online]. Available: https://neuronmocap.com/

[170] D. B. Chaffin, G. B. Andersson, and B. J. Martin, "Occupational Biomehcnical Models," in *Occupatinal Biomechanics*, 3rd ed. Wiley & Sons, Inc., 1999, ch. Six, pp. 181–277.

[171] A. Garg and D. B. Chaffin, "A Biomechanical Computerized Simulation of Human Strength," *A I I E Transactions*, vol. 7, no. 1, pp. 01–15, mar 1975.

[172] M. Jäger and A. Luttmann, "Critical survey on the biomechanical criterion in the NIOSH method for the design and evaluation of manual lifting tasks," *International Journal of Industrial Ergonomics*, vol. 23, no. 4, pp. 331–337, mar 1999. [Online]. Available: http://linkinghub.elsevier.com/retrieve/pii/S0169814198000493

[173] D. Anton, L. D. Shibley, N. B. Fethke, J. Hess, T. M. Cook, and J. Rosecrance, "The effect of overhead drilling position on shoulder moment and electromyography." *Ergonomics*, vol. 44, no. January 2015, pp. 489–501, apr 2001. [Online]. Available: http://www.tandfonline.com/doi/abs/10.1080/00140130120079

[174] A. Garg, K. Hegmann, B. Schwoerer, and J. Kapellusch, "The effect of maximum voluntary contraction on endurance times for the shoulder girdle," *International Journal of Industrial Ergonomics*, vol. 30, no. 2, pp. 103–113, aug 2002.

[175] R. M. Yerkes and J. D. Dodson, "The relation of strength of stimulus to rapidity of habit-formation," *Journal of Comparative Neurology and Psychology*, vol. 18, no. 5, pp. 459–482, nov 1908. [Online]. Available: http://doi.wiley.com/10.1002/cne.920180503

[176] C. G. Drury, "Ergonomics Practice in Manufacturing," *Ergonomics*, vol. 34, no. 6, pp. 825–839, jun 1991.

[177] J. A. Gambatese, M. Behm, and J. W. Hinze, "Viability of Designing for Construction

Worker Safety," *Journal of Construction Engineering and Management*, vol. 131, no. 9, pp. 1029–1036, sep 2005.

[178] S. Reddy, M. Mun, J. Burke, D. Estrin, M. Hansen, and M. Srivastava, "Using mobile phones to determine transportation modes," *ACM Transactions on Sensor Networks*, vol. 6, no. 2, pp. 1–27, feb 2010. [Online]. Available: http://portal.acm.org/citation.cfm?doid=1689239.1689243

[179] R. Akhavian and A. H. Behzadan, "Smartphone-based construction workers??? activity recognition and classification," *Automation in Construction*, vol. 71, no. Part 2, pp. 198–209, nov 2016.

[180] S. Namal, A. Senanayake, V. Chong, J. Chong, and G. Sirisinghe, "Analysis of Soccer Actions using Wireless Accelerometers," in *2006 IEEE International Conference on Industrial Informatics*, no. August. IEEE, aug 2006, pp. 664–669.

[181] S. M. N. A. Senanayake, O. A. Malik, and M. Iskandar, "Wireless Multi-Sensor Integration for ACL Rehabilitation Using Biofeedback Mechanism," in *Volume 2: Biomedical and Biotechnology*, no. November. ASME, nov 2012, p. 99. [Online]. Available: http://proceedings.asmedigitalcollection.asme.org/proceeding.aspx?doi=10.1115/IMECE2012-87809

[182] C. R. Ahn, S. Lee, and F. Peña-Mora, "Application of Low-Cost Accelerometers for

Measuring the Operational Efficiency of a Construction Equipment Fleet," *Journal of Computing in Civil Engineering*, vol. 29, no. 2, p. 04014042, mar 2015.

[183] A. Jain, P. Duin, and Jianchang Mao, "Statistical pattern recognition: a review," *IEEE Transactions on Pattern Analysis and Machine Intelligence*, vol. 22, no. 1, pp. 4–37, 2000. [Online]. Available: http://ieeexplore.ieee.org/lpdocs/epic03/wrapper.htm?arnumber=824819

[184] O. Girard, J.-P. Micallef, and G. P. Millet, "Lower-limb activity during the power serve in tennis: effects of performance level." *Medicine and science in sports and exercise*, vol. 37, no. 6, pp. 1021–9, jun 2005.

[185] J. Baker, J. Côté, and B. Abernethy, "Learning from the experts: practice activities of expert decision makers in sport." *Research quarterly for exercise and sport*, vol. 74, no. 3, pp. 342–347, sep 2003. [Online]. Available: http://www.tandfonline.com/doi/abs/10.1080/02701367.2003.10609101

[186] A. Chaouachi, M. Brughelli, K. Chamari, G. T. Levin, N. Ben Abdelkrim, L. Laurencelle, and C. Castagna, "Lower limb maximal dynamic strength and agility determinants in elite basketball players." *J. Strength Cond. Res.*, vol. 23, no. 5, pp. 1570–1577, aug 2009.

[187] H. Karimi, T. R. Taylor, P. M. Goodrum, and C. Srinivasan, "Quantitative

analysis of the impact of craft worker availability on construction project safety performance," *Construction Innovation*, vol. 16, no. 3, pp. 307–322, jul 2016. [Online]. Available: http://www.emeraldinsight.com/doi/10.1108/CI-10-2015-0050

[188] G. Wu, S. Siegler, P. Allard, C. Kirtley, A. Leardini, D. Rosenbaum, M. Whittle, D. D. D'Lima, L. Cristofolini, H. Witte, O. Schmid, and I. Stokes, "ISB recommendation on definitions of joint coordinate system of various joints for the reporting of human joint motion–part I: ankle, hip, and spine. International Society of Biomechanics." *Journal of biomechanics*, vol. 35, no. 4, pp. 543–548, 2002.

[189] G. Wu, F. C. T. Van Der Helm, H. E. J. Veeger, M. Makhsous, P. Van Roy, C. Anglin, J. Nagels, A. R. Karduna, K. McQuade, X. Wang, F. W. Werner, and B. Buchholz, "ISB recommendation on definitions of joint coordinate systems of various joints for the reporting of human joint motion - Part II: Shoulder, elbow, wrist and hand," *Journal of Biomechanics*, vol. 38, no. 5, pp. 981–992, 2005.

[190] A. K. Jain, M. N. Murty, and P. J. Flynn, "Data clustering: a review," *ACM Computing Surveys*, vol. 31, no. 3, pp. 264–323, 1999. [Online]. Available: http://portal.acm.org/citation.cfm?doid=331499.331504

[191] C. D. Brown and H. T. Davis, "Receiver operating characteristics curves and related decision measures: A tutorial," *Chemometrics and Intelligent*

Laboratory Systems, vol. 80, no. 1, pp. 24–38, jan 2006. [Online]. Available: http://linkinghub.elsevier.com/retrieve/pii/S0169743905000766